SYNTHESIS OF AZOBENZENE CONTAINING MACROCYCLES

A THESIS SUBMITTED TO
THE GRADUATE SCHOOL OF NATURAL AND APPLIED SCIENCES
OF
MIDDLE EAST TECHNICAL UNIVERSITY

BY

EGE HOŞGÖR

IN PARTIAL FULFILLMENT OF THE REQUIREMENTS
FOR
THE DEGREE OF MASTER OF SCIENCE
IN
CHEMISTRY

FEBRUARY 2021

Approval of the thesis:

SYNTHESIS OF AZOBENZENE CONTAINING MACROCYCLES

submitted by **EGE HOŞGÖR** in partial fulfillment of the requirements for the degree of **Master of Science in Chemistry, Middle East Technical University** by,

Date: 11.02.2021

I hereby declare that all information in this document has been obtained and presented in accordance with academic rules and ethical conduct. I also declare that, as required by these rules and conduct, I have fully cited and referenced all material and results that are not original to this work.

Name, Last name : Ege Hoşgör

Signature :

ABSTRACT

SYNTHESIS OF AZOBENZENE CONTAINING MACROCYCLES

Hoşgör, Ege
Master of Science, Chemistry
Supervisor: Prof. Dr. Akın Akdağ

February 2021, 159 pages

Aromatic azo compounds are one of the well-known research topics of recent times due to their photoisomeric properties under ultraviolet or visible light. Generally, these substances undergo isomerization from the thermodynamically more stable *trans* isomer to the *cis* isomer when irradiated with appropriate light radiation. The incorporation of azo groups to the macrocycle skeleton is an important part of the supramolecular chemistry. Azobenzene photoisomerization is the key mechanism of molecular motors that can be controlled by light. These are further proposed to act as catch and release receptors. In this study, macrocycles were constructed from 2-aminobenzoic acid. The benzoic acids were linked together with ethylene glycol units through ester linkage (diethylene glycol, triethylene glycol, tetraethylene glycol). Then, the amino parts were converted to azo linkage with $Pb(OAc)_4$. Moreover, *L*-phenylalanine was incorporated into these macrocycles to get chiral macrocycles. The photophysical and photochemical properties of these macrocycles were investigated both experimentally and theoretically.

Keywords: azobenzene, macrocycles, photoisomerization, chirality

ÖZ

AZOBENZEN İÇEREN MAKROHALKA SENTEZİ

Hoşgör, Ege
Yüksek Lisans, Kimya
Tez Yöneticisi: Prof. Dr. Akın Akdağ

Şubat 2021, 159 sayfa

Aromatik azo bileşikler, ultraviyole ya da görünür bölge ışığı altında gösterdikleri fotoizomerik özelliklerinden dolayı son dönemlerin popüler konularından biridir. Genellikle, bu maddeler, uygun radyasyon verildiğinde termodinamik olarak daha kararlı olan *trans* izomerinden, *cis* izomerine dönüşürler. Makrohalka iskelet yapılarına azo gruplarının katılması, supramolekürler kimyanın önemli bir alanıdır. Azobenzenler, ışık aracılığıyla kontrol edilebilen makrohalkalı moleküler motorların anahtar mekanizmalarını oluştururlar. Bu maddeler yakala ve bırak reseptörleri olarak bu tezde önerilmiştir. Bu çalışmada, 2-aminobenzoik asit, etilen glikollerle birleştirilerek esterler elde edilmiştir. Uçlarda bulunan amino grupları $Pb(OAc)_4$ kullanılarak azo gruba çevirilerek azo makrohalkalar sentezlenmiştir. Bunun ötesinde *L*-fenilalanin kullanılarak kiral makrohalka yapıları sentezlenmiştir. Bu bileşiklerin fotofiziksel ve fotokimyasal özellikleri deneysel ve teorik olarak incelenmiştir.

Anahtar Kelimeler: azobenzen, makrohalka, fotoizomerizasyon, kiralite

To my beloved Mother and Father

ACKNOWLEDGMENTS

This thesis owes its existence to the generous intellectual and moral support provided by many people. The COVID-19 outbreak has affected the world severely, and during this time, it was hard to focus and keep working on completing this thesis while isolating myself from all the news about the global pandemic. I wish to thank all the people whose assistance was a milestone in this challenging time.

First and foremost, I would like to express my sincere gratitude to my supervisor Prof. Dr. Akın Akdağ, for his endless patience, guidance, and encouragement during this stressful time. Since my undergraduate years, whenever I feel like giving up, he encouraged me to look at science in new and creative ways and gave me confidence to complete this study. He has taught me the way of questioning knowledge and encouraged me to expand my limits.

I would like to thank the rest of the committee members: Prof. Dr. Cihangir Tanyeli, Prof. Dr. Özdemir Doğan, Assoc. Prof. Dr. Serhan Türkyılmaz and Assoc. Prof. Dr. Stellios Arseniyadis for assisting me with their valuable comments, thoughts and criticisms in shaping the final draft of this study.

In my third year of my bachelor's degree Assoc. Prof. Dr. Stellios Arseniyadis gave me a chance to work as an intern student in his laboratory at the Queen Mary University of London. I gained much valuable experience by working with him. I would like to thank him for giving me the opportunity.

I would like to thank TUBITAK (118Z710) for scholarship. The work for the project (118Z710) is not included into this thesis.

My time at METU would not have been the same without many great people. Especially, I would like to thank Gizem Çalışgan Ünay and Perihan Öztürk Düzenli for their mentorship, who shared their time and ideas through discussions. They were always with me when I needed to endure challenging situations. I am most lucky to have known these powerful women.

I would like to thank to my group members: Bengi Şentürk, Ece Ayça Erdoğan, Berçin Verda Asya, Oğuzhan Albayrak, Fatmanur Aydemir, Ozan Ünver, Bulem Çakmak, Nihat Aksoy, and Sadia Tul Munna. Their companionship, curiosity of research, and a good sense of humor made the path joyful. I wish them all the best in their careers.

I am grateful to all my beloved friends, Başak Mumcu, Tuğçe Özkan, Umut Aydemir, and İzel Akdeniz Gürel who are always there with me in all aspects of my life.

My *framily*, Selena Değer, Tarkan Üsküdar, Berna Taşçı, Oytun Demirörs, Ezgi Demiral, Serkan Durukan, Kutay Ağırbaş, and Görkem Özcan, have made winters bearable and summers enjoyable. I am deeply thankful for their valuable comments in shaping my process, unfailing good humor, and never-ending belief in me.

I owe more than thanks to my dearest, Doruk Baykal, who always make me feel stronger than I thought. His true love and passion for science are always very inspiring. This journey would not have been the same without his sense of sharing, love, and beautiful smile. He was there when I was about to give up, together with our lovely cats, Dobby and Mona.

Last but not least, I would like to thank my dearest family to whom this thesis is dedicated, for instilling in me the wonder of learning: Ayşe Gündüz Hoşgör, Hasan Hoşgör, and Pamuk. I love you so much!

TABLE OF CONTENTS

LIST OF SCHEMES

SCHEMES

LIST OF FIGURES

FIGURES

LIST OF TABLES

CHAPTER 1

INTRODUCTION

1.1 Photoresponsive Materials

Over the last two decades, many types of photoresponsive materials have gained popularity and been synthesized for control over molecular motion through external variables such as pH, electricity, magnetism, and light.[1] This offers numerous opportunities in modern chemistry, biochemistry and materials science.[1,2] In the literature, photochemical reactions are classified as *cis-trans* isomerisation, tautomerization, electrocyclic reactions, and heterolytic and homolytic cleavage of bonds.[2] Compounds bearing azo groups, also known as diazenes, are unique due to their tendency towards *cis-trans* isomerisation.

1.1.1 Azo Compounds

1.1.1.1 Structure

Azo compounds, also known as diazenes, consist of two or more moieties linked by azo bridges and they are characterized by **R–N=N-R'** linkage. These moieties have critical roles on the physical and chemical properties of azo compounds. Azo compounds can be classified in two major groups: Aliphatic and aromatic.[3]

1.1.1.1.1 Aliphatic Azo Compounds

If alkyl groups are attached on one side of the azo group, the molecule is classified as aliphatic azo compound. In the literature, these molecules were originally known as “azoalkanes” however, “dialkyldiazenes” appears to be the modern

nomenclature.[3,4] In general, aliphatic azo compounds show lower overall stability as compared to their aromatic counterparts.

Aliphatic diazenes have known tendencies towards thermal decomposition through homolytic cleavage of the carbon-nitrogen bonds. Therefore, aliphatic azo compounds are commonly used as radical initiators. A popular example would be 2,2'-azobisisobutyronitrile (AIBN), which was first reported by Thiele and Heuser in 1896.[5] The well-established decomposition mechanism of AIBN to radicals and a molecule of nitrogen is as follows (Scheme 1):

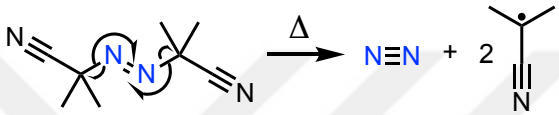

Scheme 1. Mechanism of the decomposition of AIBN

The decomposition mechanism of AIBN molecule gives rise to the quantitative formation of nitrogen and free radicals.[6,7]

1.1.1.1.2 Aromatic Azo Compounds

If aryl groups are attached on each side of the azo bridge, the molecule is classified as aromatic azo compound. Aromatic rings and the azo group extend the conjugation in the molecule. In aliphatic azo compounds, the carbon atom covalently bonded to the azo bridge is sp^3 hybridized however, in aromatic azo compounds, said carbon atom is sp^2 hybridized. Eilhard Mitscherlich first reported the popular example 'azobenzene' in 1834 (Figure 1).[8]

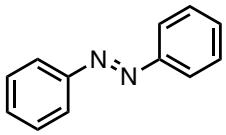

Figure 1. *trans*-Azobenzene

1.1.1.2 Properties

Azo compounds have received great attention due to their thermal, chemical, photochemical, and biological properties,[9] which make them worth studying.

1.1.1.2.1 Thermal

Azobenzene and derivatives are not easily affected by higher temperatures. They are thermally stable, which renders them excellent candidates for heat resistant substances.[6] Hybridization of carbon atom attached to azo group in the aromatic azo compounds explains the stability. The conjugation of nitrogen atoms, both of them are sp^2 hybridized. This brings conjugation to the molecule which lowers the total energy of the system. Thus, stabilizes the molecule.

1.1.1.2.2 Photochemical

Photochemically, aliphatic and aromatic azo compounds absorb light at certain wavelengths associated with electronic excitation. Aromatic azo compounds do not undergo photodissociation reaction like their aliphatic counterparts.[6]

Azo compounds have *cis* and *trans* configurations that are transformable to each other by a stimulus. Azobenzene derivatives have definite absorption spectra for each isomer. The typical spectrum for *trans*-azobenzene has an intense absorption band at around 320 nm, which corresponds to π-π* transition and a weaker absorption band at around 440 nm associated with the n-π* transition. The intensities of these bands differ significantly for each isomer.[6]

trans-Azobenzene is planar and has C_{2h} symmetry. The N=N bond distance is around 1.26Å.[9] The n-π* transition band of *trans* isomer is more intense than carbonyl compounds. By selection rules,[10] for *trans* isomer, the n-π* transition is symmetry forbidden however, it is allowed for the *cis* isomer, which explains the difference in intensities. Non-planar distortions and vibrational motion define the difference.[11] Electronic nature of the substituents modify the absorption.

1.1.1.2.3 Color

Azo aromatic compounds are excellent candidates for colorants and they represent a significant volume of the dye industry.[12] Azo dyes have represented 70% of all dyes in the printing market until the harmful effects of azo dyes, on both the environment and humans were discovered. After the discovery of their carcinogenic properties in 2002, the EU pushed laws against the production of azo dyes.[13] Some examples of such compounds are *o*-toluidine (ot), *p*-amino azobenzene (pa), *o*-aminoazotoluene (oa), *p*-toluidine (pt), and 4-chloroaniline (Figure 2).[13] Aryl amines are no longer used to dye textiles in the European industry.

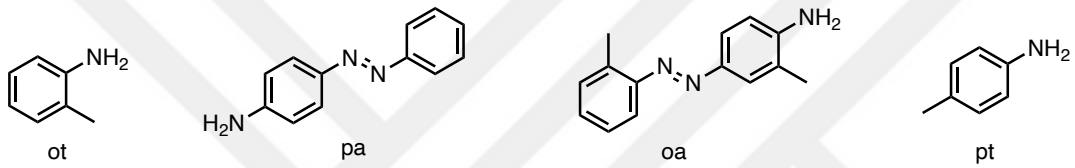

Figure 2. Some carcinogenic compounds used in the dye industry

The blazing color of azo dyes are dependent on the substituents. Azo dyes can be dissected into three major components: the backbone, chromophoric substituents, and the solubilizing groups. The backbone refers to the core unsubstituted azobenzene structure, whereas chromophoric substituents refer to the substituents contributing significantly to the electronic structure. Methyl orange, mordant red, and azo violet are some examples from the literature (Figure 3).

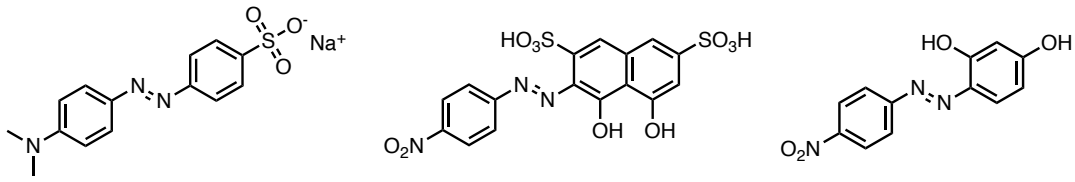

Figure 3. Examples of most well-known azo dyes[12]

1.1.1.2.4 Oxidation

Both aliphatic and aromatic azo compounds oxidized to azoxy derivatives (Scheme 2) under appropriate reaction conditions. Azoxy compounds are well-known starting materials for organic synthesis.[14] By the use of strong oxidants like perbenzoic acid azobenzene derivatives oxidize to azoxybenzenes. In addition, the two diastereomers of azobenzenes undergo *N*-oxidation at specific rates.[6]

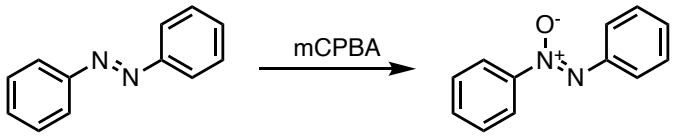

Scheme 2. Oxidation of *trans*-azobenzene to *trans*-azoxybenzene

1.1.1.2.5 Reduction

Reduction of azobenzene yields hydrazobenzene (Scheme 3), which is a common precursor for dyes. Hydrogenation of azobenzene with metallic reducing agents such as Mg, Fe, and Zn, in either acidic or alkaline media, gives hydrazobenzene with inorganic side products.[15] Another method to reduce azobenzene to hydrazobenzene, is the catalytic hydrogenation with Pd and H_2.[15]

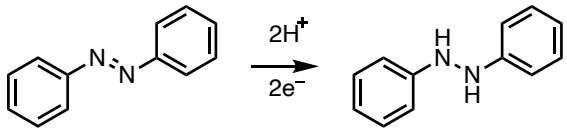

Scheme 3. Reduction of *trans*-Azobenzene

1.1.1.3 Synthesis

1.1.1.3.1 Diazotization or Azo Coupling Reaction

The classical method for synthesizing aromatic azo compounds is an azo coupling reaction between a diazotized aromatic amine and an aromatic nucleophile. The diazotization reaction of aromatic amines, which planted the seeds of the azo dye industry, was first reported by Peter Greiss in 1858. Some important aspects of this

transformation are as follows:[16] Use of a Bronsted acid is essential in order to liberate the nitrosonium ion from $NaNO_2$ *via* elimination of a molecule of water. The nitrosonium ion is a strong electrophile, which is susceptible to nucleophilic attack by aniline. After a nucleophilic attack followed by elimination of water diazonium salt forms. The diazonium salt can then undergo electrophilic aromatic substitution with an electron rich aromatic compound such as aniline.[17]

Since the aromatic diazonium salts are resonance stabilized *i.e.* the positive charge is delocalized, they are not very strong electrophiles. Thus, the reaction rate is dictated by the nucleophile and it is essential to use electron-rich arenes like aniline or phenol derivatives to synthesize azobenzenes with higher yields.[18]

The most accepted mechanism for this reaction is electrophilic aromatic substitution of electron rich nucleophile with diazonium salt (Scheme 4).[18]

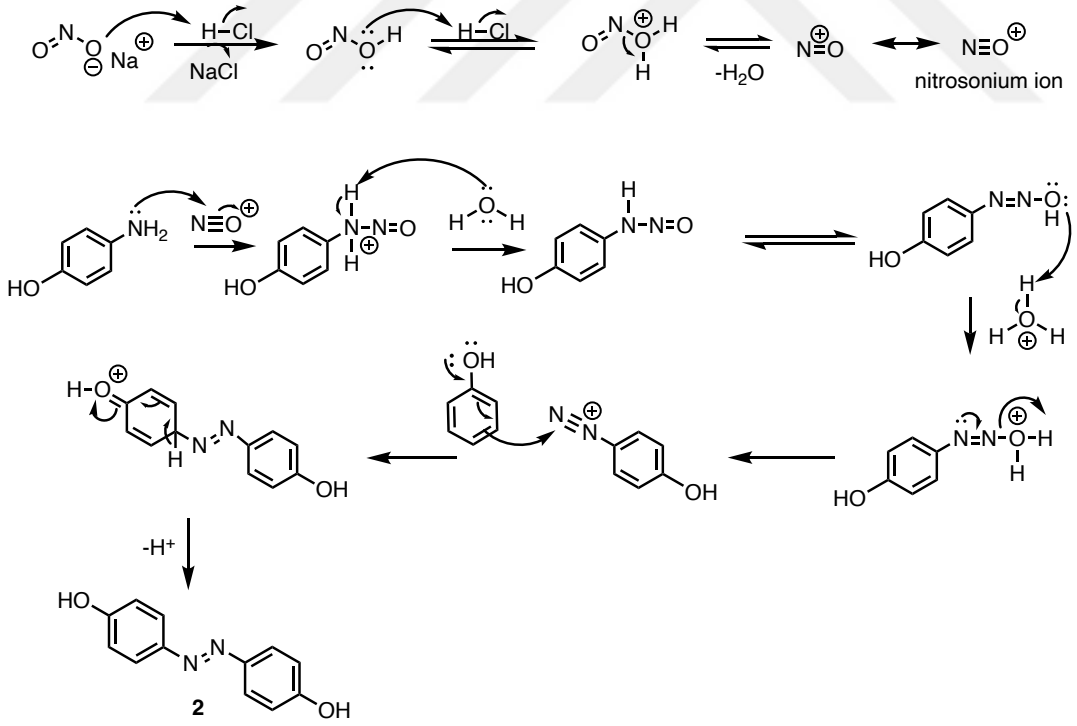

Scheme 4. Mechanism of a classical azo coupling reaction

1.1.1.3.2 Mills Reaction

The reaction of aromatic nitroso derivatives and aryl amines in acetic acid is another route to azobenzenes. The most famous example for this coupling is between phenylhydroxylamine and 4-methoxyaniline. An oxidant is used to oxidize the hydroxylamine to the related nitroso compound. Ferric chloride and dichromic acid are some common examples of oxidants.[19] Overoxidation to nitro compounds is possible. The proposed mechanism of this reaction is depicted on Scheme 5.[20]

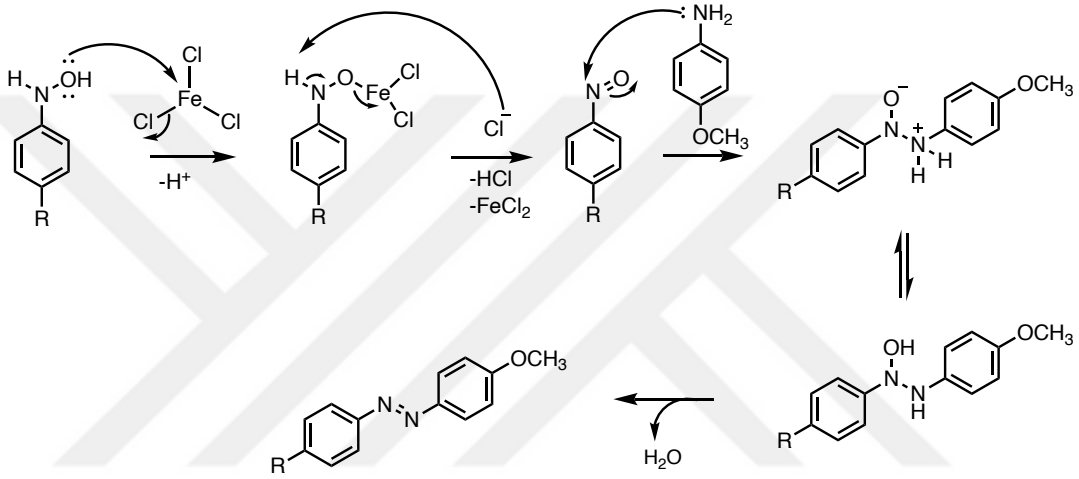

Scheme 5. Mechanism of Mills Reaction

1.1.1.3.3 Wallach Rearrangement

Another effective method to synthesize azobenzenes is the rearrangement of azoxybenzenes to 2- or 4-hydroxy-substituted azobenzenes using strong acids.[21] Azoxybenzenes can be effectively synthesized from nitrobenzenes by reduction. Substituents on the azoxybenzene guide the rearrangement. For instance, 4,4'-nitroazoxybenzene rearranges to 2-hydroxy-4,4'-azobenzene, whereas unsubstituted azoxybenzene rearranges to 4-hydroxyazobenzene. The proposed mechanism of this reaction is depicted on Scheme 6.[18]

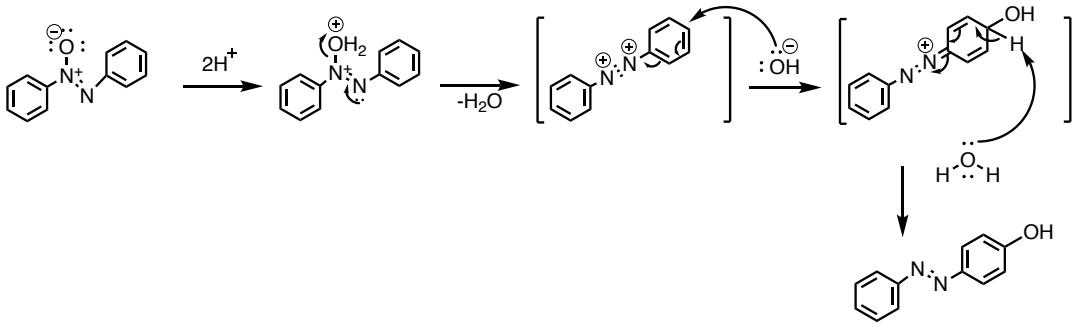

Scheme 6. Mechanism of Wallach Transformation

1.1.1.3.4 Copper Catalyzed Aerobic Coupling of Aniline

A new approach to synthesize unsymmetrical azo compounds from easily achievable anilines was published in 2010 (Scheme 7). In this reaction, dioxygen is used as the oxidant with a catalyst such as CuBr. The mechanism of this transformation is not yet completely understood. [22]

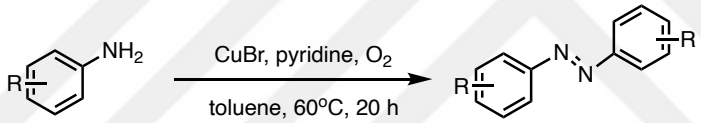

Scheme 7. Coupling Reaction of Aniline with O_2

1.1.1.3.5 Coupling Reaction of Aniline via 1,8-Diazabicyclo[5.4.0]undec7-ene (DBU) and *N*-Chlorosuccinimide

Another method to synthesize symmetrical azo compounds is a single step coupling reaction of aromatic amines with *N*-chlorosuccinimide and DBU (Scheme 8). Mechanism of this reaction is a modified mechanism, which is proposed by us, given in results and discussion part.[23]

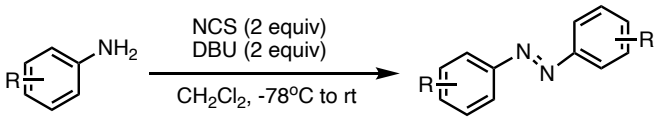

Scheme 8. Coupling Reaction of Aniline with NCS/DBU

1.1.1.3.6 Oxidation Reaction by Lead Tetraacetate

From the oxidation of primary aromatic amines with lead tetraacetate (LTA), symmetric or asymmetric azo compounds can be obtained.[24] The reaction goes through an hydrazo intermediate, which are oxidized to azo compounds. Recently, oxidative macrocyclization with lead tetra-acetate is widely used for the synthesis of azo bearing macrocycles.[25]

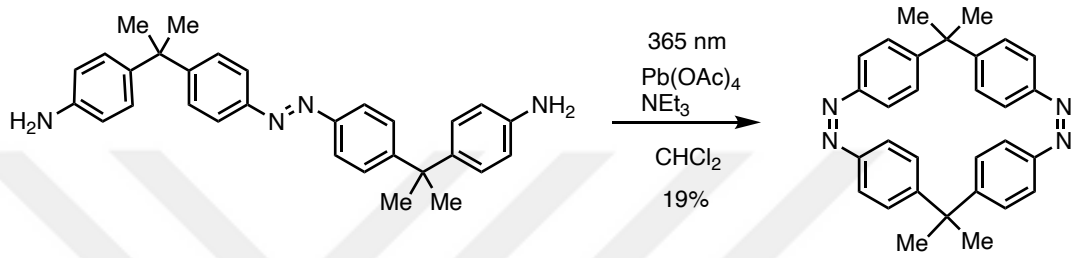

Scheme 9. Oxidative Macrocyclization with lead (IV)acetate

1.1.1.4 Reactions

1.1.1.4.1 Electrophilic Aromatic Substitution Reaction

In electrophilic aromatic substitution reactions, one hydrogen atom of the ring is replaced with an electrophile to form a substituted aromatic ring (Figure 5). The mechanisms of electrophilic substitution reactions depend on the rate-determining formation of a cationic intermediate followed by the rapid loss of a proton. The ring substituents determine the rate of the reaction by either stabilizing or destabilizing the intermediate.[26] The extended conjugation of the phenylazo group provides resonance stability to the benzenonium intermediate (Figure 4).[26]

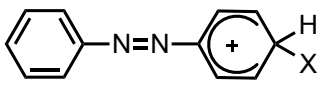

Figure 4. Benzenonium ion intermediate[26]

For example, chlorination of benzene in the presence of a Lewis acid gives chlorobenzene in appreciable yields.[27] Bromination, nitration, sulphonation products were successfully synthesized and isolated for certain azo molecules. [26]

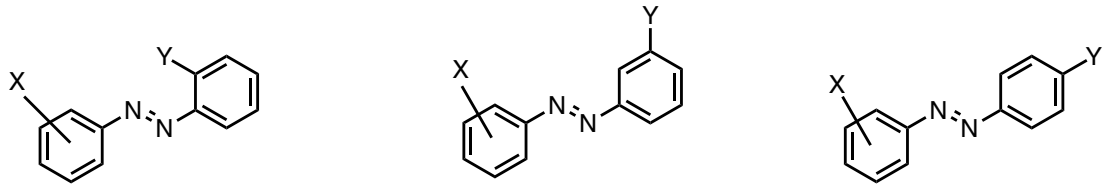

Figure 5. Substitution of azobenzene

1.1.1.4.2 Photoisomerization

Photoisomerization between the *cis* and *trans* form of azobenzene derivatives is one of the most well-known photochemical reactions.[28] After the discovery and isolation of *cis*-azobenzene,[29] the study of photoisomerization mechanism received great attention from scientists. Despite significant developments and growth in the field, the mechanism of photoisomerization is not completely understood.[30] The experimental data to prove ideas of such mechanism is limited due to the *cis* isomer's thermal instability. Using molecular orbital theory, electronic properties of *cis*- and *trans*- azobenzene are studied (Figure 6).

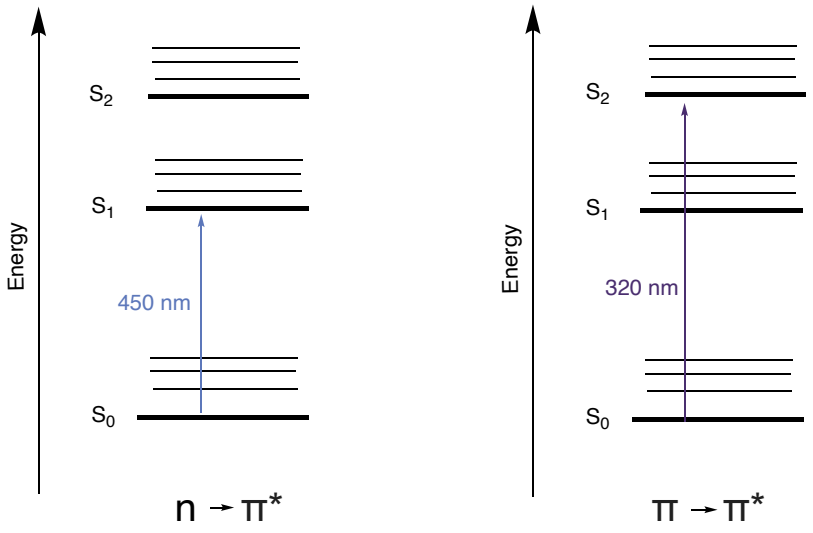

Figure 6. Absorption explained using molecular orbital theory

Both diastereomers of azobenzene show two absorption bands in the UV-Vis region,[30] which are associated with π-π* and n-π* electronic transitions. In the carbon analogs of azobenzene such as stilbene, a strong UV band around 320 nm arises from the symmetry allowed π-π* transition without the symmetry forbidden n-π* transition band. [31,32] The mechanistic difference between two systems caused by the unshared electron pairs of nitrogen atoms indicates different isomerization pathways. [32] The n-π* and π-π* electronic transitions excite azobenzene to first and second singlet excited states S_1 and S_2, respectively.[33]

Stilbene can be interconverted between its diastereomers in complete conversion however, for azobenzene, complete conversion is unlikely. [34,35] In order to fully understand the mechanistic pathway, the electronic properties of each isomer should be taken into consideration. The molar extinction coefficient, ε, of the π-π* absorption band of the *trans* isomer is around $3x10^4$ $M^{-1}\cdot cm^{-1}$, whereas the n-π* band is weaker, with an extinction coefficient of around 400 $M^{-1}\cdot cm^{-1}$.[35] However, the *cis* isomer has a shifted π-π* absorption band shorter wavelengths with a weaker intensity ε ≅ 7-$9x10^3$ $M^{-1}\cdot cm^{-1}$. Due to the allowed n-π* transition, the second absorption band is stronger than that of the *trans* isomer ε ≅ 1500 $M^{-1}\cdot cm^{-1}$. [35] In general, irradiating *trans*-azobenzene with the light of wavelength between 320-380 nm promotes *trans* to *cis* isomerization, whereas irradiating *cis* isomer between 400-450 nm promotes *cis* to *trans* isomerization. By the irradiation with light at a certain wavelength, it is possible to control the position of each *trans*-*cis* photostationary state. [36]

1.1.1.4.2.1 Rotation and Inversion Mechanisms

Several mechanisms have been proposed for azobenzene photoisomerization since the discovery of *cis*-azobenzene. There exists no certain explanation for the isomerization process, which makes the research subject popular. Mainly, two different pathways are proposed (Scheme 11). A rotation around the central C-N=N-C double bond and an in-plane inversion of the N=N double bond. [28] In the

rotational pathway, the weakening of the N=N π bond by excitation occurs to free the rotation around the center. The dihedral angle of the CNNC changes while the NNC remains at 120°.[32] On the other hand, in the inversion mechanism C-N=N-C dihedral angle fixed at 0° while N=N-C angle changes to 180°. During inversion mechanism, one of the nitrogen atoms of the transition state becomes sp hybridized and the proposed transition states become polar. Finally, relaxation from transition states results in *cis* and *trans* isomers. [32] The nonbonding electrons of nitrogen atom excite from S_0 to S_1 (n-π*) during the inversion mechanism. However, during rotation mechanism S_0 to S_2 (π-π*) transition occurs. [36]

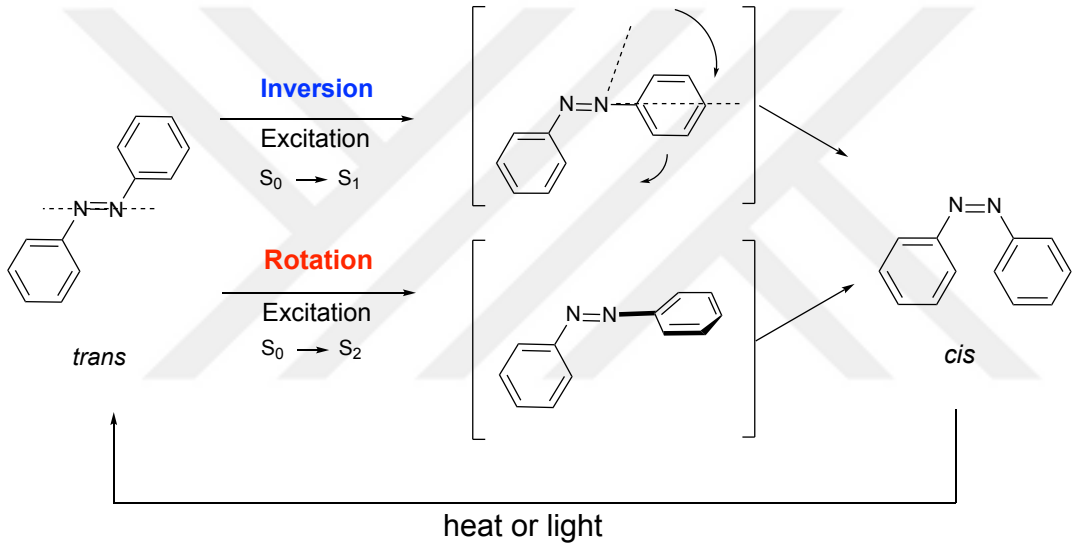

Scheme 10. Isomerization mechanism of azobenzene[36]

1.1.1.5 Uses

Aromatic azo compounds constitute one of the significant parts of chemical industry and are commonly used as organic dyes and pigments since almost any color in the spectrum can be obtained with appropriate structural modifications.[37] Beside the dye industry, azo compounds are widely used as food additives, acid-base indicators,[38] photoswitchable catalysis,[39] and light triggered therapeutic agents,[40] due to their extensive biological activities. Organic azo compounds are prevalent for drug delivery systems as well. For instance, Rafi et al. reported photoswitchable

nanomechanical systems with light driven molecular jacks, including azobenzene as drug delivery systems. Azobenzene in this system leads to a change in the distance of nanolayers upon photoisomerization, and the material could release the drug at a definite time and place for phototherapy.[40] Recently, photoisomerization of azo compounds have been applied in biological systems to control the activity of a large variety of biomolecules like enzymes and polypeptides.[41] The design and modifications of the light sensitive biomolecule are important because of the 'caging' approach. The key part of the biomolecule is surrounded by a light-sensitive protecting group, which controls the biomolecule activity with light. The azo substituted caging group undergoes an irreversible conversion until it becomes uncaged and releases the biomolecule.[42]

1.1.2 Azo Functional Macrocycles

The discovery of macrocyclic compounds has become a milestone in organic chemistry since these discoveries initiated host-guest and supramolecular chemistry.[43] For the last two decades, many scientists have been working on the design and synthesis of macrocyclic polyethers such as crown ethers.[44] For instance, Donald J. Cram, Jean-Marie Lehn, and Charles J. Pederson were awarded the Nobel Prize in Chemistry 1987 "for their development and use of molecules with structure-specific interactions of high selectivity" [45] and Jean-Pierre Sauvage, Sir J. Fraser Stoddart, and Ben L. Feringa were awarded the Nobel Prize in Chemistry 2016 "for the design and synthesis of molecular machines" [46] which are closely associated with supramolecular chemistry.

The skeleton of macrocycles can be altered by different functional groups for the specific purpose as they gain additional chemical and physical properties. The introduction of azo groups into the macrocyclic compounds is one of the most well-known modifications of supramolecular systems.[47] Due to the photoisomerization property of azo compounds, the geometry of the macromolecule changes upon irradiation (Scheme 11). This ability makes azo macrocycles perfect light-triggered switches, which can be used in light-driven molecular machines. Plenty of various

azo-macrocyclic molecules are used with a particular focus on supramolecular interactions.[43]

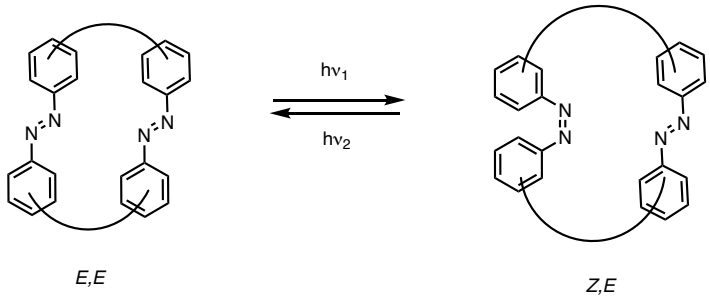

Scheme 11. Photoisomerization of azomacrocycles[43]

1.1.2.1 Effect of Chirality

Chirality is the characteristic of living organisms and nature. During the evolution of life, one kind of chirality is favored and had a chain effect on all transformations. If a molecule is not superimposable on to its mirror image, it is called a chiral molecule. In a point chiral molecule, one or more carbon centers are sp^3 hybridized and bonded to four different groups. Such a carbon center is called "asymmetric carbon". It is possible to have a chiral molecule without an asymmetric carbon as well. This type of chirality is called planar or axial chirality.[48] The most crucial part is that chirality can be seen at every scale like subatomic and supramolecular, macroscopic, and even galactic.[49] In nature, most of the amino acids, sugars, and so many synthetic molecules are chiral. In supramolecular chemistry, self-assembly of molecules which is defined as an autonomous organization of compounds into patterns, has an important role.[50] Supramolecular chirality arises as a result of biological molecular self-assembly. For instance, proteins can exhibit different conformations such as α-helices and β-sheets.[48] Supramolecular chirality can be induced through the non-covalent weak interactions, such as π-stacking, hydrogen bonding, electrostatic interaction, and host-guest interaction.[51]

1.1.2.2 Structure

The smallest example of an azo macrocyclic compound is benzo[c]cinnoline (Figure 7), and it can be considered as cyclic analogs of azobenzene. Like the other azo compounds, cinnolines are used in dye synthesis and some electrochromic polymers. Some larger cinnoline derivatives bonded with ethylene bridges are used for molecular switches due to their photochemical characteristics.[47-48]

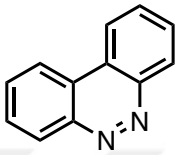

Figure 7. The structure of benzo[c]cinnoline

When the macrocycle consists of at least two or more azobenzene moiety, it is called oligobenzophane (Figure 8). In these macrocycles, azobenzene groups can be bonded in different positions by sp^3 hybridized spacers forming flexible, non-conjugated azobenzophanes or without sp^3 hybridized spacers conjugated more rigid azobenzophanes. The simplest example of a conjugated one is cyclotrisazobenzene. [43] The benefit of azobenzophanes is related to the difference in its photoisomerization from azobenzene. Unlike azobenzene, macrocyclic azobenzophanes offer multiple molecular states depending on their azo units. If an azobenzophane contains two azo units, than that azobenzophane can have three different states as *Z*,*Z* *E*,*E* and *E*,*Z* depending on the geometry and photoisomerization conditions.

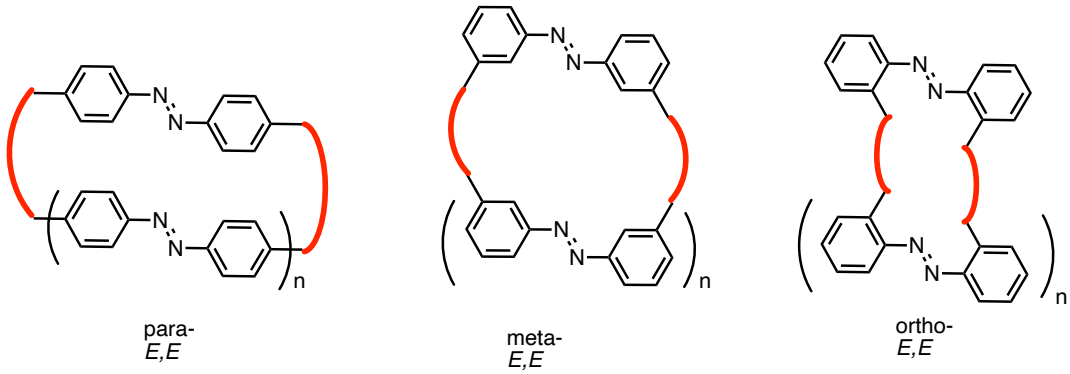

Figure 8. Azobenzophanes bonded in *para*-, *meta*-, *ortho*- positions[43]

1.1.2.2.1 Azobenzocrowns

Crown ethers have gained worldwide fame in the last 50 years due to their unique binding abilities to metal cations. So many different macrocyclic compounds have been synthesized and studied since the discovery of crown ethers. Azobenzene moiety attached to the crown ethers as a part of the skeleton have been synthesized (Figure 9), and the metal ion complexation of these cycles have been investigated.[52] For the synthesis of azo bearing crowns, Williamson reaction has been used from dihydroxyazobenzene and alkylating agents.[43]

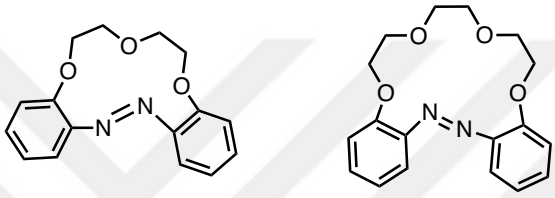

Figure 9. Examples of azobenzocrown ethers

Azo bearing crowns are popular candidates for light switches due to their photosensitive properties. The azo bridge of the cycle results in photoisomerization for light driven transport of potassium and sodium. Unique examples are ‘‘butterfly crown ethers’’ (Figure 10), which have been synthesized by Shinkai et al. [53] These photoswitchable cycles bind to metal cations depending on the geometry of the azo group. The increase of cavity size in the *cis* isomer results in binding cations whereas the *trans* isomer releases the same cation. With the effect of *trans-cis* isomerization on crown ethers, many different applications have been discovered.[43]

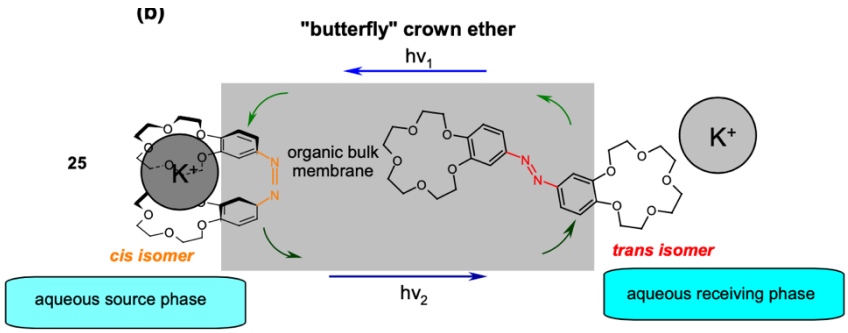

Figure 10. An example of a butterfly crown ether[43]

CHAPTER 2

AIM OF THE STUDY

Aromatic azo compounds are well-known for their unique photoisomerization reactions. Ever since their discovery, numerous types of azo compounds have been synthesized, and their photochemistry and photophysics have been extensively studied. Azo compounds undergo *trans* to *cis* isomerization upon irradiation with certain wavelengths of light. Therefore, introducing azo moiety into macrocycles possibly offers unique sensing ability as mentioned in the introduction part. A literature survey reveals that, azo functional macrocycles are less studied among azo derivatives, due to their challenging syntheses. With this in mind, the aim of this study was the synthesis of chiral and achiral macrocycles containing azo groups, and exploration of their photoisomerization and sensing properties. In this study, macrocycles **I**, **II**, **III**, and **IV** were synthesized as shown below, and photoisomerization and sensing studies were carried out.

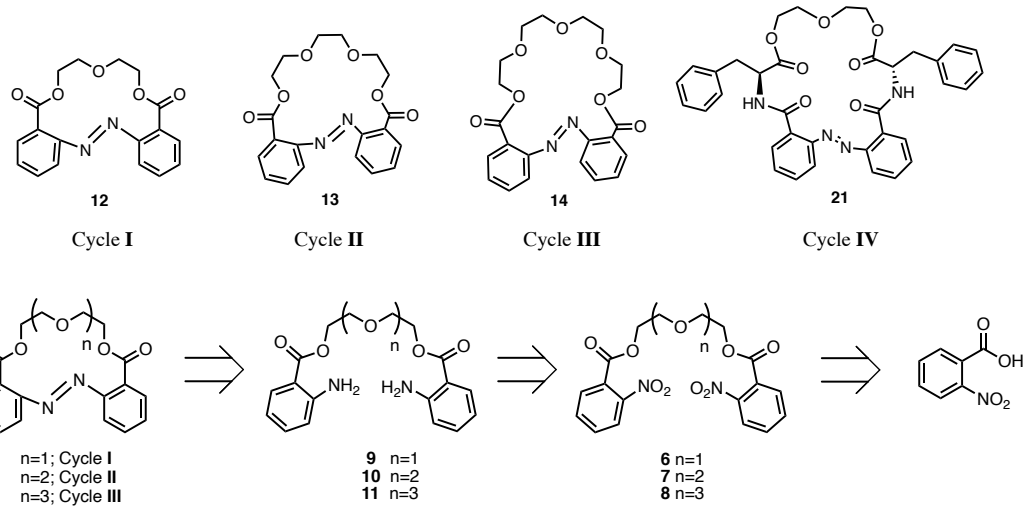

CHAPTER 3

RESULTS AND DISCUSSIONS

3.1 Synthesis

3.1.1 Synthesis of Azobenzene

Since the discovery of azobenzene, several different synthetic methods have been reported. In order to find the optimum conditions for the synthesis of diazo compounds, all well-known methods were surveyed. Five procedures among the reported ones were targeted in this thesis. Initially, azobenzene and its common derivatives were synthesized. These methods are discussed below.

Firstly, the coupling reaction of nitrobenzene in the presence of zinc powder and sodium hydroxide in ethanol was experimented as shown in Scheme 13. The corresponding azobenzene was synthesized in *ca.* 30% yield. The ^{1}H NMR spectrum (Figure 11) showed the formation of azobenzene which is different than ^{1}H spectrum of nitrobenzene. Furthermore, IR spectrum (Figure 12) shows formation of -N=N- bond which has a stretching frequency around 1599 cm^{-1}.

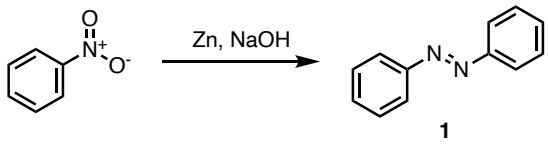

Scheme 12. Reductive coupling of nitrobenzene

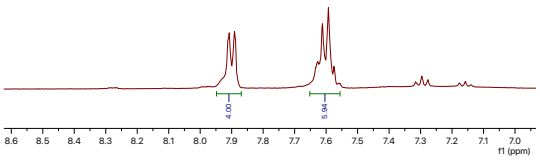

Figure 11. ^{1}H NMR Spectrum of Azobenzene

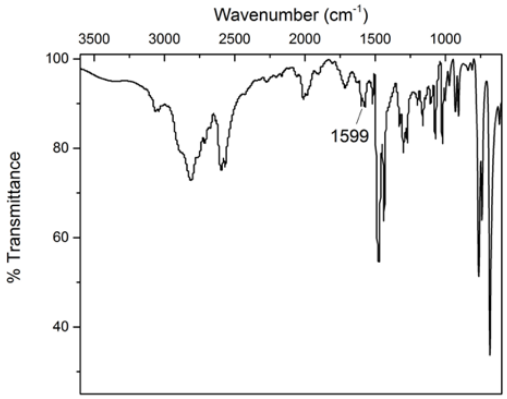

Figure 12. IR Spectrum of Azobenzene

Since the reductive coupling of nitrobenzene using elemental zinc gave poor yields, alternative methods were sought. As an alternative method, oxidative coupling was experimented with aniline using *N*-chlorosuccinimide (NCS) as the oxidant and 1,8-diazabicyclo[5.4.0]undec-7-ene (DBU) as base. Aniline was treated with DBU and cooled to -78°C. Then, NCS was added portion-wise to the medium and stirred -78°C for 20 minutes. Afterwards, the mixture was allowed to reach room temperature and saturated $NaHCO_3$ solution was then added to the mixture. Organic phase was separated and washed with HCl in order to remove DBU from the organic phase. The organic phase was then stripped of solvent *in vacuo* to give the crude azobenzene in 75% yield (Scheme 13).

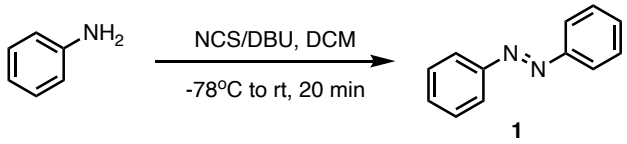

Scheme 13. NCS/DBU coupling of Azobenzene

The mechanism of this reaction proceeds through DBU mediated chlorine transfer from NCS to aniline to give *N*-chloroaniline. Nucleophilic attack by a free aniline then forms *N,N'*-diphenylhydrazine.[54]

Another DBU mediated chlorine transfer from NCS to the hydrazine followed by β–elimination yields azobenzene, as depicted in Scheme 14.

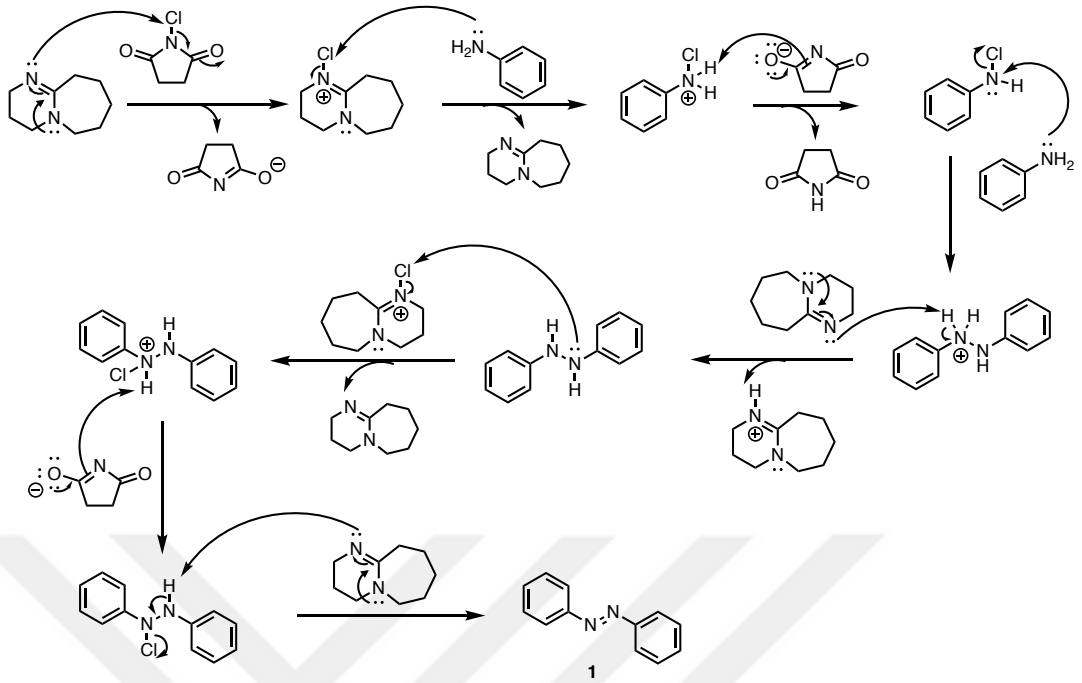

Scheme 14. Mechanism of NCS/DBU method

3.1.2 Synthesis of 4,4'-dihydroxyazobenzene, 4,4'-diallyoxyazobenzene, 4,4'-diacetoxyazobenzene and 4,4'-diacetamidoazobenzene

A classical synthesis of azobenzene was also employed in our surveys. Although this method requires electron rich aromatic compounds, we tried this method for comparison. In this synthesis 4,4′-dihydroxyazobenzene (**2**) was targeted due to the fact that hydroxy groups could be our starting point for macrocyclization. *p*-aminophenol was subjected to diazotization with sodium nitrite under acidic conditions (Scheme 15). The diazo compound was subsequently treated with phenol to get compound **2**. In the ^{1}H NMR spectrum, as shown in Figure 11, compound **2** showed two doublets. The acidic protons resonated at 10.1 ppm. This is in agreement with reported literature spectrum.[55]

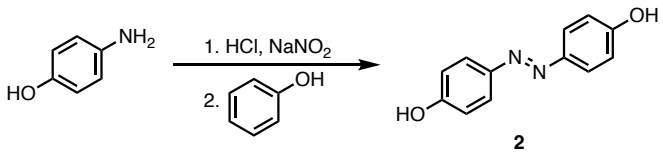

Scheme 15. Diazotization of *p*-aminophenol

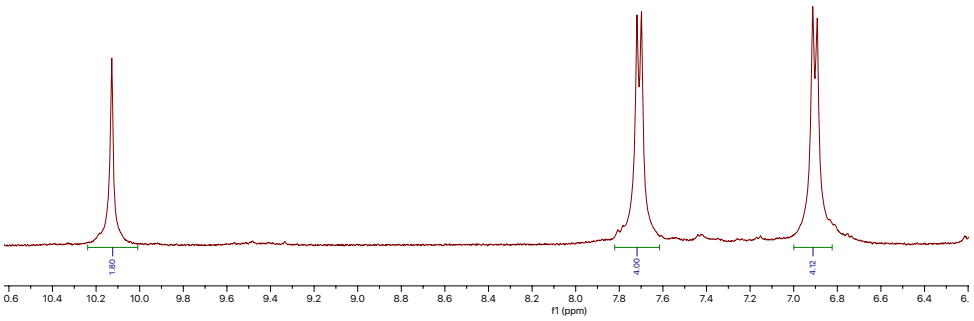

Figure 13. ^{1}H NMR Spectrum of 4,4′-dihydroxyazobenzene

With 4,4′-dihydroxyazobenzene in hand, we focused on derivatization of this compound with allyl bromide. Compound **2** was treated with K_2CO_3 then with allyl bromide in acetone. 4,4′-diallyoxyazobenzene was obtained in 43% yield (Scheme 16). The compound was further purified with recrystallization from methanol.

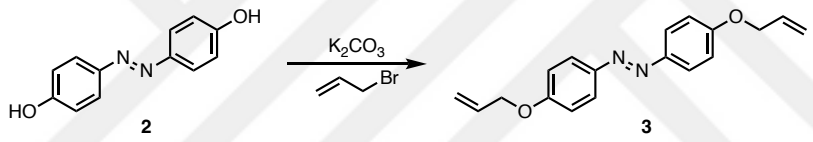

Scheme 16. Synthesis of 4,4′-diallyoxyazobenzene

The 4,4′-diallyoxyazobenzene was characterized with ^{1}H NMR spectrum and the assigned protons are given in Figure 14. The vinylic protons of the compound **3,** showed a doublet of doublet of triplet at 6.1 ppm for two protons and two doublets of doublet at 5.4 and 5.3 ppm for four protons. The allylic protons showed doublet of triplet at 4.6 ppm for four protons.

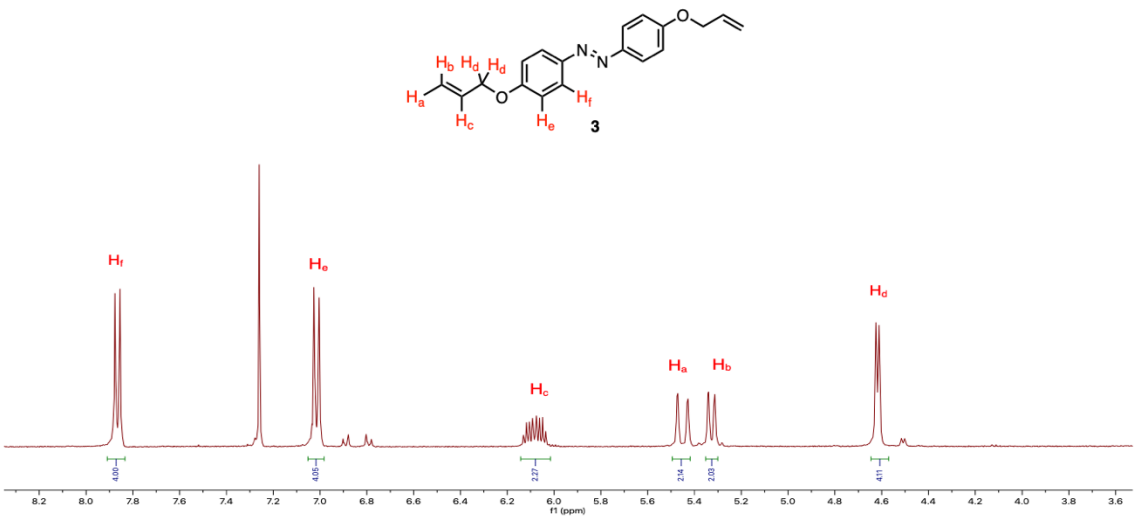

Figure 14. ^{1}H NMR spectrum of 4,4′-diallyoxyazobenzene

Epoxidation of compound **3** with *m*-CPBA, yielded a complex mixture (Scheme 17). The complication of this reaction might be due to the presence of azo moiety which is also prone to oxidation.

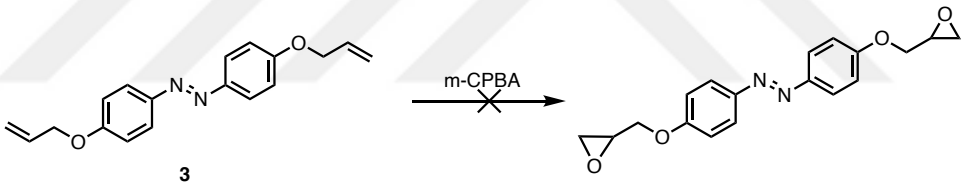

Scheme 17. Epoxidation of 4,4′-diallyoxyazobenzene

With the failed experiment from the epoxidation we turned our attention to *p*-acetoxyaniline coupling. *p*-Acetoxyaniline was synthesized by modifying the literature procedure.[56] Then, the aniline was coupled with NCS/DBU method (*vide infra*) to get 4,4'-diacetoxyazobenzene in 36% yield (Scheme 18). ^{1}H NMR spectrum of corresponding azo compound given in Appendix A with some impurities unidentified.

p-acetoxyaniline

4

Scheme 18. Synthesis of compound **4**

With this result in mind, tartaric acid was thought to replace acetyl group. The lengthy and tedious procedures discouraged us to further advance in this route. Instead, we decided to go forward with *p*-phenylenediamine. *p*-Nitroaniline was acetylated with acetic anhydride, then the nitro group was reduced with H_2 and Pd/C as catalyst. The resulting 4-acetamido aniline was subjected to coupling in the presence of CuBr in pyridine with bubbling O_2 to yield compound **5** in 25% yield. Copper-catalyzed oxidative coupling reaction with O_2 with certain aniline derivatives were reported by Jiao et. al.[22] In this reaction, copper(I) is ligated by pyridine and the complex is oxidized to copper (II) by dioxygen. (Scheme 19)

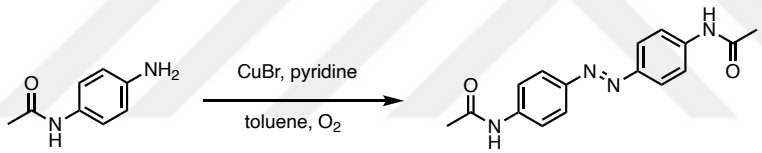

5

Scheme 19. Synthesis of compound **5**

Compound **5** in hand, we turned our attention to a possible macrocycle with tartaric acid as linker. The macrocycle *B* given in Scheme 20, was designed. The synthesis started with *p*-nitroaniline coupled with tartaric acid in boiling *o*-xylenes. The compound *A* was synthesized in 23% yield. The nitro group was subjected to reduction using acidic conditions (Fe, HCl), and neutral conditions (Pd/C, H_2) in methanol. Despite all the efforts, the reduced compound was not observed.

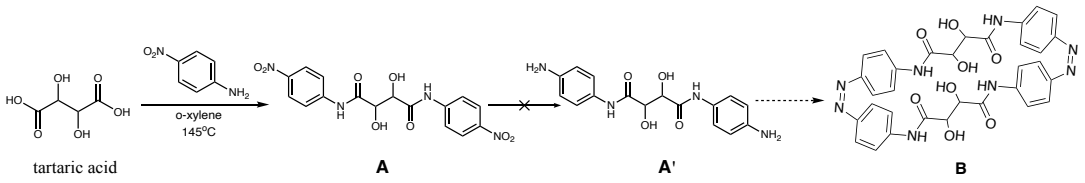

Scheme 20. Synthetic route for possible macrocycle with tartaric acid

3.1.3 Retrosynthetic Analysis of Achiral Azo Macrocycles

With the failure of our first attempt on azo containing chiral macrocycle, we turned our attention to the synthesis of achiral macrocycles. Accumulated synthetic knowledge about the azo bridge also oriented us to the new macrocycles. Linker synthesis was the starting point for the new macrocycles as seen in the retrosynthetic analysis. (Scheme 21)

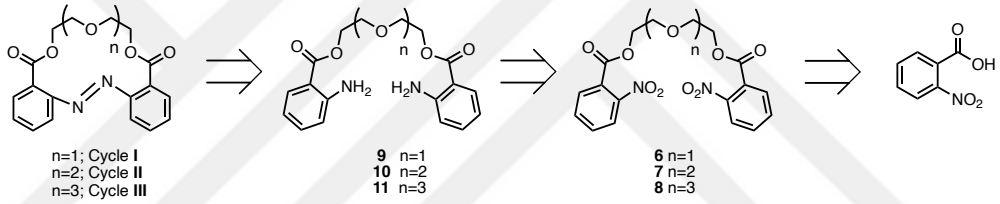

Scheme 21. Retrosynthetic analysis of achiral macrocycles

3.1.4 Synthesis of Achiral Azo Macrocycles

With the experience about azo coupling reactions, we thought that closing macrocycles will proceed through the appropriate azo coupling method to give desired compounds. Cycle **I**, **II**, **III** were designed up to this strategy. (Scheme 22)

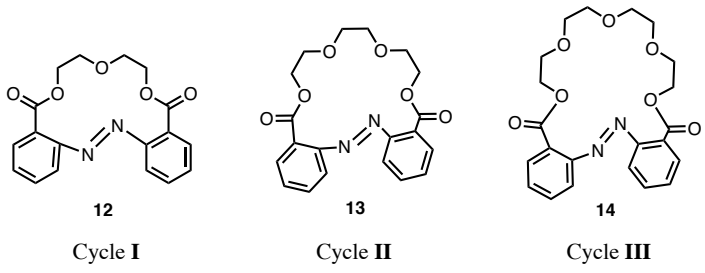

Scheme 22. Design of Cycle **I**, **II**, and **III**

Diethylene glycol, triethylene glycol, and tetraethylene glycol were used respectively for the synthesis of the macrocycles. These three macrocycles were envisioned to be synthesized in the same manner. Commercial *o*-nitrobenzoic acid was converted to *o*-nitrobenzoyl chloride with refluxing in thionyl chloride. Addition of thionyl chloride to *o*-nitrobenzoic acid is exothermic, thus the reaction medium was kept at 0°C during the addition. After two hours of refluxing, the excess thionyl chloride was evaporated and the remaining chloride in the flask was used as it is. The chloride was treated with ethylene glycols (diethylene glycol, triethylene glycol, and tetraethylene glycol) to give the desired *o*-nitrobenzoate linked through the glycols. The esters were obtained more than 90% yield. *o*-Nitrobenzoates were, then, attempted for reduction to *o*-aminobenzoates in methanol and Pd/C with a H_2 balloon on the top. However, yields for the reduction are not enough to continue the synthesis. High pressure reactor vessel was preferred to obtain higher yields in this step. (Scheme 23)

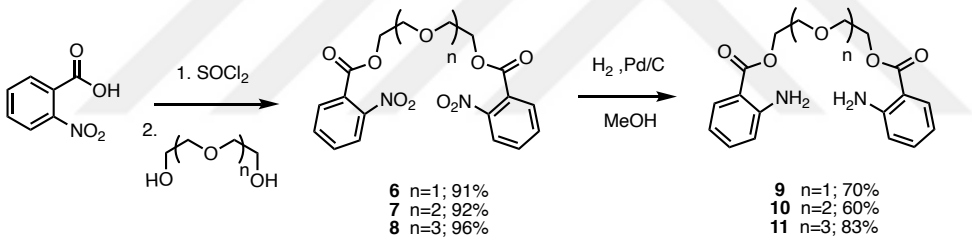

Scheme 23. Synthetic pathway of *o*-aminobenzoates linked through glycols

With this results in hand, an intramolecular cyclization via diazo formation were not successful with the above-mentioned methods. Therefore, a new method was necessary. An extensive literature survey revealed that diazo compounds could also be synthesized with lead (IV) acetate. For organic chemists, lead (IV) acetate is a well-known versatile oxidant and used also for azo cyclization reactions.[24] Oxidative coupling reaction was performed with lead (IV) acetate and *o*-aminobenzoates. As it is elaborated below, the reaction proceeded to the desired compounds with lead (IV) acetate. Ethylene glycol aminobenzoates were dissolved in CH_2Cl_2 with excess Et_3N under argon atmosphere. The solvents and all other reagents are carefully dried. These conditions were found to be vital for reaction to proceed smoothly.

Afterwards, lead (IV) acetate was added to the mixture. For the work-up the volatiles were removed under vacuum and the residue was loaded to alumina column in order to separate the macrocycles. These macrocycles could not be separated on silica column. During the purification, the main problem was to separate the cycle from the starting material. As it can be seen, an acidic work-up could easily remove the starting material from the macrocycle. However, macrocycle decomposed under these conditions. Corresponding macrocycles were synthesized less than 8% yield (Scheme 24).

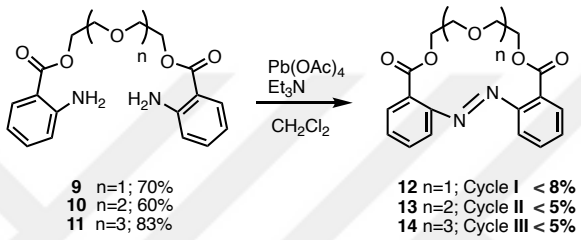

Scheme 24. Oxidative macrocyclization of *o*-aminobenzoates

The following mechanism was proposed for oxidative cyclization with lead(IV) acetate is shown in Scheme 25. The mechanism starts with aniline attack to lead(IV) acetate which decomposes to aniline radical. Two aniline radicals combined to form hydrazine. The hydrazine coordinates to lead(IV) acetate again and the elimination with lead(II) acetate leads to the formation of azo compounds.[24]

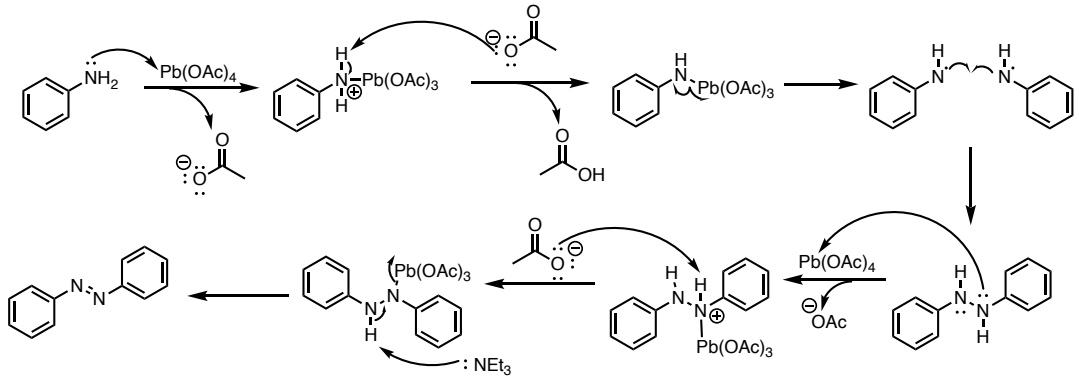

Scheme 25. Proposed mechanism of oxidative coupling with lead(IV)acetate

Cycle **I** was characterized with ^{1}H NMR spectrum and the assigned protons are given in Figure 16-a. The aromatic protons of the compound **12,** showed a doublet of doublet at 7.7 ppm for two protons and multiplet at 7.5 ppm for six protons. The diethylene glycol protons showed two multiplets at 4.4 ppm and 3.8 ppm for eight protons. Furthermore, IR spectrum (Figure 16-b) shows formation of -N=N- bond which has a stretching frequency around 1590 cm^{-1}. ^{13}C NMR showed nine carbons which are present in the compound. (Figure 16-c) Further characterization with HRMS shows the formation of compound **12** in Appendix D without any doubt.

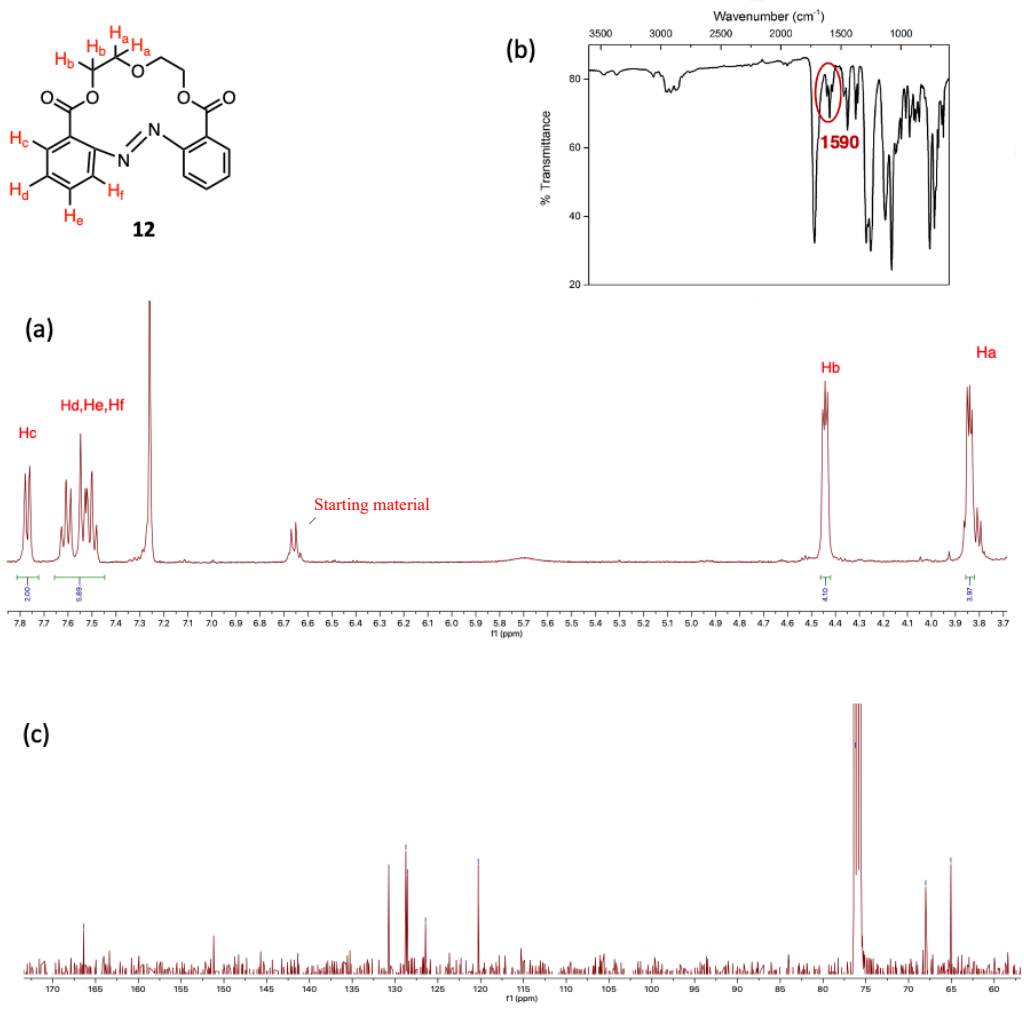

Figure 15. Characterization of Cycle **I**

Cycle **II** was characterized with ^{1}H NMR spectrum and the assigned protons are given in Figure 17-a. The aromatic protons of the compound **13,** showed a doublet of doublet at 7.9 ppm for two protons and multiplet at 7.6 ppm for six protons. The triethylene glycol protons showed two multiplets at 4.5 ppm and 3.8 ppm for eight protons and one singlet at 3.6 ppm for four protons. ^{13}C NMR showed ten carbons which are present in the compound (Figure 17-c). IR spectrum of the compound **13** showed azo peak at 1591 cm^{-1} (Figure 17-b). Further characterization with HRMS shows the formation of compound **13** in Appendix D.

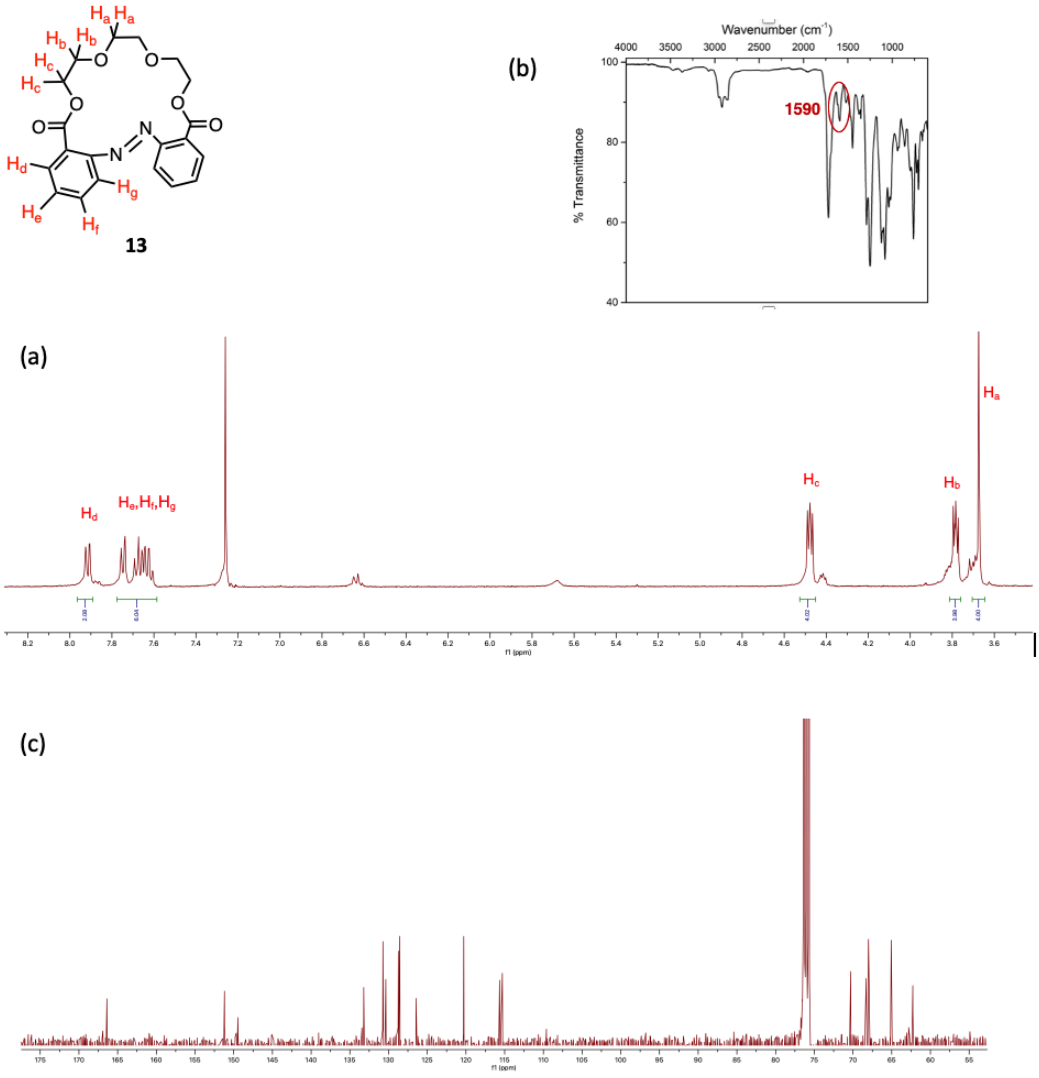

Figure 16. Characterization of Cycle **II**

Cycle **III** was characterized with ^{1}H NMR spectrum and the assigned protons are given in Figure 18. The aromatic protons of the compound **14,** showed a doublet of doublet at 7.8 ppm for two protons and multiplet at 7.5 ppm for six protons. The tetraethylene glycol protons showed four multiplets at 4.4 ppm, 3.7 ppm, 3.4 ppm, and 3.3 ppm for sixteen protons. ^{13}C NMR showed eleven carbons which are present in the compound (Figure 18-c). IR spectrum of the compound **14** showed azo peak at 1594 cm^{-1} (Figure 18-b).

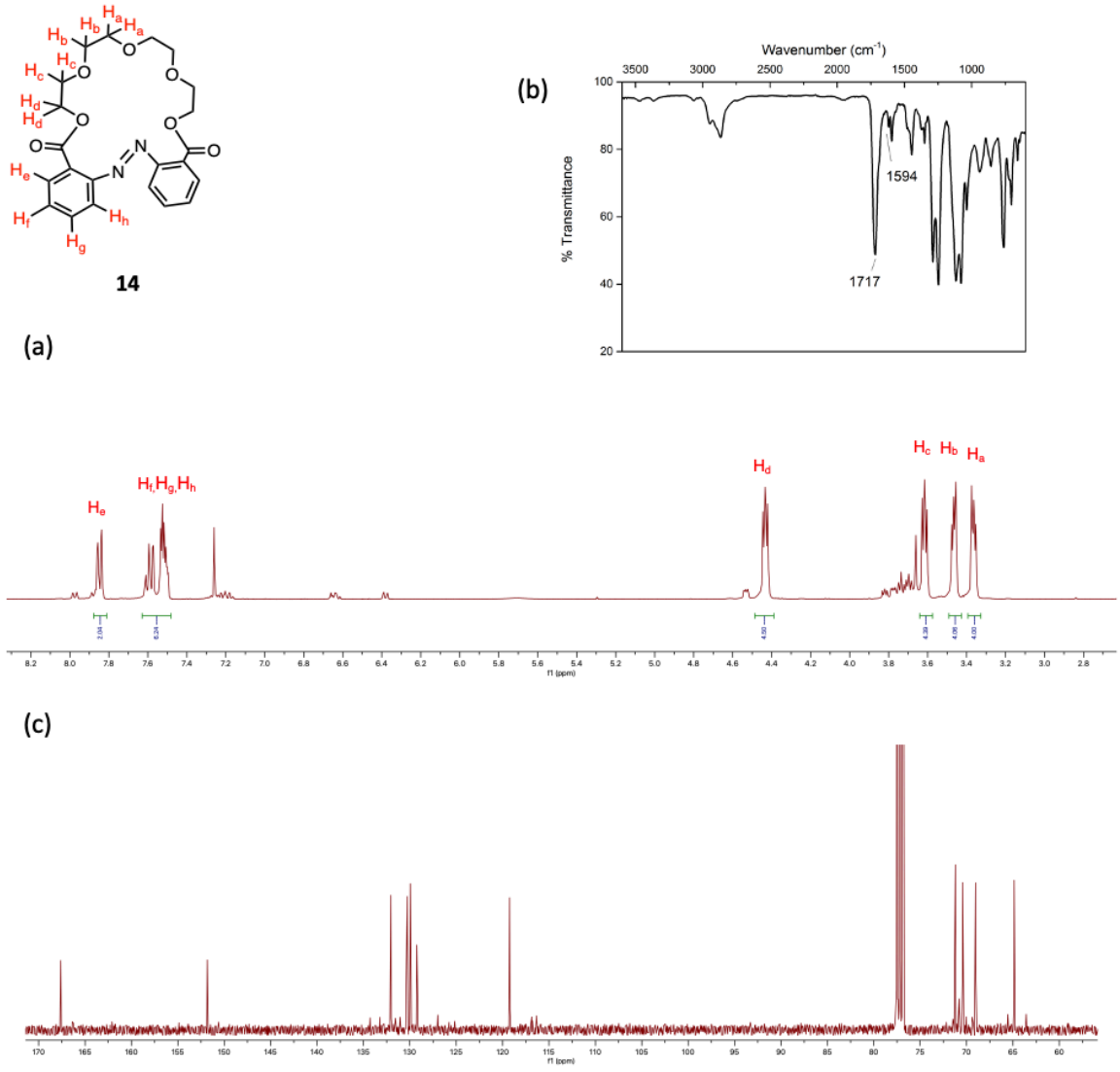

Figure 17. Characterization of Cycle **III**

3.1.5 Synthesis of Reference Compound 17

Before moving on the photochemical and photophysical experiments of Cycle **I, II,** and **III**, our aim is to synthesize an acyclic azo compound with similar electronic properties. The photochemistry of this acyclic compound will be a reference for the photoisomerization of azo cycles. Therefore, dimethyl 2,2'-(diazene-1,2-diyl)(E)-dibenzoate, compound **17**, and the synthetic pathway to which, was designed (Scheme 26).

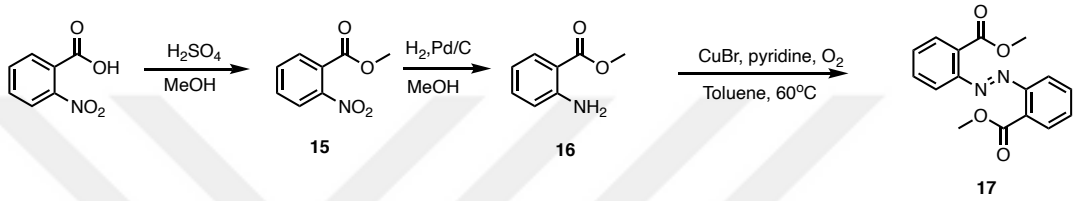

Scheme 26. Synthesis of Compound **17**

This pathway starts with the Fisher esterification of *o*-nitrobenzoic acid in the presence of H_2SO_4 and CH_3OH. The yield of methyl *o*-nitrobenzoate, compound **15**, was 70%. Reduction of the methyl *o*-nitrobenzoate, compound **16**, was obtained in high pressure reactor vessel in methanol and Pd/C with the yield of 83%. After the synthesis of methyl *o*-aminobenzoate, three different azo coupling methods were attempted. First synthetic method was the NCS/DBU, which did not lead to the desired azo compound. Then, lead(IV) acetate was used as the alternative method but unsuccessful results oriented us to the CuBr/pyridine method. With this way, the acyclic reference compound **17**, was synthesized in 5% yield which was enough for us to perform photoisomerization experiments.

Compound **17**, was characterized with ^{1}H NMR spectrum and the assigned protons are given in Figure 19-a. The aromatic protons of the compound **17,** showed two doublet of doublet at 7.8 ppm, 7.6 ppm for six protons and multiplet at 7.5 ppm for two protons. The methyl protons showed singlet at 3.9 ppm for six protons.

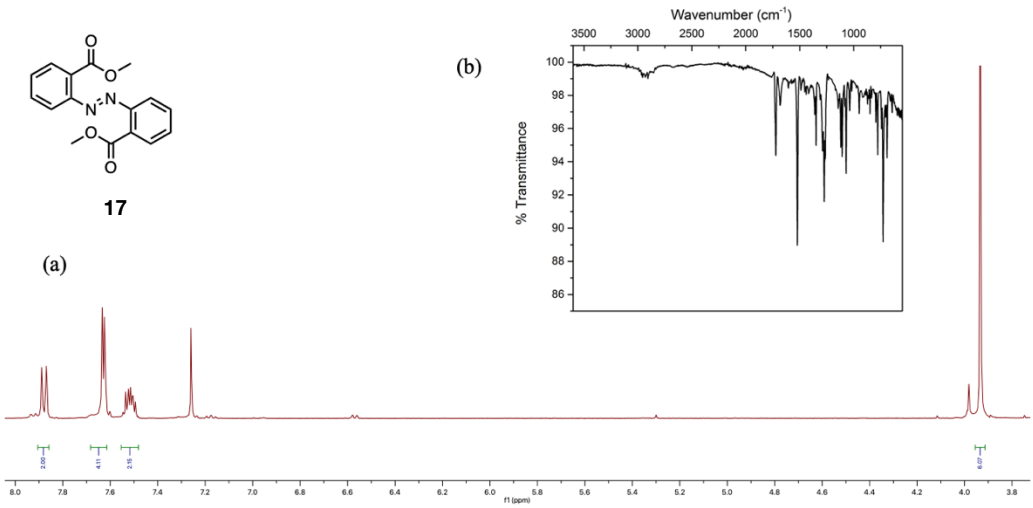

Figure 18. Characterization of compound **17**

3.1.6 Retrosynthetic Analysis of Chiral Azo Macrocycle

With the achiral cycles **I**, **II**, and **III** synthesized, we turned our attention to a chiral macrocycle with a similar backbone. Recently, addition of chiral groups to macrocycles became popular for organic chemists.[57]

For the synthesis of chiral macrocycle, *L*-phenylalanine was selected as chiral compound in the macrocycle because *L*-phenylalanine is a bifunctional chiral compound. The retrosynthetic analysis showed that integration of *L*-phenylalanine into macrocycle could be done through an amide linkage (Scheme 27).

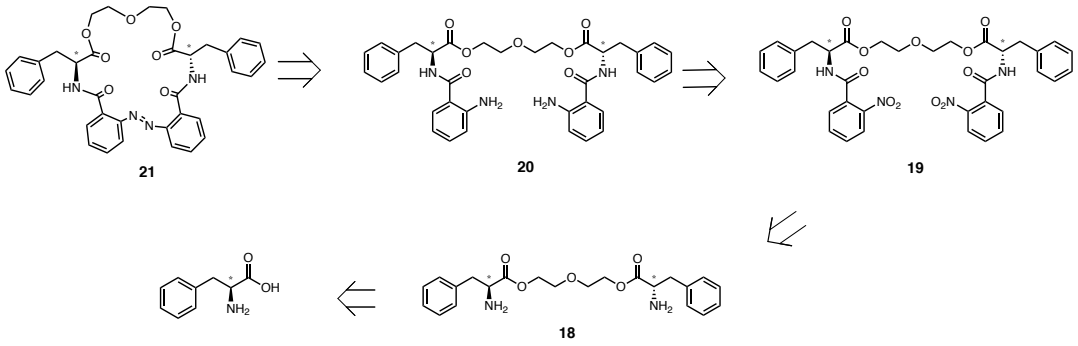

Scheme 27. Retrosynthetic Analysis of Cycle **IV**

3.1.7 Synthesis of Cycle IV

Synthesis starts with esterification of *L*-phenylalanine with diethylene glycol in the presence of *p*-TSA. Compound **18** successfully synthesized in 65% yield and coupled with *o*-nitrobenzoic acid with EDC coupling. The reaction yielded compound **19** in 42% yield. The other coupling method with carbonyldiimidazole (CDI) to increase the yield failed. Reduction of the nitro groups to amine, compound **20,** proceeds with hydrogen in the presence of Pd/C under 30 bar. Finally, compound **21** was synthesized by oxidative azo coupling reaction with lead(IV)acetate less than 9% yield (Scheme 28).

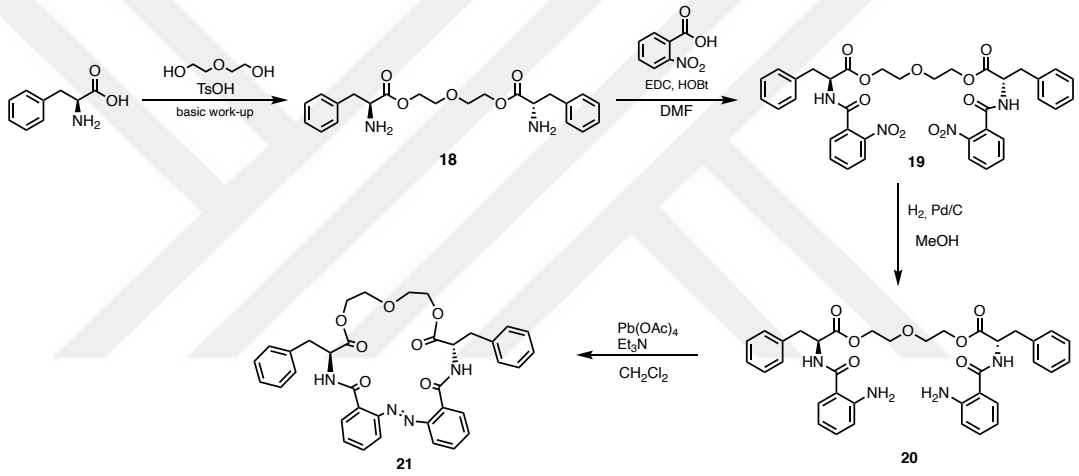

Scheme 28. Synthetic pathway of Cycle **IV**

Compound **20** had peaks at 6.6 ppm in the ^{1}H NMR spectrum and these peaks disappeared after the coupling reaction with lead(IV) acetate in the ^{1}H NMR spectrum of compound **21** (Figure 20 and 21-a).This shows that electron donating groups (-NH_2) on the aromatic ring converted into electron withdrawing group (-N=N-). Furthermore, IR spectrum of **21** shows a peak at 1592 cm^{-1} which is characteristic azo unit (Figure 21-c).^{13}C and HRMS spectra further confirmed the formation of the macrocycle.

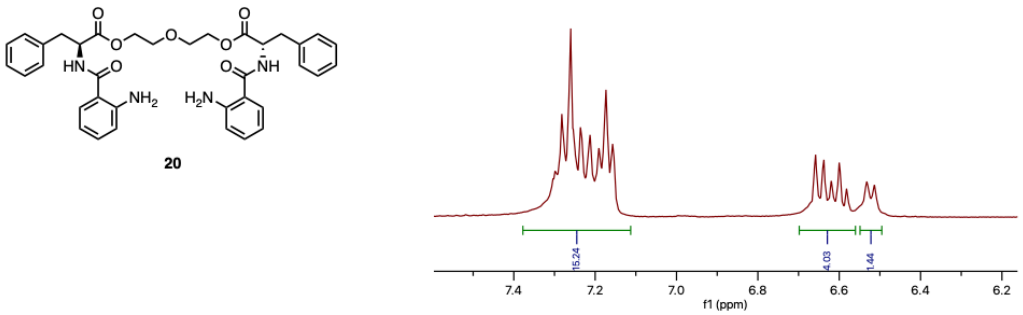

Figure 19. Aromatic region of compound **20** in ^{1}H NMR spectrum

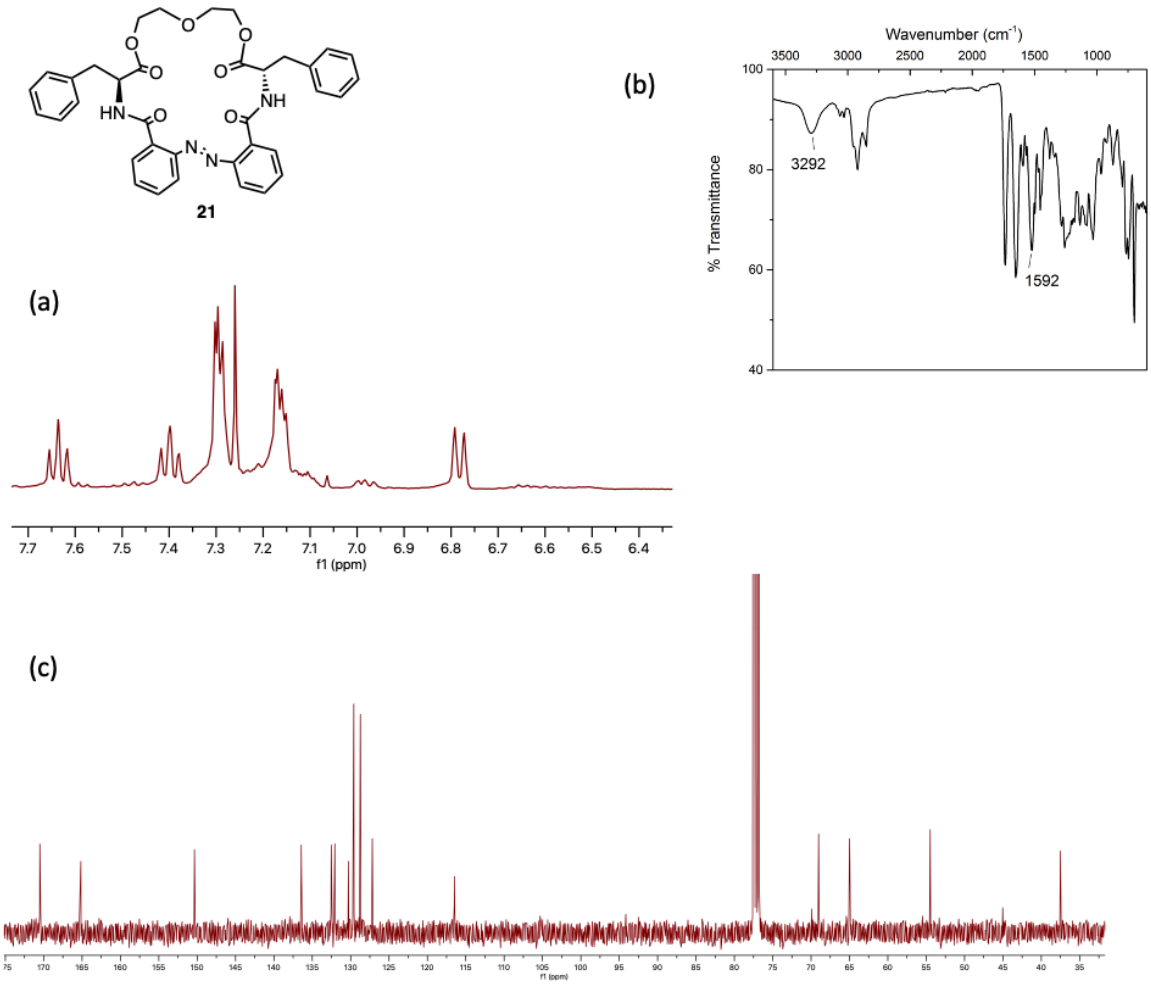

Figure 20. Characterization of Cycle **IV**

3.2 Photophysical and Photochemical Studies

Azobenzenes and their derivatives are well-known for their photoisomerization reactions. Their spectral properties are strongly dependent on the geometry of the azo bridge. Before moving on to the photoisomerization experiments with the macrocycles, *trans-cis* conversion of azobenzene was studied. Initially, UV-Vis absorption spectrum of azobenzene was measured and a λ_{max} was observed at 320 nm. This UV absorption band extended to 365 nm. With this in mind, a light source illuminating below 365 nm would be enough to convert *trans* isomer to *cis* isomer. A light source with 365 nm was used to illuminate azobenzene for 10, 25, and 55 minutes. In Figure 22, the decrease in 320 nm shows *trans*-azobenzene conversion to *cis*-azobenzene. This experiment revealed that we could successfully convert *trans*-azobenzene to *cis*-azobenzene.

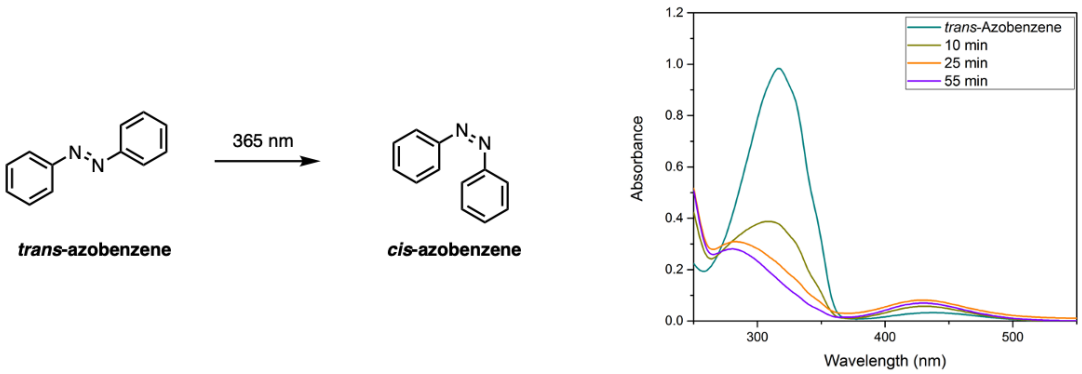

Figure 21. *Trans-cis* isomerization of azobenzene in acetonitrile

With successful photochemical conversion on azobenzene, we turned our attention to the reference compound **17**. Firstly, UV-Vis absorption spectrum of compound **17** was taken. A λ_{max} at 310 nm was observed with that absorption band extending to 365 nm. Therefore, photochemical conversion of this compound could be done with a wavelength shorter than 365 nm. Irradiating compound **17** with 365 nm light for 10, 25, and 55 min showed that the conversion from *trans* to *cis* is not as efficient as azobenzene (Figure 23). This low conversion might be due to the steric effects of compound **17** in the *cis* form.

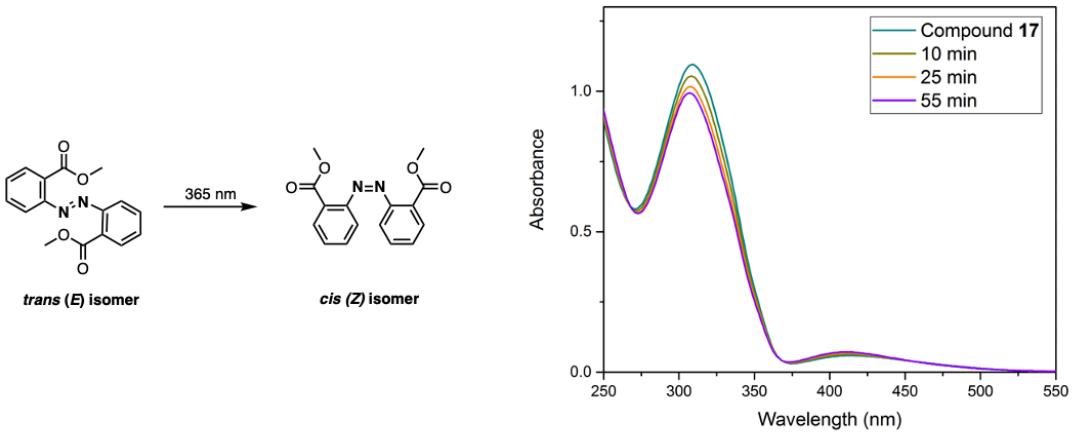

Figure 22. *Trans-cis* isomerization of compound **17** in acetonitrile

Irradiating compound **17** with 365 nm light for 90 min converted 19% to *cis* isomer. After storing the irradiated compound in the dark for two days, the compound turned back to the *trans* isomer. This conversion was followed by UV-Vis spectrometer, as shown in Figure 24.

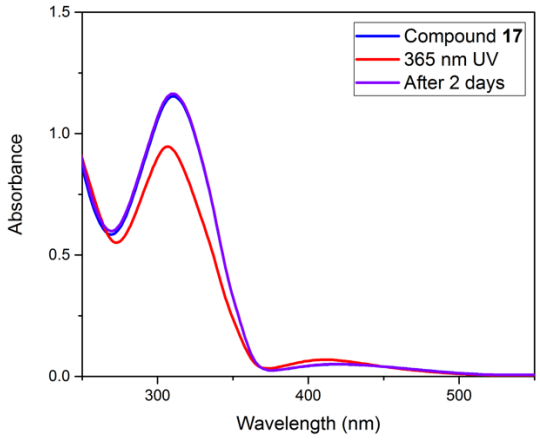

Figure 23. Back isomerization of compound **17**

After the photoisomerization experiments with reference azo compounds, we moved on to the macrocycles (Figure 25). Initially, UV-Vis absorption spectrum of Cycle **I** was taken and a λ_{max} at 310 nm observed. Irradiating Cycle **I** with 365 nm light source for 10, 25, and 55 minutes showed a conversion from *trans* to *cis* isomer, (Figure 26).

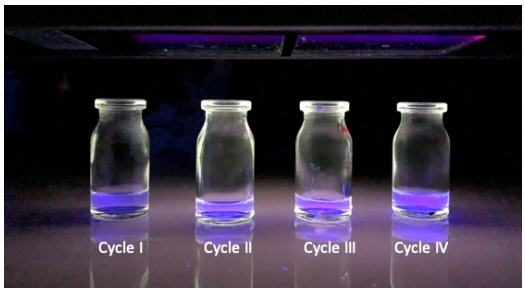

Figure 24. Irradiation of Cycle **I**, **II**, **III**, and **IV**

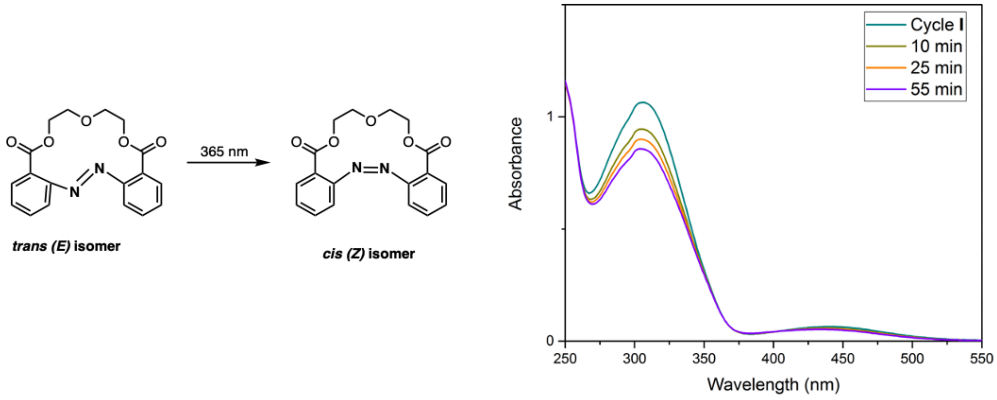

Figure 25. *Trans-cis* isomerization of Cycle **I** in acetonitrile

Cycle **I** was converted to *cis* isomer 20% after irradiating with 365 nm light for 90 min. This compound was kept five days in the dark; however, the back isomerization to *trans* isomer was not complete. This is due to rigidity of the cycle. This conversion was followed by UV-Vis spectrometer, as shown in Figure 27.

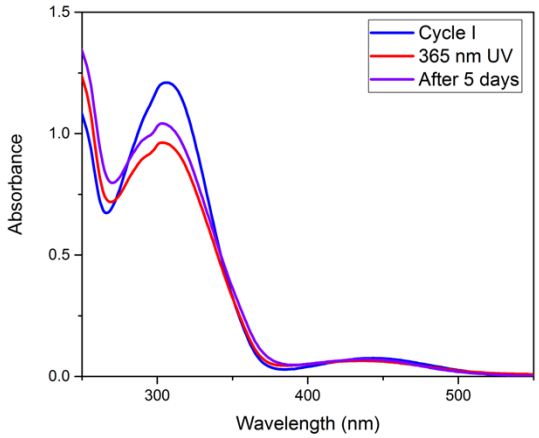

Figure 26. Back isomerization of Cycle **I**

UV-Vis absorption spectrum of Cycle **II** was taken and a λ_{max} at 310 nm also observed. Similarly, irradiating Cycle **II** with 365 nm light source for 10, 25, and 55 minutes showed 10% conversion from *trans* to *cis* isomer (Figure 28).

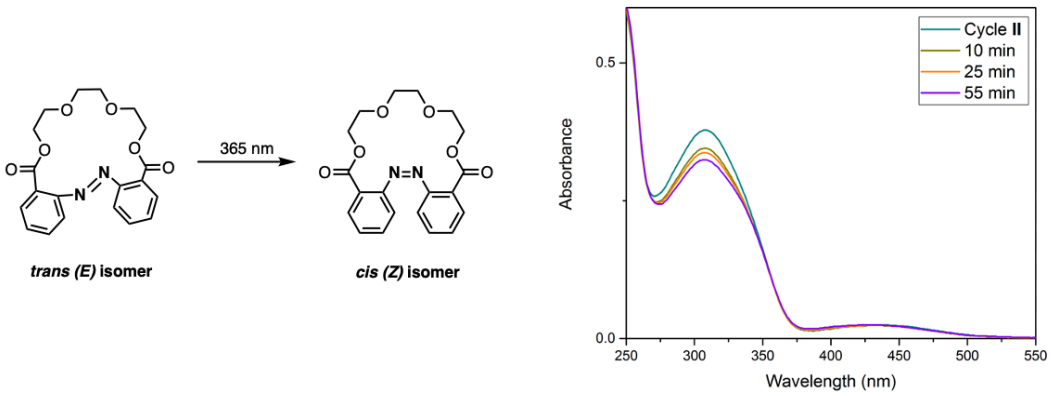

Figure 27. *trans* to *cis* isomerization of Cycle **II** in acetonitrile

Cycle **II** was also subjected to light with wavelength of 365 nm for 90 minutes. The *cis* isomer turned back to *trans* isomer. The concentration of the Cycle **II** increased due to solvent evaporation. Nevertheless, all *cis* is converted to *trans* in 5 days (Figure 29).

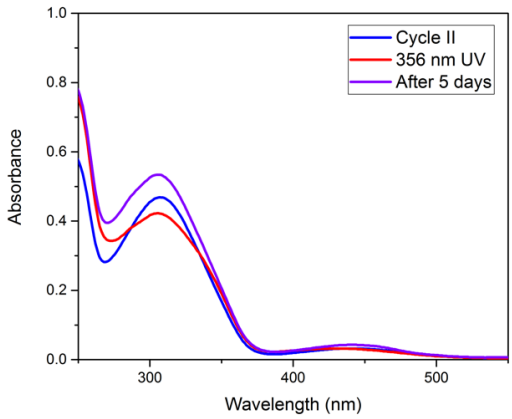

Figure 28. Back isomerization of Cycle **II**

In the UV-Vis absorption spectrum of Cycle **III** a λ_{max} at 310 nm also observed. Irradiating Cycle **III** with 365 nm light source for 10, 25, and 55 minutes showed

24% conversion from *trans* to *cis* isomer (Figure 30). Similarly, this compound was kept 5 days in the dark and the back isomerization to *trans* isomer observed (Figure 31).

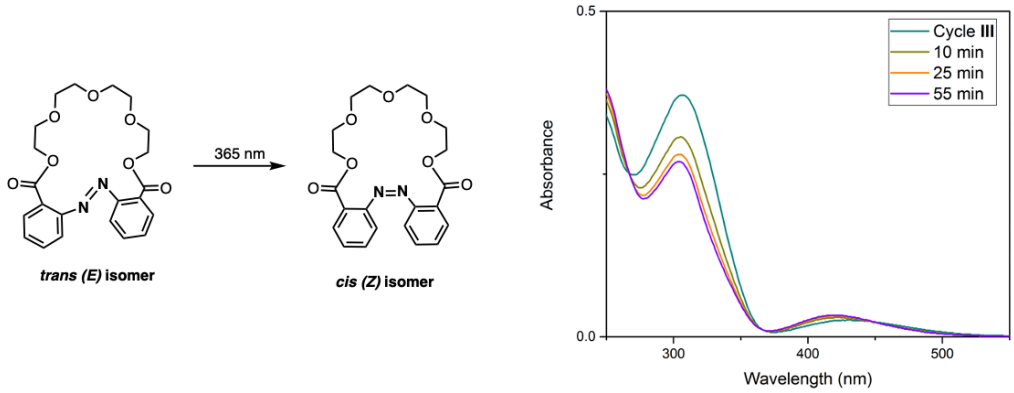

Figure 29. *Trans-cis* isomerization of Cycle **III** in acetonitrile

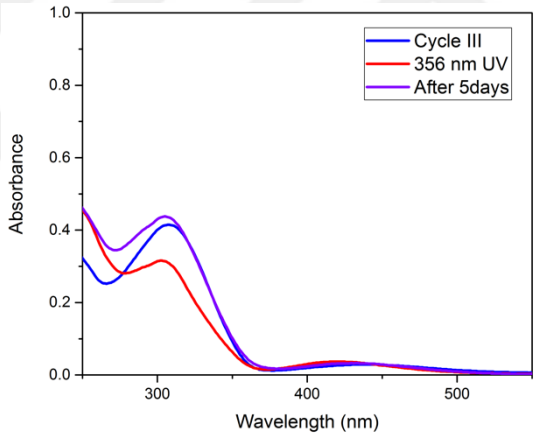

Figure 30. Back isomerization of Cycle **III**

Lastly, UV-Vis absorption spectrum of Cycle **IV** was taken. A λ_{max} at 320 nm was observed with that absorption band extending to 395 nm. Therefore, photochemical conversion of this compound could be done with a wavelength shorter than 395 nm. Irradiating Cycle **IV** with 365 nm light for 10, 25, and 55 min showed that the conversion from *trans* to *cis* is similar to azobenzene due to the larger ring size which in turn brings flexibility (Figure 32).

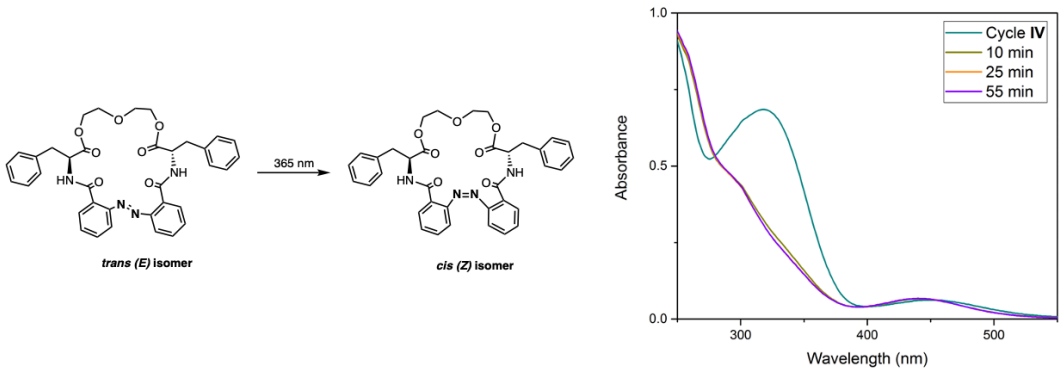

Figure 31. *trans-cis* isomerization of Cycle **IV** in acetonitrile

Cycle **IV** was converted completely to *cis* isomer after irradiating with 365 nm light for 90 min. This compound was kept 5 days in the dark and the back isomerization to *trans* isomer observed (Figure 33).

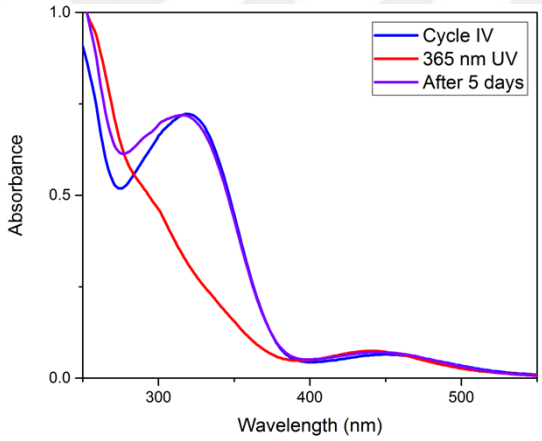

Figure 32. Back isomerization of Cycle **IV**

UV-Vis spectra of azobenzene and Cycle **IV** showed λ_{max} at 320 nm, while compound **17**, Cycle **I**, Cycle **II**, and Cycle **III** showed λ_{max} at 310 nm. This 10 nm blue shift in the first three cycles and reference compound is due to deviation from planarity. This could be seen in the geometry optimization of these compounds *(vide supra)*. The full isomerization from *trans* to *cis* is not observed for Cycle **I**, **II**, **III**, and reference compound due to the steric effects. On the contrary, Cycle **IV** is wholly converted to the *cis* form due to a larger ring. However, one might argue that the steric effects are present in Cycle **IV** as well. This led us to think that amide less

electron-withdrawing than esters. Therefore, electronic effects are also governing the *cis-trans* isomerization. Cycle **IV** showed a CD activity at 460 nm, which corresponds to n- π* transition (Figure 34).

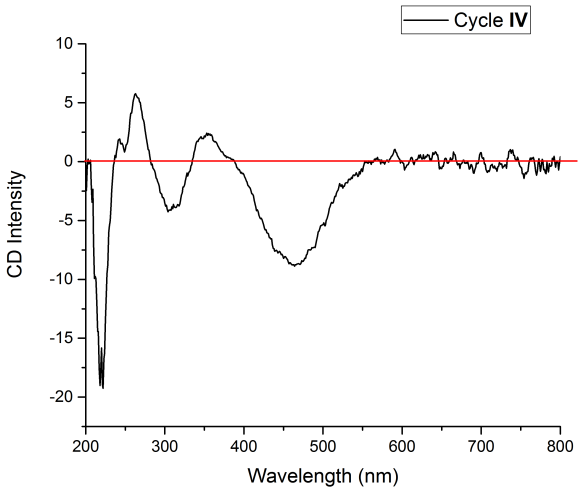

Figure 33. CD spectrum of Cycle **IV** in acetonitrile

3.2.1 Fluorescence Studies

Azobenzene does not have noteworthy fluorescence.[58] This is due to the rapid isomerization in the excited state. The cycles in this study showed fluorescence with the Stokes shift of 65 nm. Observing a fluorescence for these compounds shows that these compounds are rigid, explaining the low conversion from *trans* to *cis* upon irradiation. The fluorescence spectra are given in Appendix D.

3.2.2 Responses of Macrocycles to Alkali Metals

Cycle **I**, Cycle **II**, and Cycle **III** were dissolved in acetonitrile and equal molar of $LiClO_4$, $NaClO_4$, and $KClO_4$. Corresponding UV-Vis spectra of each solution were recorded. For Cycle **I**, Li^+ and Na^+ give a rise in the 310 nm absorption band while K^+ did not affect the UV-Vis spectrum. For Cycle **II**, only Na^+ increased the 310 nm absorption band while the other salts did not affect the UV-Vis absorption spectrum. As to Cycle **III**, Li^+ and Na^+ increased the absorption as K^+ did not change the

absorption. However, for this cycle the differentiation is less pronounced than for other cycles. Even though these cycles showed selectivity toward different cations, the differentiation is not large enough to be used in the practical world. The results are summarized in the following table.

Table 1. UV-Vis absorption spectra of Cycle **I**, **II**, and **III** with alkali metals

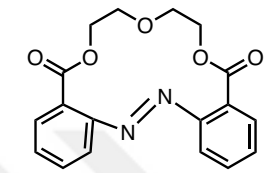

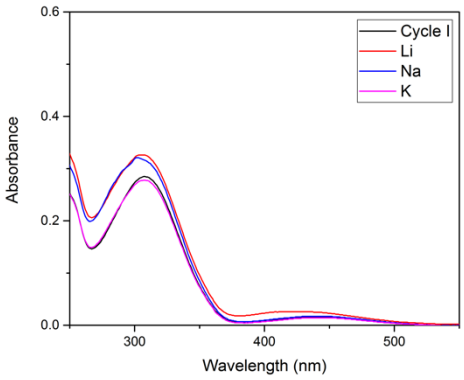

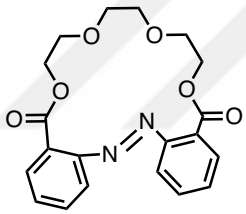

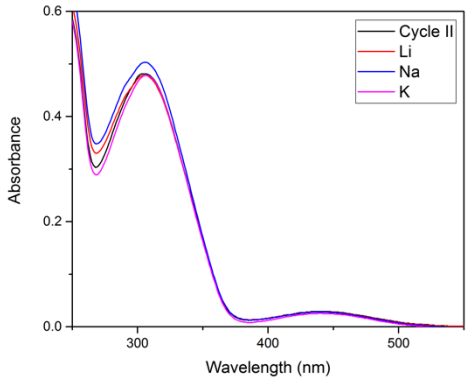

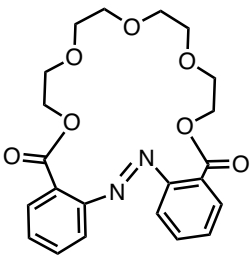

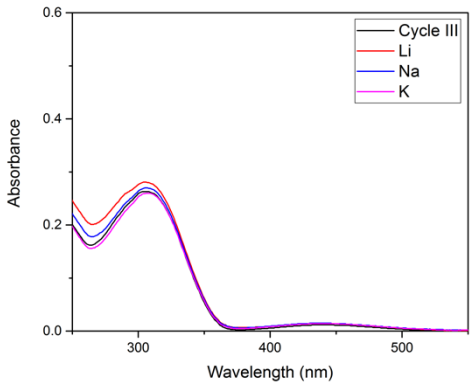

3.3 Computational Studies

Geometry optimizations were completed at the level of B3LYP/6-31G(d) as implemented in Gaussian 09.[59] The calculations were calculated for *cis* and *trans* isomers of azo compounds separately. A conformational analysis was not considered in these calculations due to the large conformational space. The calculations for each compound are discussed below.

Compound 17

The DFT calculations for compound **17** are summarized in Table 2 confirmed that *trans* isomer is more stable than *cis* isomer by 8.53 kcal/mol in terms of Gibbs Free Energies. Optimized structures, in Figure 35, showed that steric repulsions make *cis* isomer less stable than the *trans* isomer.

Table 2. DFT Calculations for compound **17**

Compound **17**	E +ZPE (Hartree)	H (Hartree)	G (Hartree)	ΔE (kcal/mol)	ΔH (kcal/mol)	ΔG (kcal/mol)
-cis	-1028.21316	-1028.19237	-1028.26316	8.01	7.97	8.53
-trans	-1028.22592	-1028.20506	-1028.27676	0	0	0

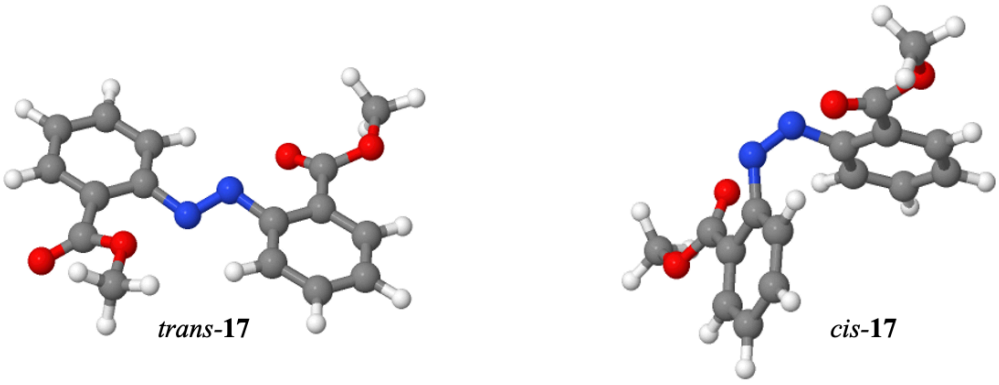

Figure 34. Optimized structures for *trans* and *cis* isomers of compound **17**

Cycle I

The DFT calculations for Cycle **I,** are summarized in Table 3 confirmed that *trans* isomer is more stable than *cis* isomer by 13.41 kcal/mol in terms of Gibbs Free Energies. The geometry optimized structures, in Figure 36, showed *trans* isomer is more relaxed than the *cis* isomer. The photoisomerization is governed by the transition state.

Table 3. DFT Calculations for Cycle **I**

Cycle **I**	E +ZPE (Hartree)	H (Hartree)	G (Hartree)	ΔE (kcal/mol)	ΔH (kcal/mol)	ΔG (kcal/mol)
-cis	-1180.78542	-1180.76387	-1180.83602	13.07	12.94	13.41
-trans	-1180.80626	-1180.78449	-1180.85739	0	0	0

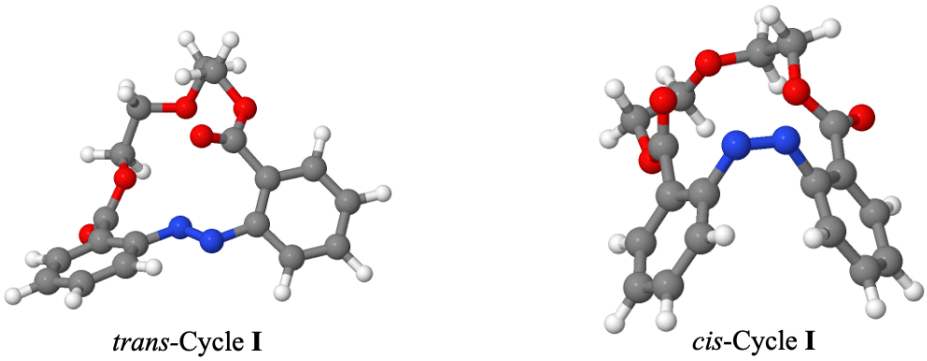

Figure 35. Optimized structures for *trans* and *cis* isomers of Cycle **I**

Cycle II

The DFT calculations for Cycle **II** are summarized in Table 4. The *trans* form is stable over *cis* form by 22.63 kcal/mol as shown in the calculations. Although the ring size increases, the energy difference is higher than the previous case. This could be because of higher energy conformer however global minimum did not searched.

Table 4. DFT Calculations of Cycle **II**

Cycle **II**	E +ZPE (Hartree)	H (Hartree)	G (Hartree)	ΔE (kcal/mol)	ΔH (kcal/mol)	ΔG (kcal/mol)
-cis	-1334.53245	-1334.50696	-1334.58826	23.02	23.26	22.63
-trans	-1334.56913	-1334.54403	-1334.62433	0	0	0

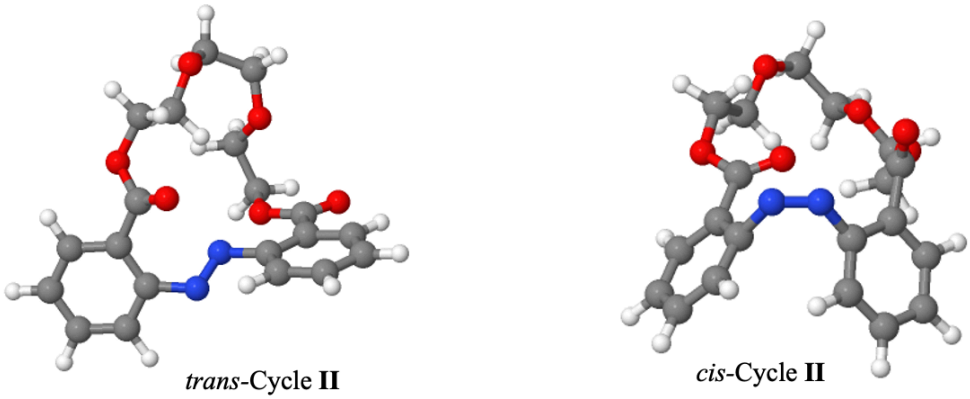

Figure 36. Optimized structures for *trans* and *cis* isomers of Cycle **II**

Cycle III

The DFT calculations for Cycle **III** are summarized in Table 5. For this compound the *trans* isomer was lower in energy by 22.86 kcal/mol. The energy difference between the diastereomers is higher due to the linker conformation. The optimized structures are given in Figure 38.

Table 5. DFT Calculations of Cycle **III**

Cycle **III**	E +ZPE (Hartree)	H (Hartree)	G (Hartree)	ΔE (kcal/mol)	ΔH (kcal/mol)	ΔG (kcal/mol)
-cis	-1488.31043	-1488.28128	-1488.37173	22.56	22.79	21.86
-trans	-1488.34638	-1488.31761	-1488.40657	0	0	0

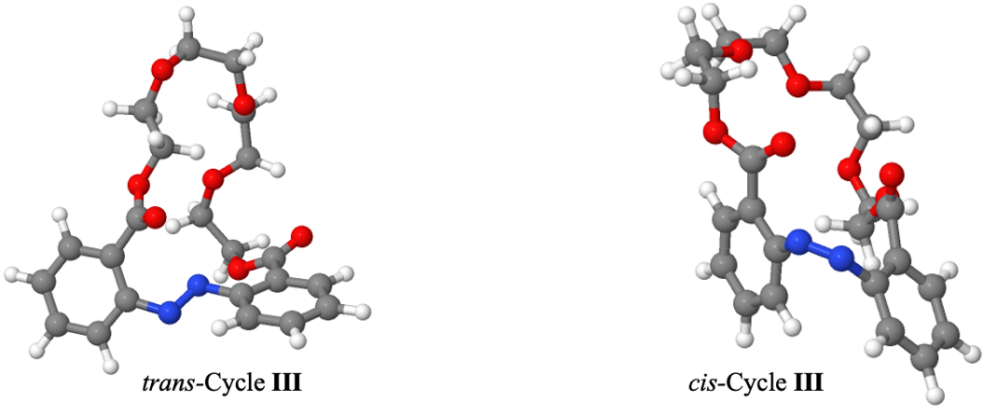

Figure 37. Optimized structures for *trans* and *cis* isomers of Cycle **III**

Cycle IV

In Table 6, the energies were summarized. It was shown, like the other macrocycles, *trans* isomer is more stable by 8.27 kcal/mol. In this case, Cycle **IV**, in Figure 39, is more relaxed in geometry compared to the other macrocycles.

Table 6. DFT Calculations for Cycle **IV**

Cycle **IV**	E +ZPE (Hartree)	H (Hartree)	G (Hartree)	ΔE (kcal/mol)	ΔH (kcal/mol)	ΔG (kcal/mol)
-cis	-2137.21412	-2137.17202	-2137.29419	7.31	7.13	8.27
-trans	-2137.22578	-2137.18338	-2137.30738	0	0	0

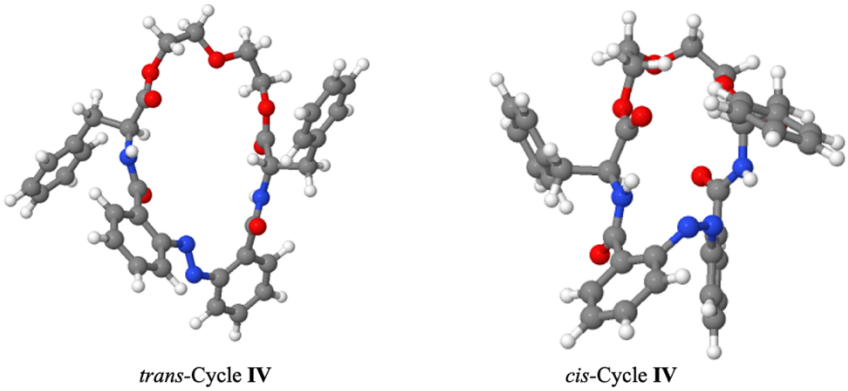

Figure 38. Optimized structures for *trans* and *cis* isomers of Cycle **IV**

In all of the macrocycles, the computational study revealed that the gauche effect for ethylene glycol units plays an essential role on conformations. However, this calls for more elaborate calculations.

CHAPTER 4

CONCLUSIONS

In this study, four novel azo-containing macrocycles were synthesized and characterized. Cycles **I**, **II**, and **III** were achiral and had linkers with diethylene glycol, triethylene glycol, and tetraethylene glycol. The last macrocycle has chiral *L*-phenylalanine incorporated; thus, it makes the compound chiral. All of these macrocycles were characterized with spectroscopic methods. The addition of the azo group in macrocycles was challenging. In our study, we decided to follow a route that azo coupling was the last step in forming the macrocycles. For the macrocyclization step, five azo coupling methods were screened. Although these steps' yields were low, the lead (IV) acetate method was found to be successful. With this method, sufficient materials were obtained for further studies.

UV-Vis absorption spectra revealed that macrocycle **I**, **II**, and **III** have an absorption λ_{max} at 310 nm, which is 10 nm lower than the reference material, compound **17**. The 10 nm change is due to the deviation from planarity, and this was further supported with DFT calculations. Cycle **IV** is not as rigid as the other macrocycles, as shown with UV-Vis studies and DFT calculations.

Well-known *trans* to *cis* isomerization of azobenzene was tested on these cycles along with the reference compound **17**. The reference compound and cycles were irradiated with a light source of 365 nm. It was shown that these compounds do not convert to *cis* fully except for Cycle **IV**. This is due to the rigidity of the macrocycles. Macrocycles have fluorescence emissions even though acyclic azo compounds lack this emission. Cycle **IV** has many promising features for chiral recognition through catch and release, which remains a future study.

Macrocycles **I**, **II**, and **III** experimented for cation recognition. Although any differentiation was not observed for K^+, Cycle **I** and **II** showed differentiation for Li^+ and Na^+. For Cycle **IV**, we were aiming for chiral recognition, which is not in this thesis's scope. We observed 60 to 70 nm Stokes shifts for Cycles **I**-**IV**. This shows some flexibility in the skeleton of these cycles. All these observations were further elaborated with DFT calculations.

CHAPTER 5

EXPERIMENTALS

5.1 Methods and Materials

All starting materials and solvents were purchased from Sigma Aldrich and were used without further purifications. The reactions were monitored by thin layer chromatography (TLC) (Merck Silica Gel 60 F254) and visualized by UV light at 254 nm.

Structural evaluation of the synthesized compounds was accomplished with the instruments stated below.

Melting points were recorded using Stuart SMP11 Instrument and the reported results are uncorrected.

^{1}H and ^{13}C nuclear magnetic resonance spectra of the compounds were recorded in deuterated solvents with Bruker Avance III Ultrashield 400 Hz NMR spectrometer. The chemical shifts were stated in parts per million (ppm) with tetramethylsilane (TMS) as internal reference. Spin multiplicities were indicated as s (singlet), d (doublet), dd (doublet of doublet), t (triplet), tt (triplet of triplet), m (multiplet) and coupling constants (*J*) were reported as in Hz (Hertz). ^{1}H NMR,^{13}C NMR, and other NMR techniques spectra of compounds were given in Appendix A. NMR spectra were processed with MestReNova program.

Infrared (IR) Spectra were recorded with Thermo Scientific Nicolet iS10 ATR-IR spectrometer. Signal locations were reported in reciprocal centimeter (cm^{-1}). The IR spectra of the compounds synthesized are given in Appendix B. IR spectra were processed with OriginPro 2015 program.

UV-Vis measurements were recorded with Shimadzu UV-2450 spectrophotometer. Spectroscopic measurements were carried out in acetonitrile of gradient grade. UV absorption spectra were processed with OriginPro 2015 program.

Fluorescence measurements were recorded with Perkin Elmer LS55 spectrofluorometer. Spectroscopic measurements were carried out in acetonitrile of gradient grade. The fluorescence spectra of the compounds synthesized are given in Appendix C. Fluorescence spectra were processed with OriginPro 2015 program.

High Resolution Mass Spectra (HRMS) were processed in positive mode on (ES+) using Time of Flight mass analyzer. The high-resolution mass spectra of compounds synthesized are given in Appendix D.

5.2 Synthesis of Azobenzene

5.2.1 Coupling of Nitrobenzene[60]

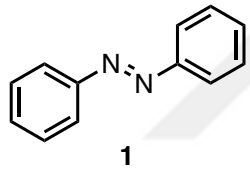

1

Nitrobenzene (5 mL, 49 mmol, 1 eq.) and NaOH (6 g) were dissolved in 100 mL ethanol. Zn powder (6 g, 2 eq.) was then introduced to the reaction medium. The mixture was refluxed for 2 hours and then, filtered while hot. The filtrate was evaporated *in vacuo* to give the product (2.78 g, 30%). IR:1599 cm^{-1} (N=N stretching).

5.2.2 Coupling of Aniline with NCS/DBU[23]

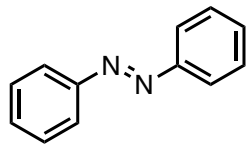

1

Aniline (0.5 g, 5 mmol, 1 eq.) was dissolved in 5 mL of CH_2Cl_2 and DBU (1.5 g, 10 mmol, 2 eq.) was introduced to the solution. The solution was stirred at room

temperature for 10 min before cooling down to -78°C. *N*-chlorosuccinimide (1.3 g, 10 mmol, 2 eq.) was then added to the reaction mixture. The orange solution was stirred for 20 min at -78°C. Afterwards, the solution was quenched by $NaHCO_3$ solution. The mixture was then extracted with 10 mL water and then 10 mL of 1 M HCl solution. The organic layers were combined, dried over anhydrous $MgSO_4$, and concentrated *in vacuo*. (0.75 g, 76%) ^{1}H NMR (DMSO-d_6, 400 MHz) δ 7.89 (d, J = 7.9 Hz, 4H), 7.64 – 7.54 (m, 6H). ^{13}C NMR (101 MHz, $CDCl_3$) δ 133.8, 130.9, 129.1, 122.8.

5.3 Synthesis of Aromatic Azo Compounds

5.3.1 Synthesis of **4,4'-dihydroxyazobenzene**[61]

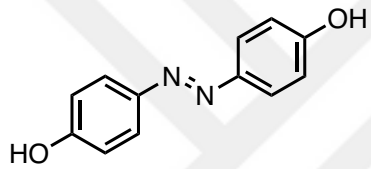

2

A 10 mL solution of 1 M HCl and *p*-aminophenol (2.0 g, 18 mmol, 1 eq.) was cooled to 0°C in an ice bath. A solution of $NaNO_2$ (1.5 g) in 15 mL water was then introduced to the reaction medium at 0°C in order to prepare the diazonium salt. 1 hour later, phenol (0.86 g, 18 mmol, 1 eq.) in 10 mL of 3 M NaOH solution was added dropwise to the reaction medium. The resulting mixture was stirred at room temperature for 2 hours. Concentrated HCl solution was then added to adjust the pH below 5. Suction filtration was used to collect the precipitate. The precipitate was washed with cold water and recrystallized from ethanol. (1.62 g, 41%) ^{1}H NMR (DMSO-d_6, 400 MHz) δ 10.13 (s, 2H), 7.71 (d, J = 8.5 Hz, 4H), 6.91 (d, J = 8.5 Hz, 4H). IR: 3354 cm^{-1} (O-H stretching), 1590 cm^{-1} (N=N stretching).

5.3.2 Synthesis of **4,4'-diallyoxyazobenzene**[62]

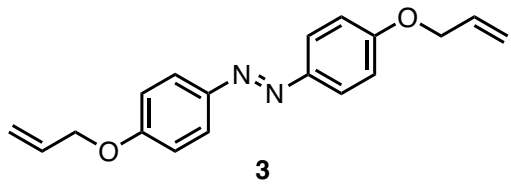

3

To a solution of 4,4'-dihydroxyazobenzene (0.5 g, 2.3 mmol, 1 eq.) and K_2CO_3(1.9 g, 6 eq.) in 10 mL acetone, allyl bromide (0,72 mL, 8.3 mmol, 3 eq.) was added at room temperature. The reaction mixture was stirred for 17 hours and the solvent was evaporated *in vacuo*. The residue was dissolved in EtOAc. The EtOAc solution was then washed first with $NaHCO_3$ solution, then 3% NaOH solution, and then with Brine. The organic layer was dried over anhydrous $MgSO_4$, filtered, and evaporated *in vacuo*. The residual crude product was recrystallized from methanol. (0.30 g, 44%) ^{1}H NMR ($CDCl_3$, 400 MHz) δ 7.85 (d, *J* = 8.9 Hz, 4H), 7.01 (d, *J* = 8.9 Hz, 4H), 6.08 (ddt, *J* = 17.3, 10.5, 5.3 Hz, 2H), 5.45 (dq, *J* = 17.3, 1.6 Hz, 2H), 5.33 (dt, *J* = 10.5, 1.4 Hz, 2H), 4.62 (dt, *J* = 5.4, 1.6 Hz, 4H).

5.3.3 Synthesis of **4,4'-diacetoxyazobenzene**

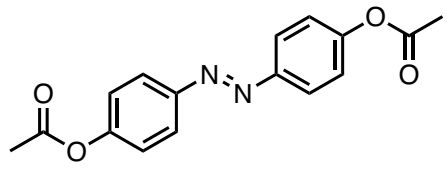

4

p-Aminophenyl acetate (0.07 g, 0.5 mmol, 1 eq.) was dissolved in 5 mL of CH_2Cl_2 and DBU (0.14 g, 0.9 mmol, 2 eq.) was introduced to the reaction mixture. The mixture was stirred at room temperature for 10 min before cooling down to -78°C. *N*-chlorosuccinimide (0.12 g, 0.9 mmol, 2 eq.) was added to the reaction mixture. The orange solution was stirred for 20 min at -78°C. Afterwards, the solution was quenched by $NaHCO_3$ solution. The mixture was then extracted with 10 mL water and then 10 mL of 1 M HCl solution. The organic layers were combined, dried over anhydrous $MgSO_4$, and concentrated *in vacuo*. (0.05 g, 36%) ^{1}H NMR ($CDCl_3$, 400

MHz) δ 7.52 (d, *J* = 8.9 Hz, 4H), 7.01 (d, *J* = 8.5 Hz, 4H), 2.75 (s, 6H). IR: 1726 cm^{-1} (C=O stretching), 1543 cm^{-1} (N=N stretching).

5.3.4 Synthesis of **4,4'-diacetamidoazobenzene**[22]

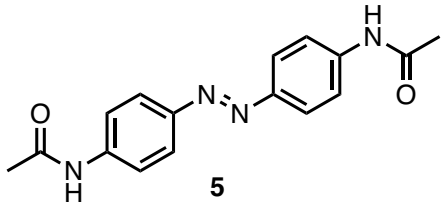

5

In a 100 ml round bottom flask *N*-(4-aminophenyl) acetamide (0.5 g, 3.3 mmol, 1 eq.) was dissolved in 20 mL of toluene. CuBr (0.015 g, 0.09 mmol, 0.03 eq.) and pyridine (0.02 mL) were then introduced to the reaction mixture. O_2 gas was bubbled through the reaction flask for 7 hours. The resulting brownish precipitate was then filtered off. (0.25 g, 25%) ^{1}H NMR (DMSO-d_6, 400 MHz) δ 10.27 (s, 2H), 7.80 (q, *J* = 8.9 Hz, 8H), 2.09 (s, 6H). IR: 3480 cm^{-1} (N-H stretching), 1665 cm^{-1} (C=O stretching), 1597 cm^{-1} (N=N stretching).

5.4 Synthesis of Cycle I, Cycle II, Cycle III

5.4.1 Synthesis of diethylene glycol bis(o-nitrobenzoate), Compound **6**

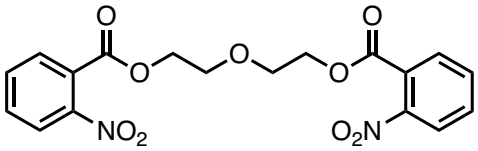

6

o-Nitrobenzoic acid (9.0 g, 53.8 mmol, 1.00 eq.) and $SOCl_2$ (11.72 mL, 161.5 mmol, 3 eq.) combined in a 250 ml round bottomed flask and cooled to 0°C. The solution was stirred for 3 hours and the excess $SOCl_2$ was evaporated *in vacuo* to give 6.42 mL of a viscous liquid. 2.14 mL of the residue was transferred into another flask, and treated with diethylene glycol (0.77mL, 8.08mmol, 1eq.) under argon. The flask was then fitted with a condenser and a drying tube. The mixture was refluxed for 2,5 hours. The

resulting mixture was neutralized with 20% Na_2CO_3 solution and extracted 3 times with $CHCl_3$. The combined organic layers were then dried over anhydrous $MgSO_4$, filtered, and evaporated *in vacuo* to give brown solids. The crude product was used in the next step without purification (3.00 g, 91.8%) ^{1}H NMR ($CDCl_3$, 400 MHz) δ 7.93 (dd, *J* = 7.5, 1.7 Hz, 2H), 7.77 (dd, *J* = 7.1, 2.0 Hz, 2H), 7.67 (m, 4H), 4.52 (m, 4H), 3.83 (m, 4H) ppm. ^{13}C NMR ($CDCl_3$, 101 MHz) δ 165.3, 147.9, 132.9, 131.6, 129.8, 127.4, 123.8, 68.5, 65.2. IR: 1722 cm^{-1} (C=O stretching), 1523 cm^{-1} (NO_2 antisym stretching),1348 cm^{-1} (NO_2 sym stretching). HRMS: (TOF-MS) m/z: $[M+H]^+$ Calcd for $C_{18}H_{17}N_2O_9^+$ 405.0934, found 405.0928.

5.4.2 Synthesis of triethylene glycol bis(o-nitrobenzoate), Compound **7**

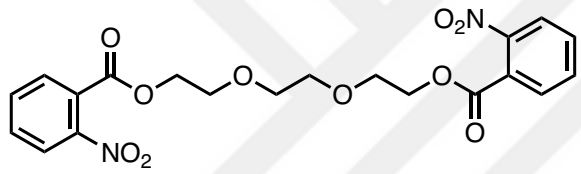

7

o-Nitrobenzoic acid (9.0 g, 53.8 mmol, 1.00 eq.) and $SOCl_2$ (11.72 mL, 161.5 mmol, 3 eq.) combined in a 250 ml round bottomed flask and cooled to 0°C. The solution was stirred for 3 hours and the excess $SOCl_2$ was evaporated *in vacuo* to give 6.42 mL of a viscous liquid. 2.14 mL of the residue was transferred into another flask, and treated with triethylene glycol (1.10 mL, 8.08mmol, 1eq.) under argon. The flask was then fitted with a condenser and a drying tube. The mixture was refluxed for 2,5 hours. The resulting mixture was neutralized with 20% Na_2CO_3 solution and extracted 3 times with $CHCl_3$. The combined organic layers were then dried over anhydrous $MgSO_4$, filtered, and evaporated *in vacuo* to give brown oil. The crude product was used in the next step without purification. (3.34 g, 92.2%) ^{1}H NMR ($CDCl_3$, 400 MHz) δ 7.92 (dd, *J* = 7.8, 1.5 Hz, 2H), 7.75 (dd, *J* = 7.8, 1.4 Hz, 2H) 7.68-7.66 (m, 4H), 4.48 (m, 4H), 3.79 (m, 4H), 3.68 (s,4H) ppm. ^{13}C NMR ($CDCl_3$, 101 MHz) δ 165.3, 147.9, 132.9, 131.7, 129.8, 127.4, 123.8, 70.4, 68.5, 65.2. IR: 1728 cm^{-1} (C=O stretching), 1529 cm^{-1}

(NO_2 antisym stretching), 1349 cm^{-1} (NO_2 sym stretching). HRMS: (TOF-MS) m/z: $[M+H]^+$ Calcd for $C_{20}H_{21}N_2O_{10}^+$ 449.1196, found 449.1141.

5.4.3 Synthesis of tetraethylene glycol bis(o-nitrobenzoate), Compound **8**

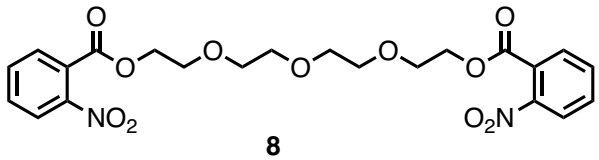

8

o-Nitrobenzoic acid (9.0 g, 53.8 mmol, 1.00 eq.) and $SOCl_2$ (11.72 mL, 161.5 mmol, 3 eq.) combined in a 250 ml round bottomed flask and cooled to 0°C. The solution was stirred for 3 hours and the excess $SOCl_2$ was evaporated *in vacuo* to give 6.42 mL of a viscous liquid. 2.14 mL of the residue was transferred into another flask, and treated with tetraethylene glycol (1.40 mL, 8.08mmol, 1 eq.) under argon. The flask was then fitted with a condenser and a drying tube. The mixture was refluxed for 2,5 hours. The resulting mixture was neutralized with 20% Na_2CO_3 solution and extracted 3 times with $CHCl_3$. The combined organic layers were then dried over anhydrous $MgSO_4$, filtered, and evaporated *in vacuo* to give brown oil. The crude product was used in the next step without purification. (3.80 g, 95.5%) ^{1}H NMR ($CDCl_3$, 400 MHz) δ 7.92 (m, 2H), 7.70 (m, 4H), 4.48 (m, 4H), 3.79 (m, 4H), 3.66 (bs, 8H) ppm. ^{13}C NMR ($CDCl_3$, 101 MHz) δ 165.4, 148.0, 132.9, 131.7, 129.8, 127.5, 123.8, 70.5, 70.4, 68.5, 65.3. HRMS: (TOF-MS) m/z: $[M+H]^+$ Calcd for $C_{22}H_{25}N_2O_{11}^+$ 493.1458, found 493.1458.

5.4.4 Synthesis of diethylene glycol bis(*o*-aminobenzoate), Compound **9**

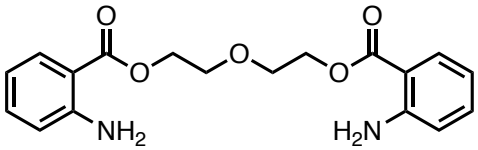

9

A solution of diethylene glycol bis(*o*-aminobenzoate) (3.0 g, 7.41 mmol) in 40 mL MeOH and Pd/C (0.2 g) were combined in a Parr® high pressure reactor vessel. The reaction mixture was stirred under H_2 gas at 50 bars of pressure for 1 hour. The solution was then filtered through a pad of Celite® 545 and the solvent was evaporated to give a brown oil. (1.77 g, 70%) ^{1}H NMR ($CDCl_3$, 400 MHz) δ 7.89 (dd, *J* = 8.1, 1.7 Hz, 2H), 7.28 (m, 2H), 6.77 – 6.63 (m, 4H), 5.49 (s, 4H), 4.46 (dd, *J* = 5.6, 3.9 Hz, 4H), 3.90 – 3.83 (m, 4H) ppm. ^{13}C NMR ($CDCl_3$, 101 MHz) δ 167.7, 149.2, 144.4, 134.1, 131.3, 117.1, 117.0, 69.1, 63.3. IR: 3462 cm^{-1}, 3369 cm^{-1} (N-H stretching), 1684 cm^{-1} (C=O stretching). HRMS: (TOF-MS) m/z: $[M+H]^+$ Calcd for $C_{18}H_{21}N_2O_5^+$ 345.1450, found 345.1435.

5.4.5 Synthesis of triethylene glycol bis(*o*-aminobenzoate), Compound **10**

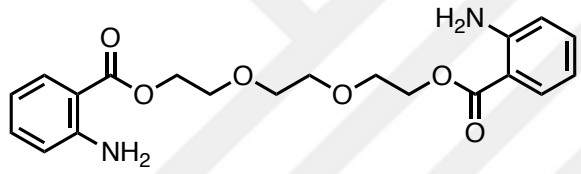

10

A solution of triethylene glycol bis(*o*-aminobenzoate) (3.0 g, 6.70 mmol) in 40 mL MeOH and Pd/C (0.2 g) were combined in a Parr® high pressure reactor vessel. The reaction mixture was stirred under H_2 gas at 50 bars of pressure for 1 hour. The solution was then filtered through a pad of Celite® 545 and the solvent was evaporated to give a brown oil. (1.5 g, 60%) ^{1}H NMR ($CDCl_3$, 400 MHz) δ 7.96 – 7.79 (m, 2H), 7.28 (dd, *J* = 12.7 Hz, 2H), 6.81 – 6.56 (m, 4H), 4.43 (d, *J* = 4.7 Hz, 4H), 3.95 – 3.58 (m, 8H). ^{13}C NMR ($CDCl_3$, 101 MHz) δ 167.8, 150.1, 134.1, 131.3, 116.7, 116.3, 110.7, 70.6, 69.2, 63.4. IR: 3472 cm^{-1}, 3366 cm^{-1} (N-H stretching), 1687 cm^{-1} (C=O stretching). HRMS:(TOF-MS) m/z: $[M+H]^+$ Calcd for $C_{20}H_{25}N_2O_6^+$ 389.1713, found 389.1710.

5.4.6 Synthesis of tetraethylene glycol bis(*o*-aminobenzoate), Compound **11**

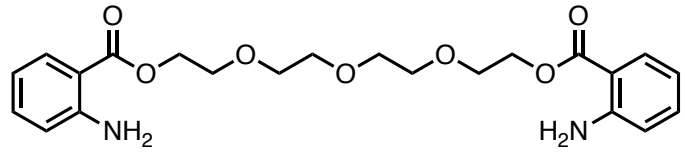

11

A solution of tetraethylene glycol bis(*o*-aminobenzoate) (3.0 g, 6.50 mmol) in 40 mL MeOH and Pd/C (0.2 g) were combined in a Parr® high pressure reactor vessel. The reaction mixture was stirred under H_2 gas at 50 bars of pressure for 1 hour. The solution was then filtered through a pad of Celite® 545 and the solvent was evaporated to give a brown oil. (2.34 g, 83.26%) ^{1}H NMR ($CDCl_3$, 400 MHz) δ 7.90 (d, *J* = 7.9 Hz, 2H), 7.28 (d, *J* = 6.8 Hz, 2H), 6.66 (dd, *J* = 7.9, 4.0 Hz, 4H), 4.44 (t, *J* = 4.8 Hz, 4H), 3.82 (m, 4H), 3.70 (s, 8H) ppm. ^{13}C NMR ($CDCl_3$, 101 MHz) δ 168.5, 150.4, 134.2, 134.1, 131.1, 116.7, 110.7, 71.3, 71.1, 64.3, 51.6. IR: 3469 cm^{-1}, 3358 cm^{-1} (N-H stretching), 1685 cm^{-1} (C=O stretching). HRMS: (TOF-MS) m/z: $[M+H]^+$ Calcd for $C_{22}H_{29}N_2O_7^+$ 433.1975, found 433.1977.

5.4.7 Synthesis of **Cycle I,** Compound **12**

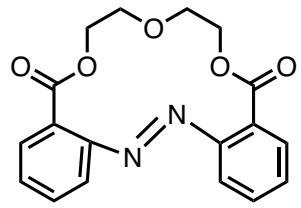

12

To a solution of diethylene glycol bis(*o*-aminobenzoate) (1.77 g, 5.14 mmol, 1 eq.) in 20 mL of CH_2Cl_2, Et_3N (7.17 mL, 51.4 mmol, 10 eq.) was added. A solution of $Pb(OAc)_4$ (5.24 g, 11.8 mmol, 2.3 eq.) in 10 mL of CH_2Cl_2 was then prepared and added to the reaction mixture under argon atmosphere. The mixture was stirred overnight at room temperature. The volatiles were removed *in vacuo*. The residue was purified with column chromatography using neutral alumina as stationary phase.

The product was obtained as orange crystals. (146 mg, 8%) m.p: 110°C ^{1}H NMR ($CDCl_3$, 400 MHz) δ 7.77 (dd, *J* = 7.7, 1.0 Hz, 2H), 7.65 – 7.46 (m, 6H), 4.48 – 4.41 (m, 4H), 3.89 – 3.80 (m, 4H). ^{13}C NMR ($CDCl_3$, 101 MHz) δ 166.4, 151.2, 130.7, 128.7, 128.5, 126.4, 120.3, 68.0, 65.1. IR: 1729 cm^{-1} (C=O stretching), 1579 cm^{-1} (N=N stretching). HRMS: (TOF-MS) m/z: $[M+H]^+$ Calcd for $C_{18}H_{17}N_2O_5^+$ 341.1137, found 341.1137.

5.4.8 Synthesis of **Cycle II**

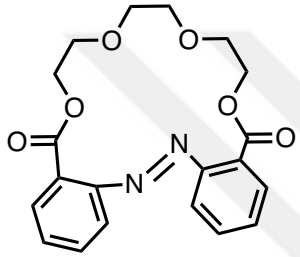

13

To a solution of triethylene glycol bis(*o*-aminobenzoate) (1.33 g, 3.42 mmol, 1 eq.) in 20 mL of CH_2Cl_2, Et_3N (5.0 mL, 34.2 mmol, 10 eq.) was added. A solution of $Pb(OAc)_4$ (3.04 g, 6.84 mmol, 2 eq.) in 10 mL of CH_2Cl_2 was then prepared and added to the reaction mixture under argon atmosphere. The mixture was stirred overnight at room temperature. The volatiles were removed *in vacuo*. The residue was purified with column chromatography using neutral alumina as stationary phase. The product was obtained as orange oil. (70 mg, 5%) ^{1}H NMR ($CDCl_3$, 400 MHz) δ 7.92 (dd, *J* = 7.9, 1.5 Hz, 2H), 7.79 – 7.58 (m, 6H), 4.51 – 4.41 (m, 4H), 3.84 – 3.75 (m, 4H), 3.67 (s, 4H). ^{13}C NMR ($CDCl_3$, 101 MHz) δ 166.4, 151.2, 133.2, 130.7, 128.6, 120.3, 70.3, 68.0, 65.1, 62.3. IR: 1719 cm^{-1} (C=O stretching), 1591 cm^{-1} (N=N stretching). HRMS: (TOF-MS) m/z: $[M+H]^+$ Calcd for $C_{20}H_{21}N_2O_6^+$ 385.1400, found 385.1400.

5.4.9 Synthesis of **Cycle III**

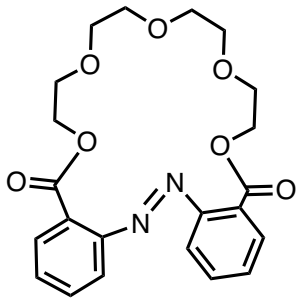

14

To a solution of tetraethylene glycol bis(*o*-aminobenzoate) (2.34 g, 5.41 mmol, 1 eq.) in 20 mL of CH_2Cl_2, Et_3N (7.8 mL, 56.2 mmol, 10.4 eq.) was added. A solution of $Pb(OAc)_4$ (5.5 g, 12.4 mmol, 2.3 eq.) in 10 mL of CH_2Cl_2 was then prepared and added to the reaction mixture under argon atmosphere. The mixture was stirred overnight at room temperature. The volatiles were removed *in vacuo*. The residue was purified with column chromatography using neutral alumina as stationary phase.The product was obtained as orange oil**.** (120 mg, 5%) ^{1}H NMR ($CDCl_3$, 400 MHz) δ 7.85 (dd, *J* = 8.0, 1.5 Hz, 1H), 7.63 – 7.47 (m, 3H), 4.48 – 4.38 (m, 2H), 3.64 – 3.59 (m, 2H), 3.51 – 3.43 (m, 2H), 3.40 – 3.30 (m, 2H). ^{13}C NMR ($CDCl_3$, 101 MHz) δ 167.6, 151.8, 132.0, 130.3, 129.9, 129.2, 119.2, 71.2, 70.4, 69.0, 64.8. IR: 1717 cm^{-1} (C=O stretching), 1594 cm^{-1} (N=N stretching). HRMS: (TOF-MS) m/z: $[M+H]^+$ Calcd for $C_{22}H_{25}N_2O_7^+$ 429.1662, found 429.1655.

5.5 Synthesis of dimethyl 2,2'-(diazene-1,2-diyl)(E)-dibenzoate (Reference Compound)

5.5.1 Esterification of *o*-nitrobenzoic acid

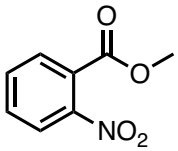

15

To a solution of *o*-nitrobenzoic acid (2 g, 12.0 mmol, 1 eq.) in 20 mL of MeOH, H_2SO_4 (0.2 mL, 2.04 mmol, 0.17 eq.) was added. The solution was refluxed for 6 hours and then concentrated to half the volume. The mixture was then diluted with 30 mL of EtOAc and extracted first with 20 mL of $NaHCO_3$ solution and then with 50 mL of Brine. Organic phase was dried over anhydrous Na_2SO_4 and evaporated *in vacuo* to give the product as a yellow oil. (1.5 g, 70%) ^{1}H NMR ($CDCl_3$, 400 MHz) δ 7.94 – 7.88 (d, 1H), 7.78 – 7.59 (m, 3H), 3.92 (s, 3H).

5.5.2 Reduction of methyl *o*-nitrobenzoate

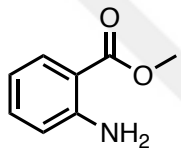

16

A solution of methyl *o*-nitrobenzoate (2.0 g, 11.0 mmol) in 20 mL of MeOH and Pd/C (0.2 g) were combined in a Parr® high pressure reactor vessel. The reaction mixture was stirred under H_2 gas at 50 bars of pressure for 1 hour. The solution was then filtered through a pad of Celite® 545. The filtrate was evaporated *in vacuo* to give the product as a pink oil. (1.04 g, 83%) ^{1}H NMR ($CDCl_3$, 400 MHz) δ 7.85 (dd, J = 8.0, 1.7 Hz, 1H), 7.26 (ddt, J = 7.8, 6.3, 1.6 Hz, 1H), 6.70 – 6.60 (m, 2H), 5.72 (bs, 2H), 3.87 (s, 3H). IR: 3479 cm^{-1} ,3369 cm^{-1} (N-H stretching),1687 cm^{-1} (C=O stretching).

5.5.3 Synthesis of dimethyl 2,2'-(diazene-1,2-diyl)(E)-dibenzoate (Reference Compound)

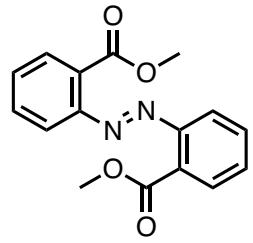

17

In a 100 ml round bottom flask methyl *o*-aminobenzoate (0.4 g) was dissolved in 20 mL of toluene. CuBr (0.02 g) and pyridine (0.02 mL) were then introduced to the reaction mixture. O_2 gas was bubbled through the reaction flask for 5 hours. Reaction mixture was concentrated *in vacuo* and flash chromatography with alumina column was performed for purification. (15 mg, 5%) ^{1}H NMR ($CDCl_3$, 400 MHz) δ 7.90 (dd, *J* = 7.6, 1.0 Hz, 2H), 7.68 – 7.62 (m, 4H), 7.54 (ddd, *J* = 7.7, 5.0, 3.6 Hz, 2H), 3.96 (d, *J* = 1.0 Hz, 6H). ^{13}C NMR ($CDCl_3$, 101 MHz) δ 167.2, 153.8, 152.3, 132.4, 130.0, 129.8, 118.5, 52.4. IR: 1722 cm^{-1} (C=O stretching), 1680 cm^{-1} (N=N stretching).

5.6 Synthesis of Cycle IV

5.6.1 Synthesis of Compound **18**[63]

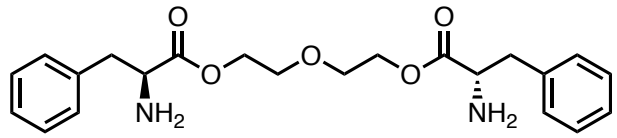

18

In a flask fitted with a Dean-Stark apparatus, a mixture of *L*-phenylalanine (5.0 g, 30.2 mmol, 2.2 eq.),diethylene glycol (1.30 mL, 13.7 mmol , 1 eq.), and *p*-toluenesulfonic acid (5.20 g, 30.2 mmol, 2.2 eq.) in 50 mL of toluene was refluxed for 16 hours. The mixture was then cooled to room temperature and evaporated *in vacuo*. The residue was recrystallized from 50 mL of H_2O. The

resulting ditosylate salt was neutralized with $NaHCO_3$ solution and extracted with CH_2Cl_2. The combined organic layers were dried over anhydrous $MgSO_4$, filtered, and evaporated *in vacuo*. (3.00g, 65%) ^{1}H NMR ($CDCl_3$, 400 MHz) δ 7.32 – 7.11 (m, 10H), 4.35 – 4.15 (m, 4H), 3.80 – 3.49 (m, 8H), 3.05 (ddd, *J* = 13.6, 8.5, 5.3 Hz, 2H), 2.86 (dd, *J* = 13.6, 7.7 Hz, 2H). HRMS: (TOF-MS) m/z: $[M+H]^+$ Calcd for $C_{22}H_{29}N_2O_5^+$ 401.2076, found 401.2078.

5.6.2 Coupling Reaction of *o*-nitrobenzoic acid and **18**

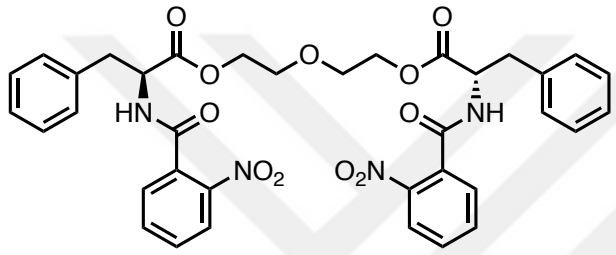

19

To a solution of *o*-nitrobenzoic acid (2.50 g, 15 mmol, 2 eq.), N-hydroxybenzotriazole (2.43 g, 18 mmol, 2.4 eq.), and **18** (3.0 g, 7.50 mmol, 1 eq.) in 30 mL of DMF, 1-ethyl-3-(3-dimethylaminopropyl)carbodiimide (3,44 g, 18.0 mmol, 2.4 eq.) and $Et(i\text{-}Pr)_2N$ (0.5 mL) were added under argon atmosphere. The mixture was stirred at room temperature for 12 hours. The mixture was then diluted with 100 mL of $CHCl_3$ and extracted 10 times with 100 mL portions of H_2O. The organic phase was then dried over anhydrous $MgSO_4$, filtered, and evaporated *in vacuo*. The residue was purified by column chromatography. The product was recrystallized from EtOAc and hexane. (2.2 g, 42%) ^{1}H NMR ($CDCl_3$, 400 MHz) δ 7.92 (d, *J* = 7.8 Hz, 2H), 7.60 – 7.44 (m, 4H), 7.33 – 7.15 (m, 12H), 6.75 (dd, *J* = 8.1, 3.4 Hz, 2H), 5.03 (td, *J* = 7.9, 7.0, 5.3 Hz, 2H), 4.30 (dtd, *J* = 16.0, 11.4, 10.5, 5.4 Hz, 4H), 3.68 (ddtd, *J* = 14.6, 11.4, 8.8, 7.1, 3.3 Hz, 4H), 3.21 (m, *J* = 7.7 Hz, 4H). ^{13}C NMR ($CDCl_3$, 101 MHz) δ 171.0, 165.7, 146.3, 135.5, 133.5, 132.1, 130.5, 130.5, 129.4, 129.3, 128.5, 127.1, 127.1, 124.4, 68.6, 64.3, 53.4, 37.5. IR: 3282 cm^{-1} (N-H stretching), 1737 cm^{-1} (C=O stretching for amide), 1651 cm^{-1} (C=O stretching

for ester), 1529 cm^{-1} (NO_2 antisym stretching), 1348 cm^{-1} (NO_2 sym stretching). HRMS: (TOF-MS) m/z: $[M+H]^+$ Calcd for $C_{36}H_{35}N_4O_{11}^+$ 699.2302, found 699.2306.

5.6.3 Reduction of Compound **19**

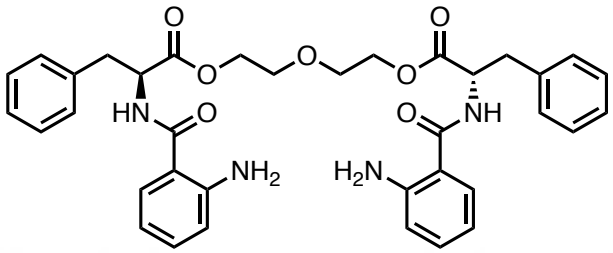

20

20 (1.2 g) was dissolved in methanol (20 mL) in a reactor and Pd/C was introduced. The reaction mixture was stirred under pressure of H_2 gas (50 bar) for 1 hour. The resulting mixture was filtrated from celite and the solvent was evaporated. Finally, red oil was obtained. (1.00 g, 86%) ^{1}H NMR ($CDCl_3$, 400 MHz) δ 7.34 – 7.11 (m, 14H), 6.72 – 6.56 (m, 4H), 6.52 (d, *J* = 7.5 Hz, 2H), 5.51 – 5.37 (bs, 4H), 5.01 (dt, *J* = 7.7, 5.7 Hz, 2H), 4.30 (dqt, *J* = 12.0, 8.4, 4.0 Hz, 4H), 3.73 – 3.62 (m, 4H), 3.23 (qd, *J* = 13.9, 6.0 Hz, 4H). IR: 3355 cm^{-1} (N-H stretching), 1735 cm^{-1}, 1639 cm^{-1} (C=O stretching). HRMS: (TOF-MS) m/z: $[M+H]^+$ Calcd for $C_{36}H_{39}N_4O_7^+$ 639.2819, found 639.2823.

5.6.4 Synthesis of **Cycle IV**

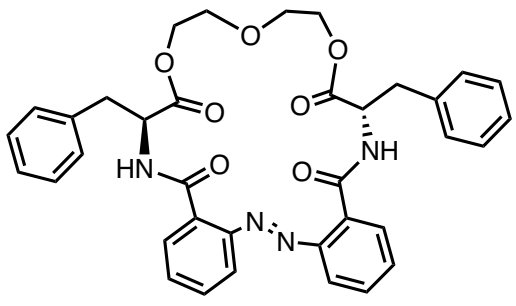

21

To a solution of compound **20** (1.0 g, 1 eq.) in 20 mL of CH_2Cl_2, Et_3N (2.2 mL, 10.4 eq.) was added. A solution of $Pb(OAc)_4$ (1.6 g, 2.3 eq.) in 10 mL of CH_2Cl_2 was then prepared and added to the reaction mixture under argon atmosphere. The mixture was stirred overnight at room temperature. The volatiles were removed *in vacuo*. The residue was purified via alumina column chromatography. The product was obtained as orange crystals. (6 mg, < 8%) m.p: 80°C ^{1}H NMR ($CDCl_3$, 400 MHz) δ 8.62 (d, 2H), 8.39 (dd, *J* = 7.9, 1.5 Hz, 2H), 7.64 (td, *J* = 7.6, 1.3 Hz, 2H), 7.40 (td, *J* = 7.7, 1.5 Hz, 2H), 7.29 (m, 6H), 7.17 (m, 4H), 6.78 (d, 2H), 5.22 (m, *J* = 8.7, 6.8, 5.1 Hz, 2H), 4.15 (m, *J* = 11.3, 5.1, 2.1 Hz, 2H), 3.27 – 3.03 (m, 10H). ^{13}C NMR ($CDCl_3$, 101 MHz) δ 170.5, 165.2, 150.4, 136.4, 132.5, 132.4, 132.1, 130.3, 129.6, 128.8, 128.7, 127.2, 116.5, 69.0, 65.0, 54.5, 37.5, 19.0. IR: 3292 cm^{-1} (N-H stretching), 1735 cm^{-1}, 1651 cm^{-1} (C=O stretching), 1592 cm^{-1} (N=N stretching). HRMS: (TOF-MS) m/z: $[M+H]^+$ Calcd for $C_{36}H_{35}N_4O_7^+$ 635.2506, found 635.2505.

REFERENCES

(1) Feringa, B. L.; Browne, W. R. Related Titles Handbook of Stimuli-Responsive Materials Handbook of Synthetic Photochemistry Functional Supramolecular Architectures Molecular Devices and Machines From Non-Covalent Assemblies to Molecular Machines Ideas in Chemistry and Molecular Science; Wiley-VCH, **2011**, Vol. 1.

(2) Hamon, F.; Djedaini-Pilard, F.; Barbot, F.; Len, C. Azobenzenes-Synthesis and Carbohydrate Applications. *Tetrahedron* **2009**, *65* (49), 10105–10123. https://doi.org/10.1016/j.tet.2009.08.063.

(3) Wang, X. Azo Polymers: Synthesis, Functions and Applications; Springer, NY, **2017**.

(4) Kempa, S.; Wallach, L. Product Class 6: Aliphatic Azo Compounds. Thieme, **2013**, 459–506. https://doi.org/10.1055/sos-sd-041-00470.

(5) Thiele, J.; Heuser, K. Liebig's Annalen. *J Liebigs Ann. Chem.* **1896**, No. 290, 1.

(6) Kumar, S. Azo Functional Polymers; Technomic Publishing Company,USA, **1992**.

(7) Zollinger, H. Azo and Diazo Chemistry: Aliphatic and Aromatic Compounds; Interscience Publishers Inc.: NY, **1961**.

(8) Mitscherlich, E. *Ann. Pharm.* **1834**, *12*, 311–314. https://doi.org/10.1002/jlac.18340120282.

(9) Tsuji, T.; Takashima, H.; Takeuchi, H.; Egawa, T.; Konaka, S. Molecular Structure and Torsional Potential of Trans-Azobenzene. A Gas Electron Diffraction Study. *J. Phys. Chem. A* **2001**, *105* (41), 9347–9353. https://doi.org/10.1021/jp004418v.

(10) Pedersen, T. G.; Ramanujam, P. S.; Johansen, P. M.; Hvilsted, S. Quantum Theory and Experimental Studies of Absorption Spectra and Photoisomerization of Azobenzene Polymers. *J. Opt. Soc. Am. B* **1998**, *15* (11), 2721. https://doi.org/10.1364/josab.15.002721.

(11) Rau, H. Photochromism; Elsevier Ltd, **1990**.

(12) Benkhaya, S.; Mrabet, S.; El Harfi, A. Classifications, Properties, Recent Synthesis and Applications of Azo Dyes. *Heliyon* **2020**, *6* (1). https://doi.org/10.1016/j.heliyon.2020.e03271.

(13) CBI. EU Legislation : Azo Dyes in Textile and Leather Articles. **2002**, 3–5.

(14) Stewart, R. Oxidation Mechanisms-Application to Organic Chemistry; NY, **1964**.

(15) Shiraishi, Y.; Katayama, M.; Hashimoto, M.; Hirai, T. Photocatalytic Hydrogenation of Azobenzene to Hydrazobenzene on Cadmium Sulfide under Visible Light Irradiation. *Chem. Commun.* **2018**, *54* (5), 452–455. https://doi.org/10.1039/c7cc08428e.

(16) Yates, E.; Yates, A. Johann Peter Griess FRS (1829-88): Victorian Brewer and Synthetic Dye Chemist. *Notes Rec.* **2016**, *70* (1), 65–81. https://doi.org/10.1098/rsnr.2015.0020.

(17) Svele, I.; Zollinger, H. Topics in Current Chemistry; **1983**.

(18) Merino, E. Synthesis of Azobenzenes: The Coloured Pieces of Molecular Materials. *Chem. Soc. Rev.* **2011**, *40* (7), 3835–3853. https://doi.org/10.1039/c0cs00183j.

(19) Davey, M. H.; Lee, V. Y.; Miller, R. D.; Marks, T. J. Synthesis of Aryl Nitroso Derivatives by Tert-Butyl Hypochlorite Oxidation in Homogeneous Media. Intermediates for the Preparation of High- Hyperpolarizability Chromophore Skeletons. *J. Org. Chem.* **1999**, *64* (13), 4976–4979. https://doi.org/10.1021/jo990235x.

(20) Ueno, K.; Akiyoshi, S. Kinetic Study on the Condensation Reaction of Aniline and Nitrosobenzenes. *J. Am. Chem. Soc.* **1954**, *76* (14), 3670–3672. https://doi.org/10.1021/ja01643a021.

(21) Furin, G. G. The Reactions of Azoxybenzenes in Acids. The Mechanism of the Wallach Rearrangement. *Russ. Chem. Rev.* **1987**, *56* (6), 532–545. https://doi.org/10.1070/rc1987v056n06abeh003288.

(22) Zhang, C.; Jiao, N. Copper-Catalyzed Aerobic Oxidative Dehydrogenative Coupling of Anilines Leading to Aromatic Azo Compounds Using Dioxygen as an Oxidant. *Angew. Chemie - Int. Ed.* **2010**, *49* (35), 6174–6177. https://doi.org/10.1002/anie.201001651.

(23) Antoine John, A.; Lin, Q. Synthesis of Azobenzenes Using N-Chlorosuccinimide and 1,8-Diazabicyclo[5.4.0]Undec-7-Ene (DBU). *J. Org. Chem.* **2017**, *82* (18), 9873–9876. https://doi.org/10.1021/acs.joc.7b01530.

(24) Aylward, J. B. The Oxidation of Organic Nitrogen Compounds with Lead Tetra-Acetate. **1968**.

(25) Heindl, A. H.; Becker, J.; Wegner, H. A. Selective Switching of Multiple Azobenzenes. *Chem. Sci.* **2019**, *10* (31), 7418–7425. https://doi.org/10.1039/c9sc02347j.

(26) Happer, D. A.; Vaughan, J.; The Chemistry of Hydrazo,Azo and Azoxy Groups.Pdf; NY , **1975**; Vol.30. https://doi.org/DOI: 10.1007/BF02389711.

(27) Roberts, B. P. W.; P.B.D. de la Mare; The Kinetics of Aromatic Halogen Substitution, Part IV. The 1-Halogenonaphthalenes and Related Compounds *J. Chem. Soc*., **1948**, 100-106.

(28) Pederzoli, M.; Pittner, J.; Barbatti, M.; Lischka, H. Nonadiabatic Molecular Dynamics Study of the Cis -Trans Photoisomerization of Azobenzene Excited to the S1 State. *J. Phys. Chem. A* **2011**, *115* (41), 11136–11143. https://doi.org/10.1021/jp2013094.

(29) Hartley, G. S. The Cis-Form of Azobenzene. *Nature* **1937**, *140* (3537), 281.

(30) Griffiths, J. II. Photochemistry of Azobenzene and Its Derivatives. *Chem. Soc. Rev.* **1972**, *1* (4), 481–493. https://doi.org/10.1039/CS9720100481.

(31) Sension, R. J.; Repinec, S. T.; Szarka, A. Z.; Hochstrasser, R. M. Femtosecond Laser Studies of the Cis-Stilbene Photoisomerization Reactions. *J. Chem. Phys.* **1993**, *98* (8), 6291–6315. https://doi.org/10.1063/1.464824.

(32) Bandara, H. M. D.; Burdette, S. C. Photoisomerization in Different Classes of Azobenzene. *Chem. Soc. Rev.* **2012**, *41* (5), 1809–1825. https://doi.org/10.1039/c1cs15179g.

(33) Lednev, I. K.; Ye, T. Q.; Matousek, P.; Towrie, M.; Foggi, P.; Neuwahl, F. V. R.; Umapathy, S.; Hester, R. E.; Moore, J. N. Femtosecond Time-Resolved UV-Visible Absorption Spectroscopy of Trans-Azobenzene: Dependence on Excitation Wavelength. *Chem. Phys. Lett.* **1998**, *290* (1–3), 68–74. https://doi.org/10.1016/S0009-2614(98)00490-4.

(34) Rodier, J. M.; Myers, A. B.; Cis-Stilbene Photochemistry: Solvent Dependence of the Initial Dynamics and Quantum Yields. *J. Am. Chem. Soc.* **1993**, *115* (23), 10791–10795. https://doi.org/10.1021/ja00076a041.

(35) Tamai, N.; Miyasaka, H. Ultrafast Dynamics of Photochromic Systems. *Chem. Rev.* **2000**, *100* (5), 1875–1890. https://doi.org/10.1021/cr9800816.

(36) Merino, E.; Ribagorda, M. Control over Molecular Motion Using the Cis-Trans Photoisomerization of the Azo Group. *Beilstein J. Org. Chem.* **2012**, 1071–1090. https://doi.org/10.3762/bjoc.8.119.

(37) Hunger, K., Ed.; Industrial Dyes; Wiley, 2003.

(38) Makuc, D.; Szacilowski, K.; Plavec, J.; Magri, D. C. Water-Soluble Colorimetric Amino[Bis(Ethanesulfonate)] Azobenzene PH Indicators: A UV-Vis Absorption, DFT, and 1 H- 15 N NMR Spectroscopy Study. *ACS Omega* **2017**, *2* (9), 6159–6166. https://doi.org/10.1021/acsomega.7b00887.

(39) Dorel, R.; Feringa, B. L. Photoswitchable Catalysis Based on the Isomerisation of Double Bonds. *Chem. Commun.* **2019**, *55* (46), 6477–6486. https://doi.org/10.1039/c9cc01891c.

(40) Abbaszad Rafi, A.; Hamidi, N.; Bashir-Hashemi, A.; Mahkam, M. Photo-Switchable Nanomechanical Systems Comprising a Nanocontainer (Montmorillonite) and Light-Driven Molecular Jack (Azobenzene-Imidazolium Ionic Liquids) as Drug Delivery Systems; Synthesis, Characterization, and in Vitro Release Studies. *ACS Biomater. Sci. Eng.* **2018**, *4* (1), 184–192. https://doi.org/10.1021/acsbiomaterials.7b00621.

(41) Wegener, M.; Hansen, M. J.; Driessen, A. J. M.; Szymanski, W.; Feringa, B. L. Photocontrol of Antibacterial Activity: Shifting from UV to Red Light Activation. *J. Am. Chem. Soc.* **2017**, *139* (49), 17979–17986. https://doi.org/10.1021/jacs.7b09281.

(42) Beharry, A. A.; Woolley, G. A. Azobenzene Photoswitches for Biomolecules. *Chem. Soc. Rev.* **2011**, *40* (8), 4422–4437. https://doi.org/10.1039/c1cs15023e.

(43) Wagner-Wysiecka, E.; Łukasik, N.; Biernat, J. F.; Luboch, E. Azo Group(s) in Selected Macrocyclic Compounds; Springer Netherlands, **2018**; Vol. 90. https://doi.org/10.1007/s10847-017-0779-4.

(44) Pedersen, C. J. Cyclic Polyethers and Their Complexes with Metal Salts. *J. Am. Chem. Soc.* **1967**, *89* (10), 2495–2496. https://doi.org/10.1021/ja00986a052.

(45) Cram, D. J.; Lehn, J.-M.; Pedersen, C. J. The Nobel Prize in Chemistry 1987 https://www.nobelprize.org/prizes/chemistry/1987/summary/.

(46) Feringa, B. L.; Sauvage Jean-Pierre; J.Fraser, S. S. The Nobel Prize in Chemistry 2016 https://www.nobelprize.org/prizes/chemistry/2016/summary/.

(47) Kolesnichenko, I. V.;Anslyn, E. V. Practical Applications of Supramolecular Chemistry. *Chem. Soc. Rev.* **2017**, *46* (9), 2385–2390. https://doi.org/10.1039/c7cs00078b.

(48) Liu, M.; Zhang, L.; Wang, T. Supramolecular Chirality in Self-Assembled Systems. *Chem. Rev.* **2015**, *115* (15), 7304–7397. https://doi.org/10.1021/cr500671p.

(49) Hegstrom, R. A.; Kondepudi, D. The Handedness of the Universe. *Sci. Am.* **1990**, *262*, 108–115.

(50) Whitesides, G. M.; Boncheva, M. Beyond Molecules: Self-Assembly of Mesoscopic and Macroscopic Components. *Proc. Natl. Acad. Sci. U. S. A.* **2002**, *99* (8), 4769. https://doi.org/10.1073/PNAS.082065899.

(51) Yin, L.; Liu, M.; Zhao, Y.; Zhang, S.; Zhang, W.; Zhang, Z.; Zhu, X. Supramolecular Chirality Induced by Chiral Solvation in Achiral Cyclic Azo-Containing Polymers: Topological Effects on Chiral Aggregation. *Polym. Chem.* **2018**, *9* (6), 769–776. https://doi.org/10.1039/c7py02002c.

(52) Wagner-Wysiecka, E.; Rzymowski, T.; Szarmach, M.; Fonari, M. S.; Luboch, E. Functionalized Azobenzocrown Ethers as Sensor Materials - The Synthesis and Ion Binding Properties. *Sensors Actuators, B Chem.* **2013**, *177*, 913–923. https://doi.org/10.1016/j.snb.2012.11.068.

(53) Shinkai, S.; Nakaji, T.; Ogawa, T.; Shigematsu, K.; Manabe, O. Photoresponsive Crown Ethers. 2. Photocontrol of Ion Extraction and Ion Transport by a Bis(Crown Ether) with a Butterfly-like Motion. *J. Am. Chem. Soc.* **1981**, *103* (1), 111–115. https://doi.org/10.1021/ja00391a021.

(54) Akdag, A.; Worley, S. D.; Acevedo, O.; McKee, M. L. Mechanism of 5,5-Dimethylhydantoin Chlorination: Monochlorination through a Dichloro Intermediate. *J. Chem. Theory Comput.* **2007**, *3* (6), 2282–2289. https://doi.org/10.1021/ct7001804.

(55) Paris, E.; Bigi, F.; Cauzzi, D.; Maggi, R.; Maestri, G. Oxidative Dimerization of Anilines with Heterogeneous Sulfonic Acid Catalysts. *Green Chem.* **2018**, *20* (2), 382–386. https://doi.org/10.1039/c7gc03060f.

(56) Habraken, E. R. M.; van der Zee, L. J. C.; van de Vrande, K. N. A.; Jupp, A. R.; Nieger, M.; Ehlers, A. W.; Slootweg, J. C. Facile Synthesis of Tuneable Azophosphonium Salts. *Eur. J. Inorg. Chem.* **2019**, *2019* (11), 1594–1603. https://doi.org/10.1002/ejic.201801546.

(57) Wang, J.; Zhuang, G.; Chen, M.; Lu, D.; Li, Z.; Huang, Q.; Jia, H.; Cui, S.; Shao, X.; Yang, S.; Du, P. Selective Synthesis of Conjugated Chiral Macrocycles: Sidewall Segments of (−)/(+)-(12,4) Carbon Nanotubes with Strong Circularly Polarized Luminescence. *Angew. Chemie - Int. Ed.* **2020**, *59* (4), 1619–1626. https://doi.org/10.1002/anie.201909401.

(58) Yoshino, J.; Kano, N.; Kawashima, T. Fluorescent Azobenzenes and Aromatic Aldimines Featuring an N-B Interaction. *Dalt. Trans.* **2013**, *42* (45), 15826–15834. https://doi.org/10.1039/c3dt51689j.

(59) M. J. Frisch, G. W. Trucks, H. B. Schlegel, G. E. S.; M. A. Robb, J. R. Cheeseman, G. Scalmani, V. Barone, B. M.; G. A. Petersson, H. Nakatsuji, M. Caricato, X. Li, H. P. H.; A. F. Izmaylov, J. Bloino, G. Zheng, J. L. Sonnenberg, M. H.; M. Ehara, K. Toyota, R. Fukuda, J. Hasegawa, M. Ishida, T. N.; Y. Honda, O. Kitao, H. Nakai, T. Vreven, J. A. Montgomery, J.; J. E. Peralta, F. Ogliaro, M. Bearpark, J. J. Heyd, E. B.; K. N. Kudin, V. N. Staroverov, R. Kobayashi, J. N.; K. Raghavachari, A. Rendell, J. C. Burant, S. S. Iyengar, J. T.; M. Cossi, N. Rega, J. M. Millam, M. Klene, J. E. Knox, J. B. C.; V. Bakken, C. Adamo, J. Jaramillo, R. Gomperts, R. E. S.; O. Yazyev, A. J. Austin, R. Cammi, C. Pomelli, J. W. O.; R. L. Martin, K. Morokuma, V. G. Zakrzewski, G. A. V.; P. Salvador, J. J. Dannenberg, S. Dapprich, A. D. D.; O. Farkas, J. B. Foresman, J. V. Ortiz, J. C.; and D. J. Fox, Gaussian, Inc., Wallingford CT, 2009. Gaussian 09, Revision A.02,.

(60) Bigelow, H. E.; Robinson, D. B.; Azobenzene. *Org. Synth.* **1942**, *22*, 28. https://doi.org/10.15227/orgsyn.022.0028.

(61) Babaei, M.; Clement, J. A.; Dayal, K.; Shankar, M. R. Steering with Light: Indexable Photomotility in Liquid Crystalline Polymers. *RSC Adv.* **2017**, *7* (83), 52510–52516. https://doi.org/10.1039/c7ra10619j.

(62) Müller, A.; Kobarg, H.; Chandrasekaran, V.; Gronow, J.; Sönnichsen, F. D.; Lindhorst, T. K. Synthesis of Bifunctional Azobenzene Glycoconjugates for Cysteine-Based Photosensitive Cross-Linking with Bioactive Peptides. *Chem. - A Eur. J.* **2015**, *21* (39), 13723–13731. https://doi.org/10.1002/chem.201501571.

(63) Guo, K.; Chu, C. C. Synthesis, Characterization, and Biodegradation of Novel Poly(Ether Ester Amide)s Based on L-Phenylalanine and Oligoethylene Glycol. *Biomacromolecules* **2007**, 2851–2861. https://doi.org/10.1021/bm070158c.

APPENDICES

A. NMR Spectra

NMR spectra were recorded at Bruket Avance III Ultrashield 400 Hz. $CDCl_3$ and DMSO were used as solvent in all records.

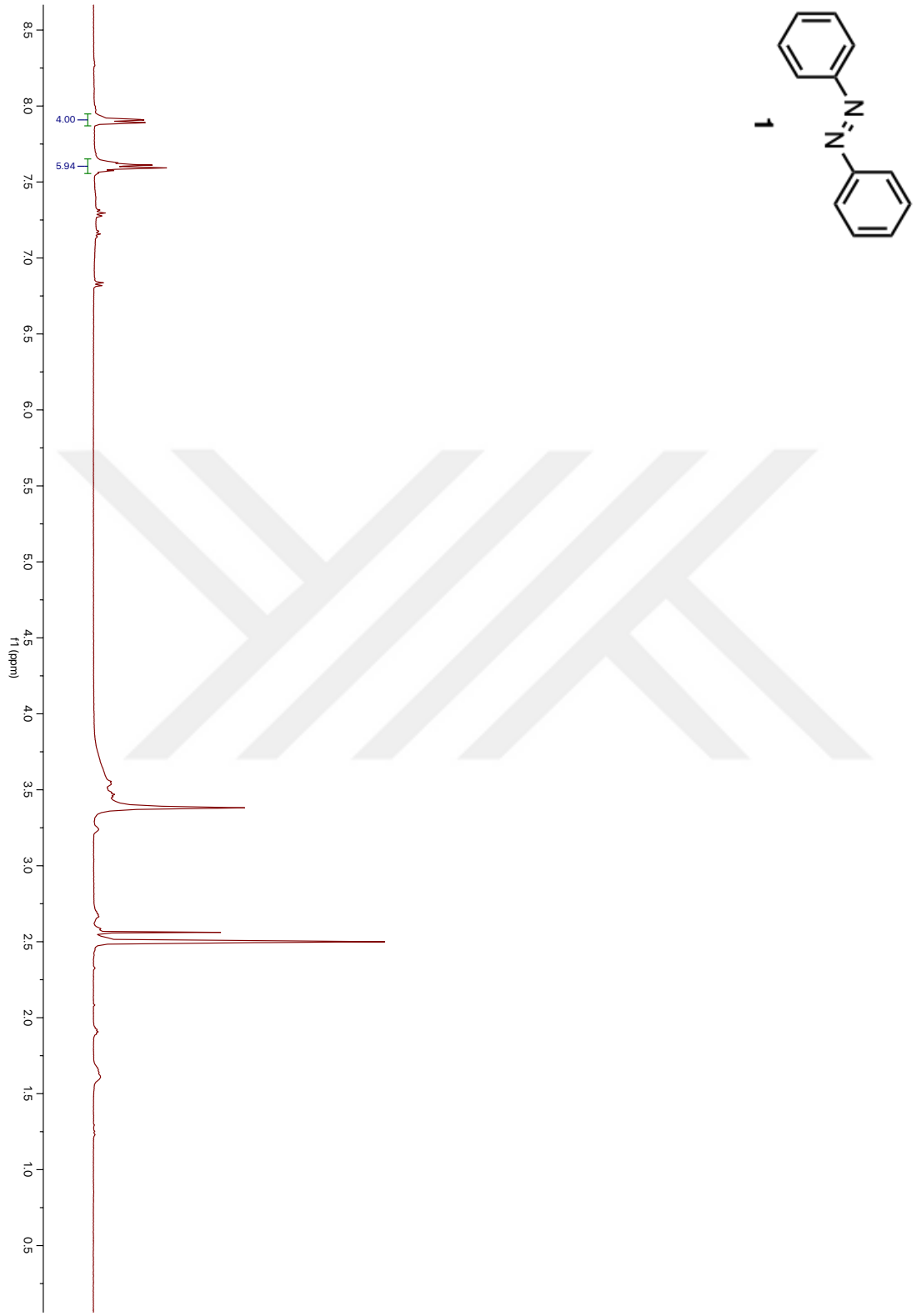

Figure 39. ^{1}H NMR Spectrum of azobenzene

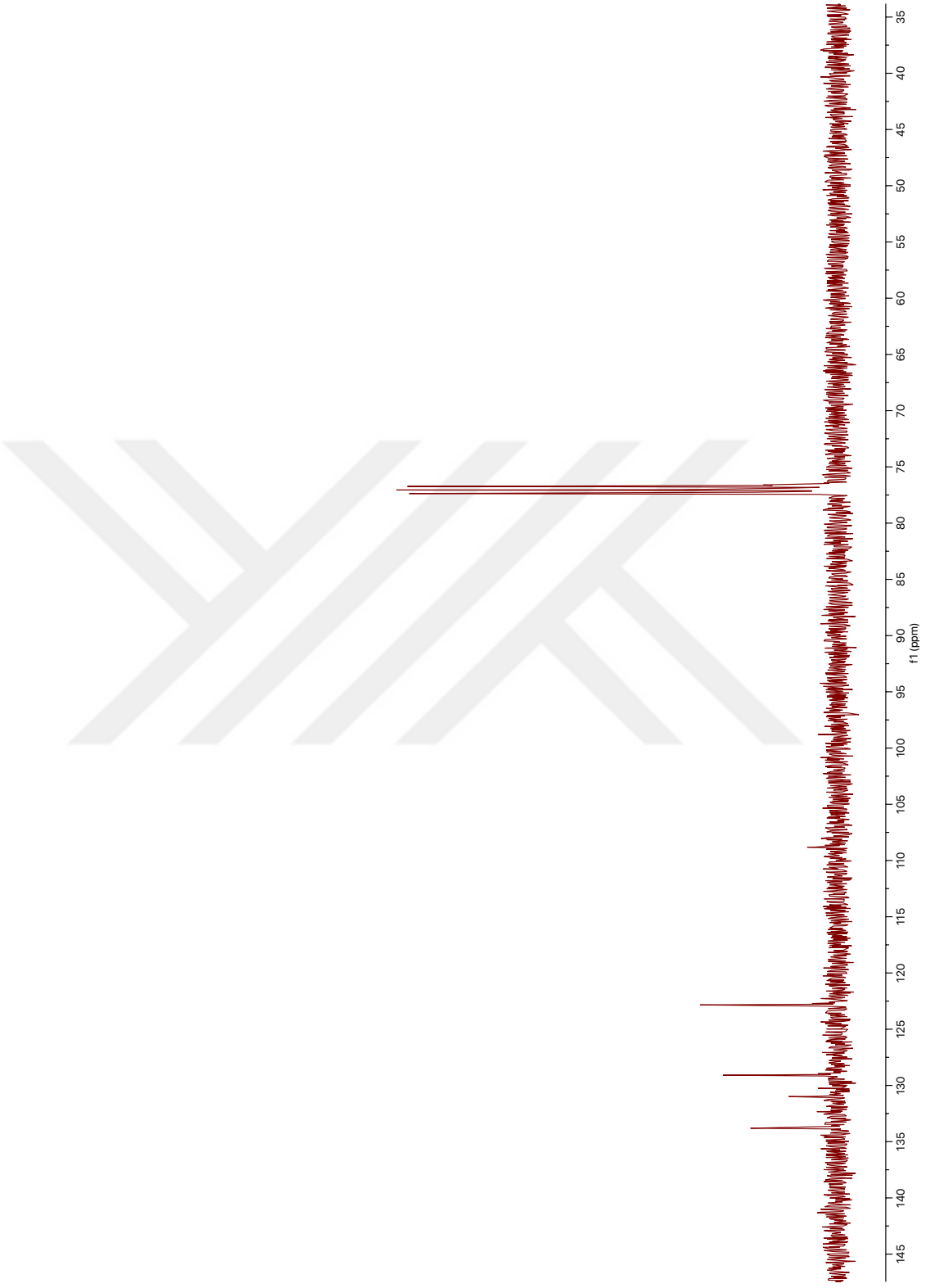

Figure 40. ^{13}C NMR Spectrum of azobenzene

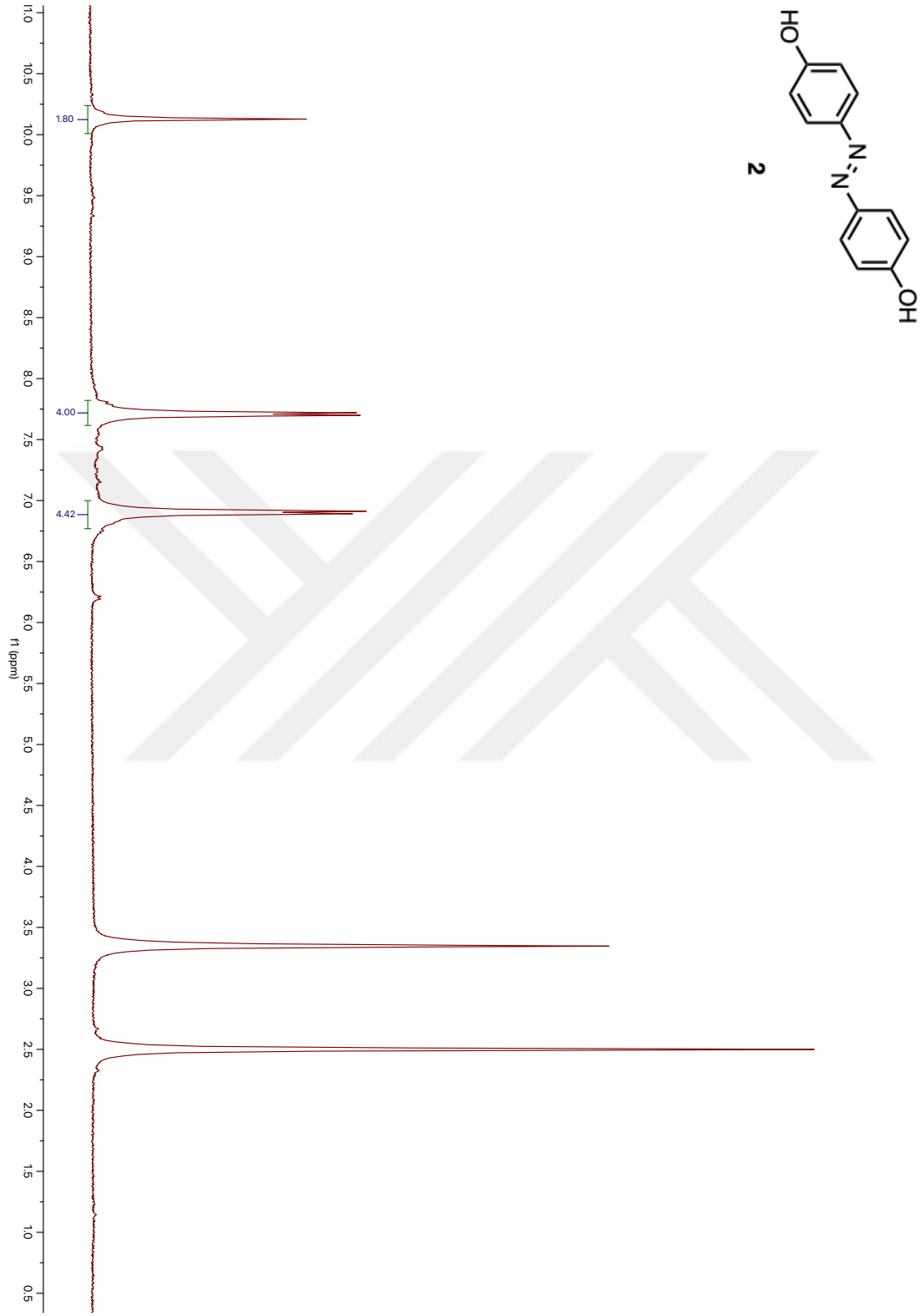

Figure 41. ^{1}H NMR Spectrum of 4,4'-dihydroxyazobenzene

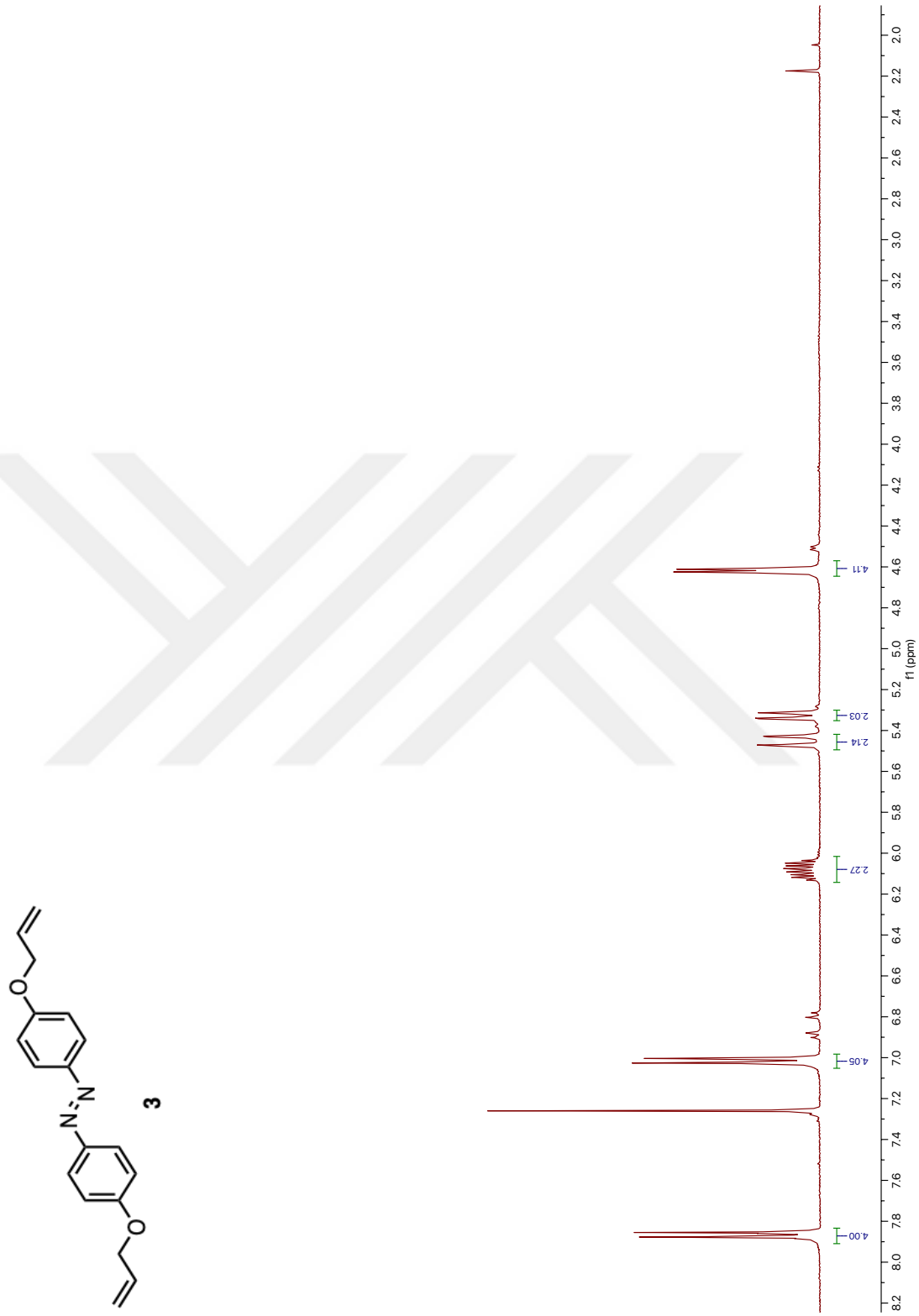

Figure 42. ^{1}H NMR Spectrum of Compound **3**

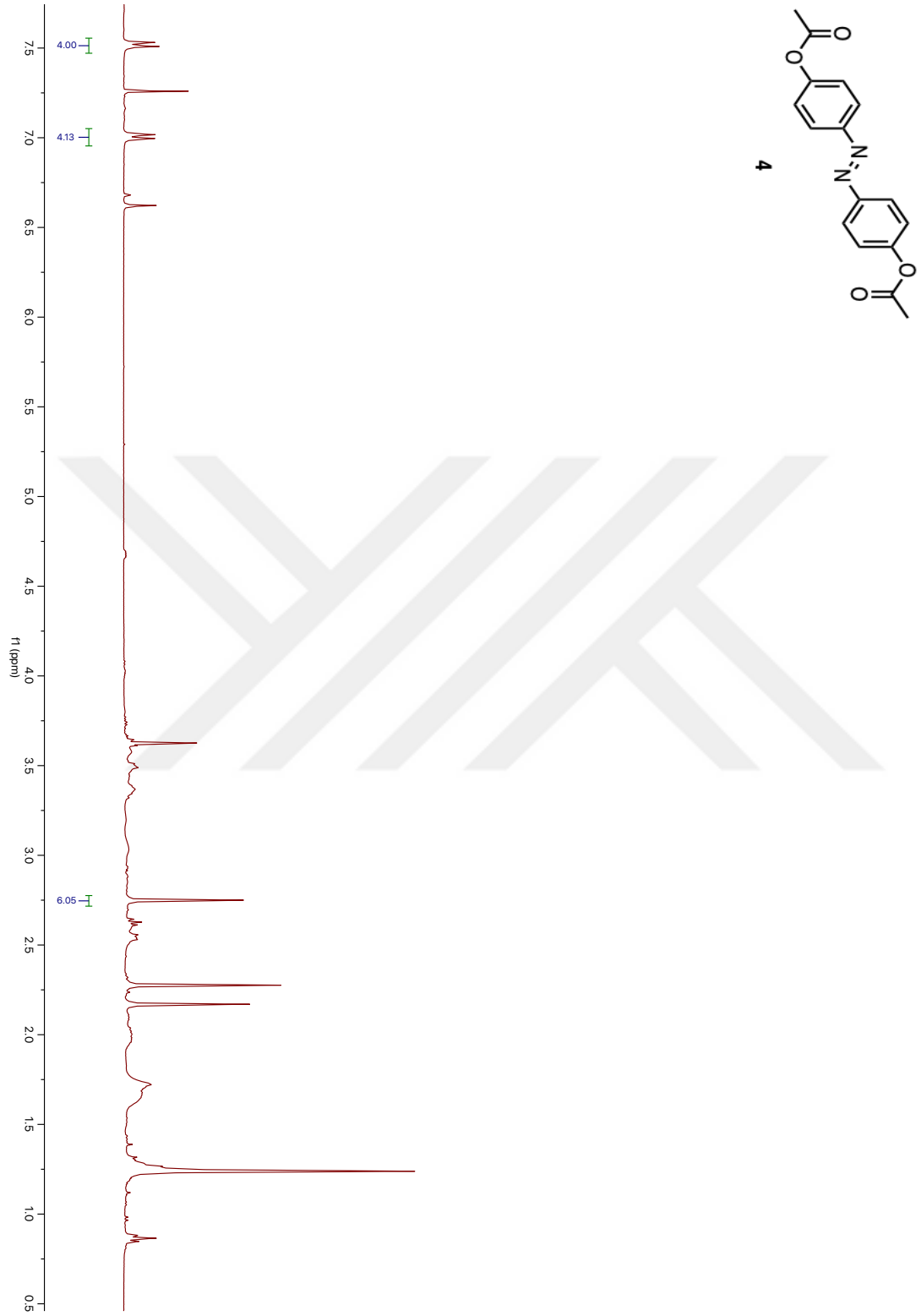

Figure 43. ^{1}H NMR Spectrum of Compound **4**

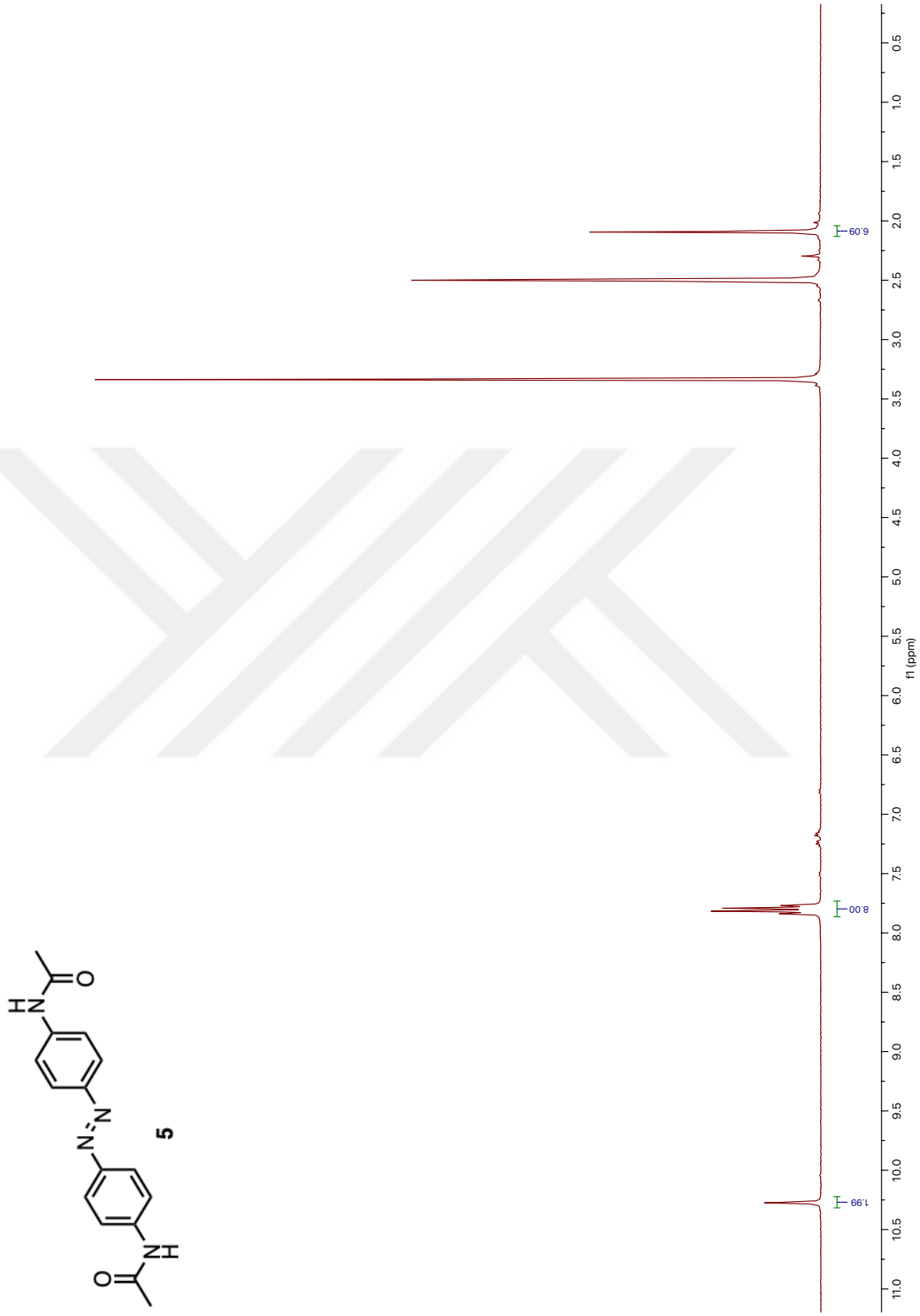

Figure 44. ^{1}H NMR Spectrum of Compound **5**

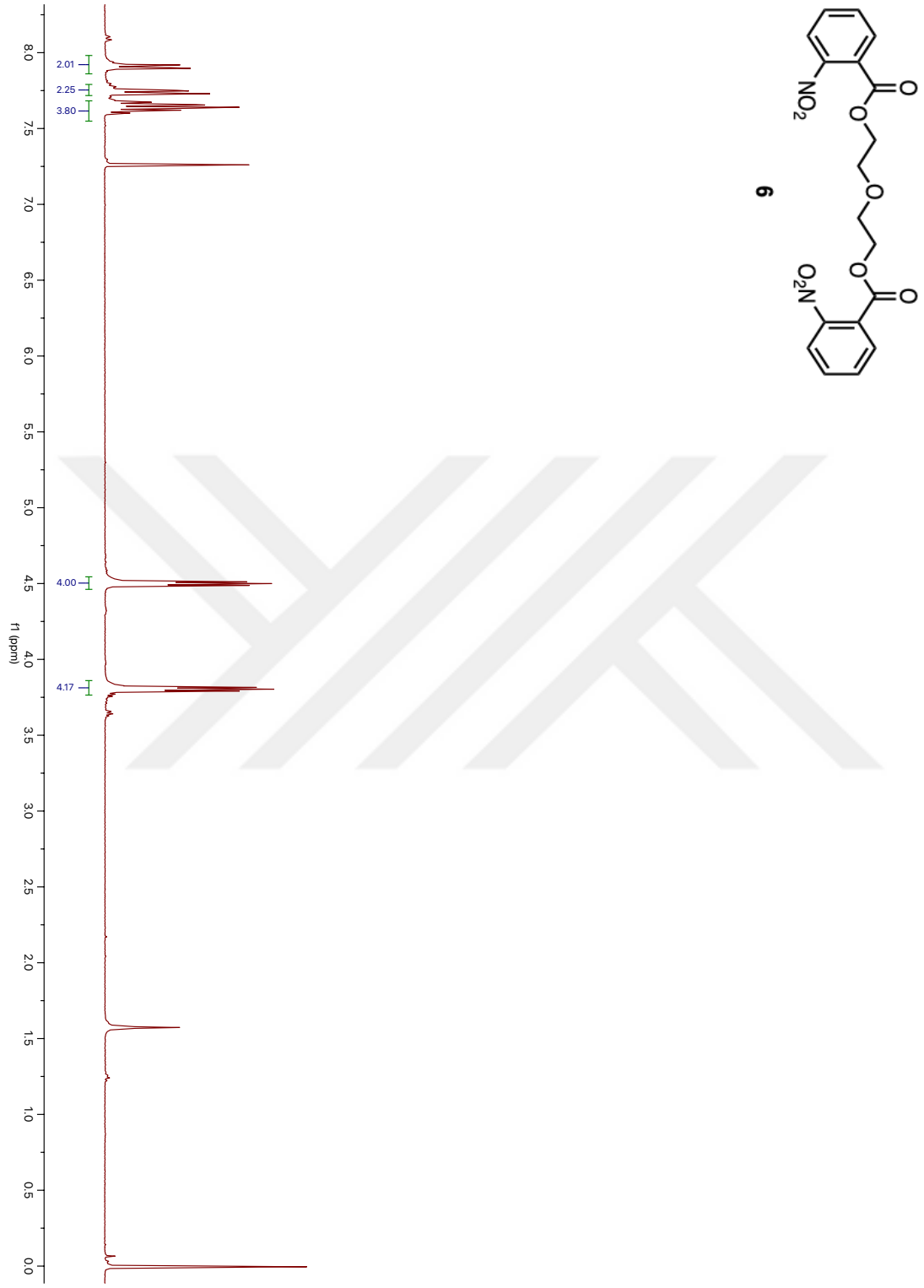

Figure 45. ^{1}H NMR Spectrum of Compound **6**

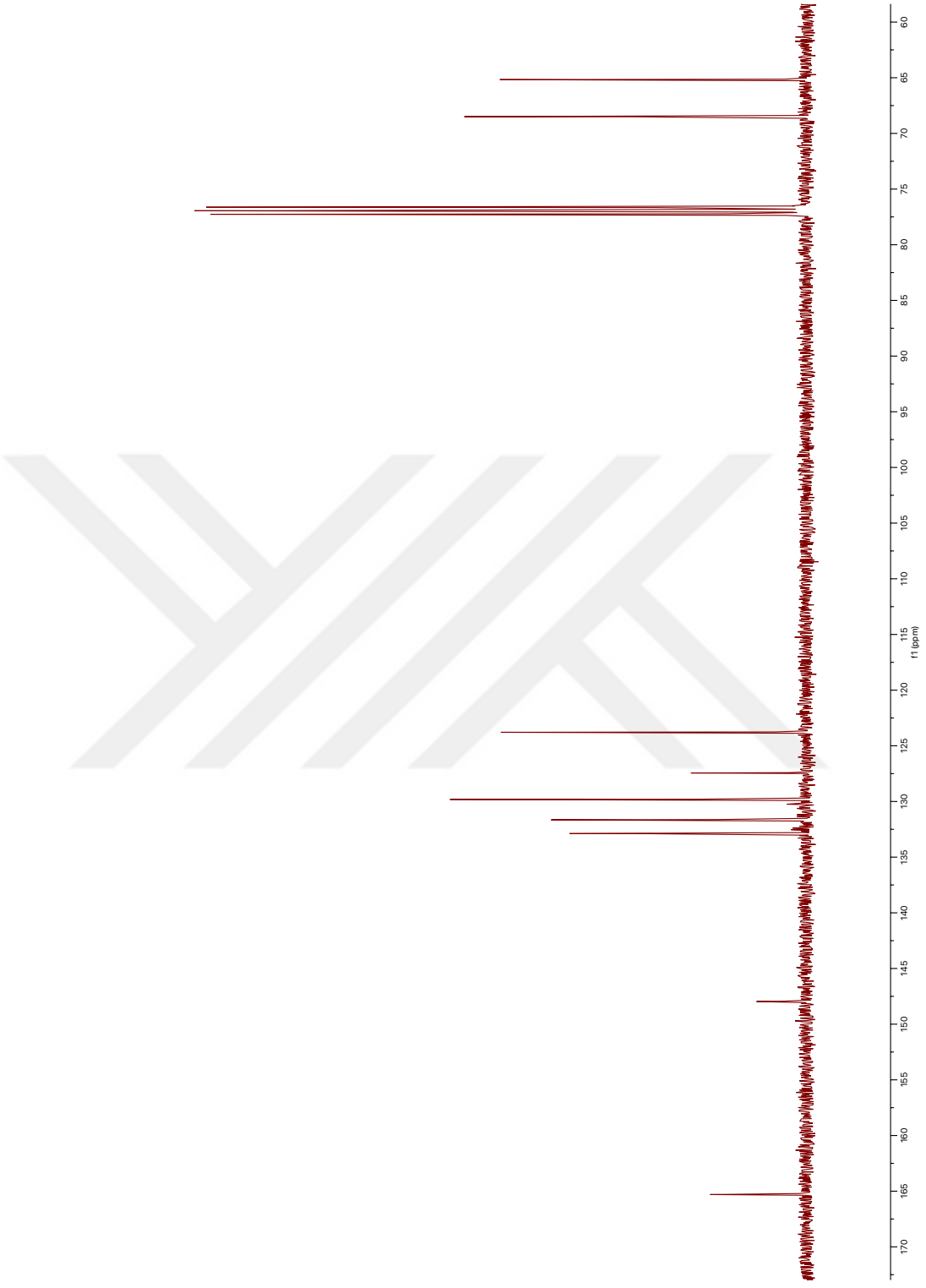

Figure 46. ^{13}C NMR Spectrum of Compound **6**

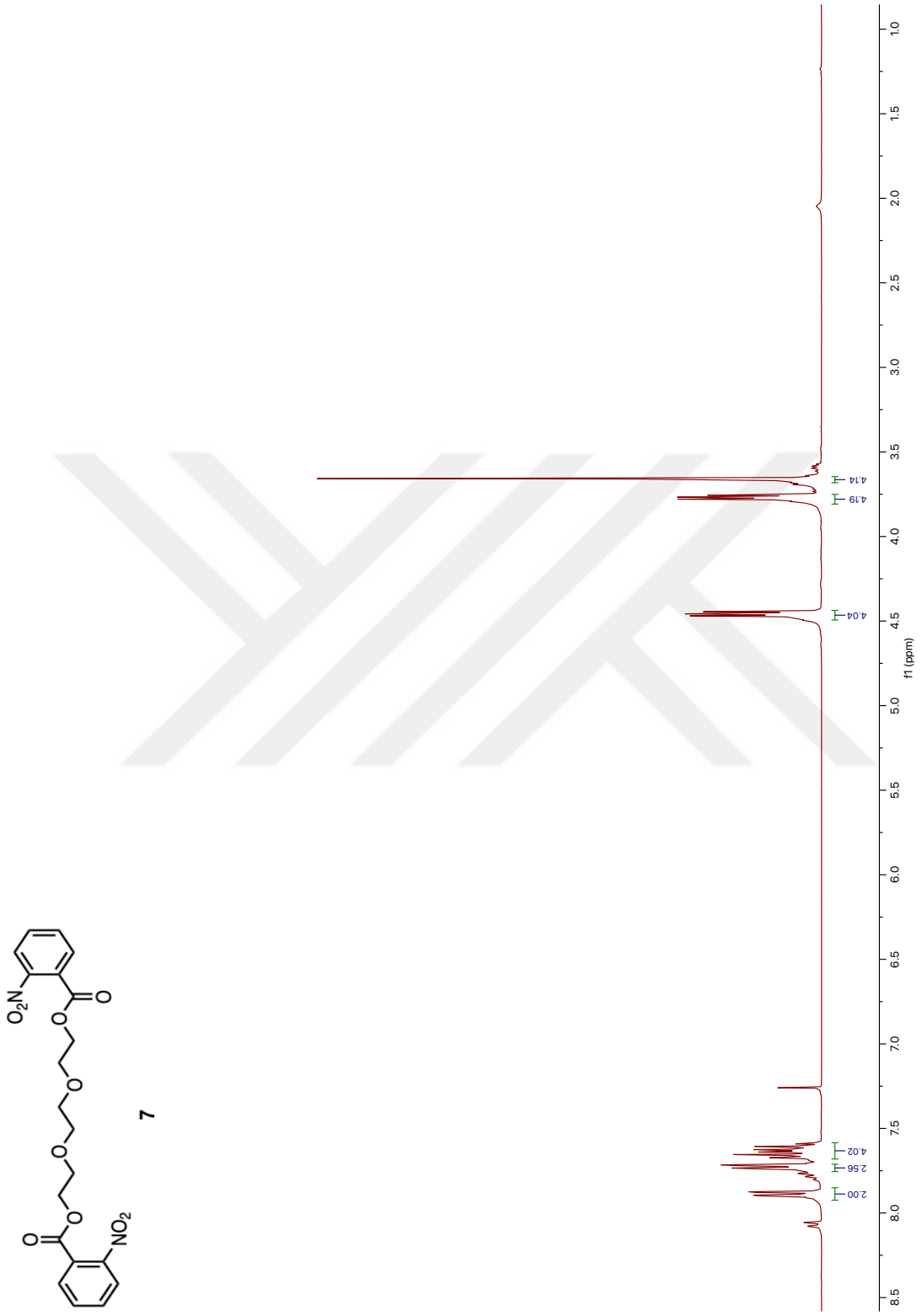

Figure 47. ^{1}H NMR Spectrum of Compound **7**

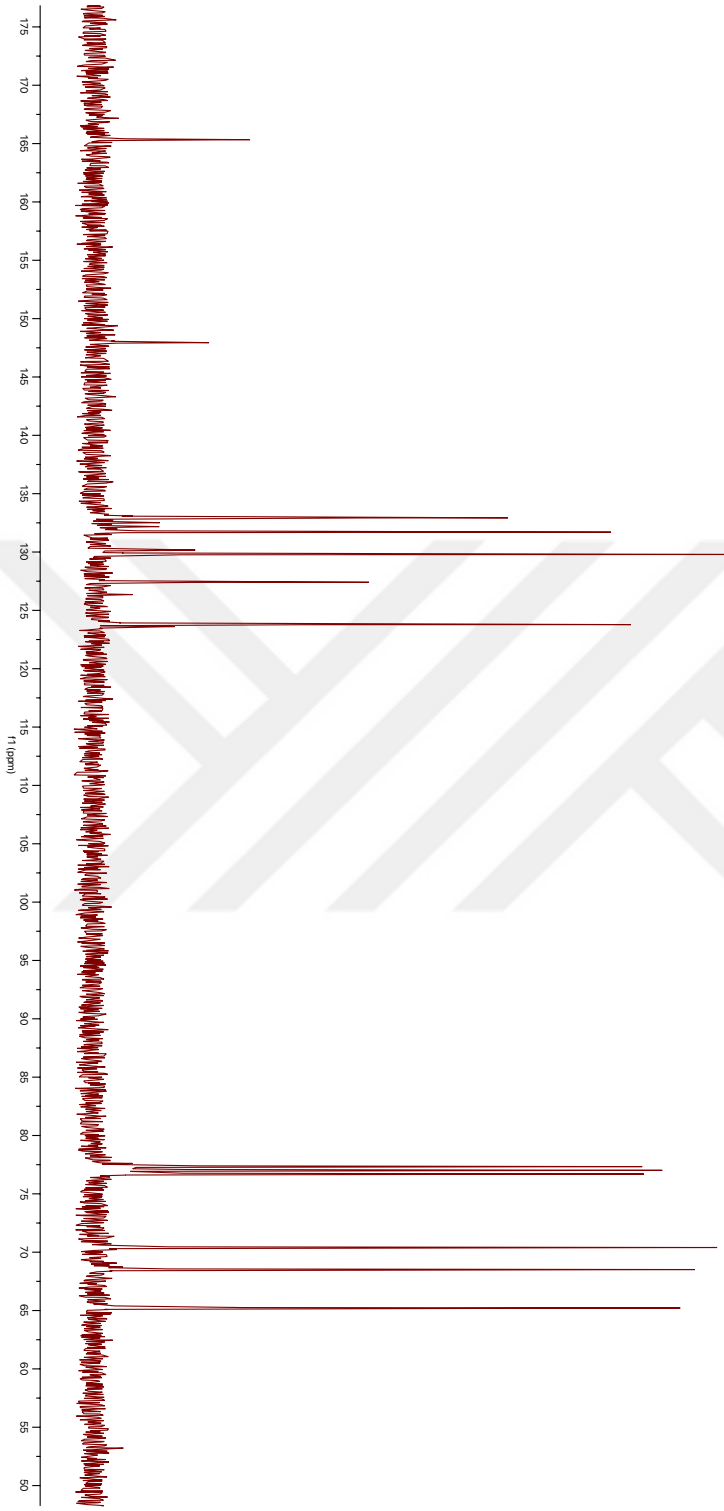

Figure 48. ^{13}C NMR Spectrum of Compound **7**

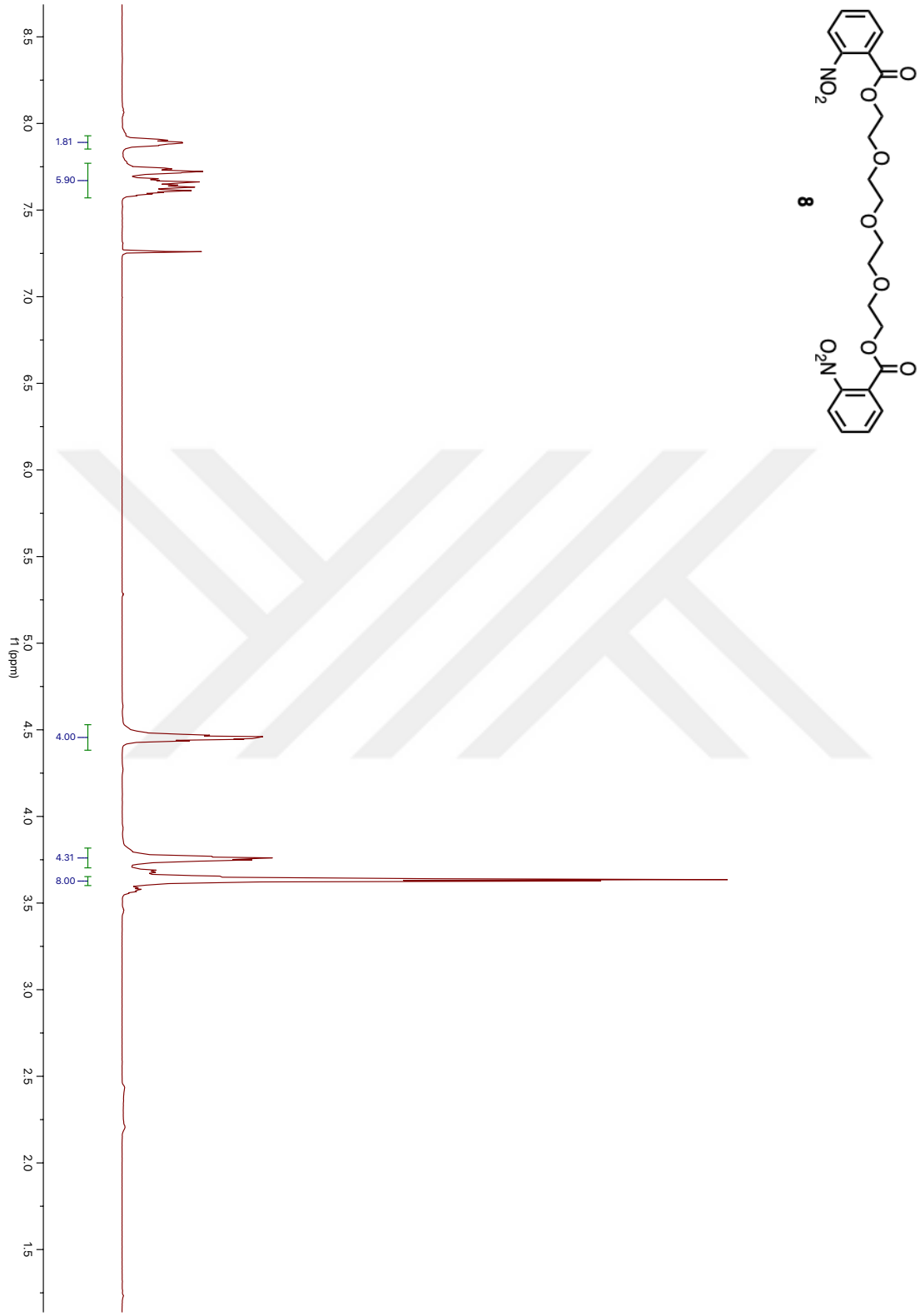

Figure 49. ^{1}H NMR Spectrum of Compound **8**

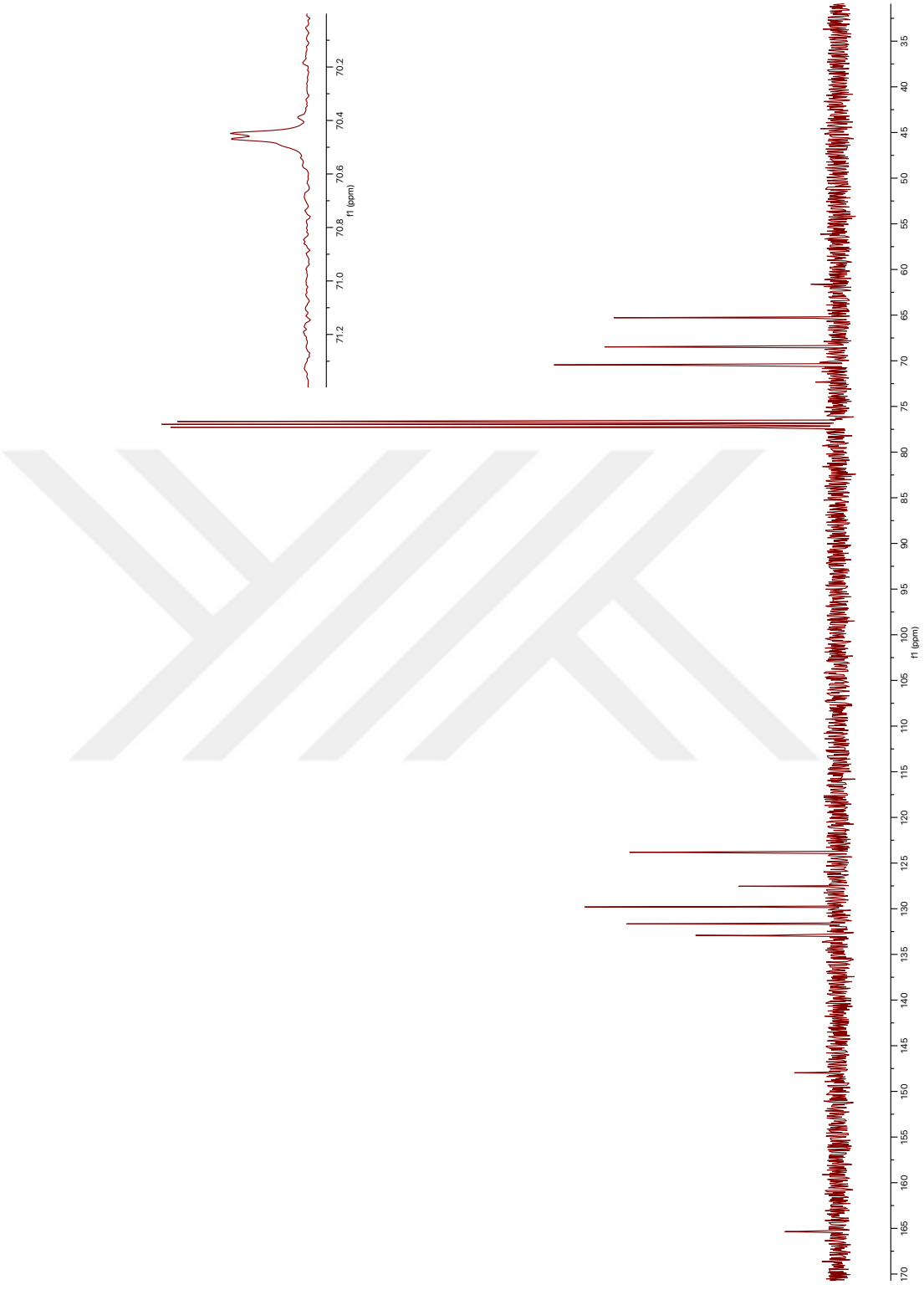

Figure 50. ^{13}C NMR Spectrum of Compound **8**

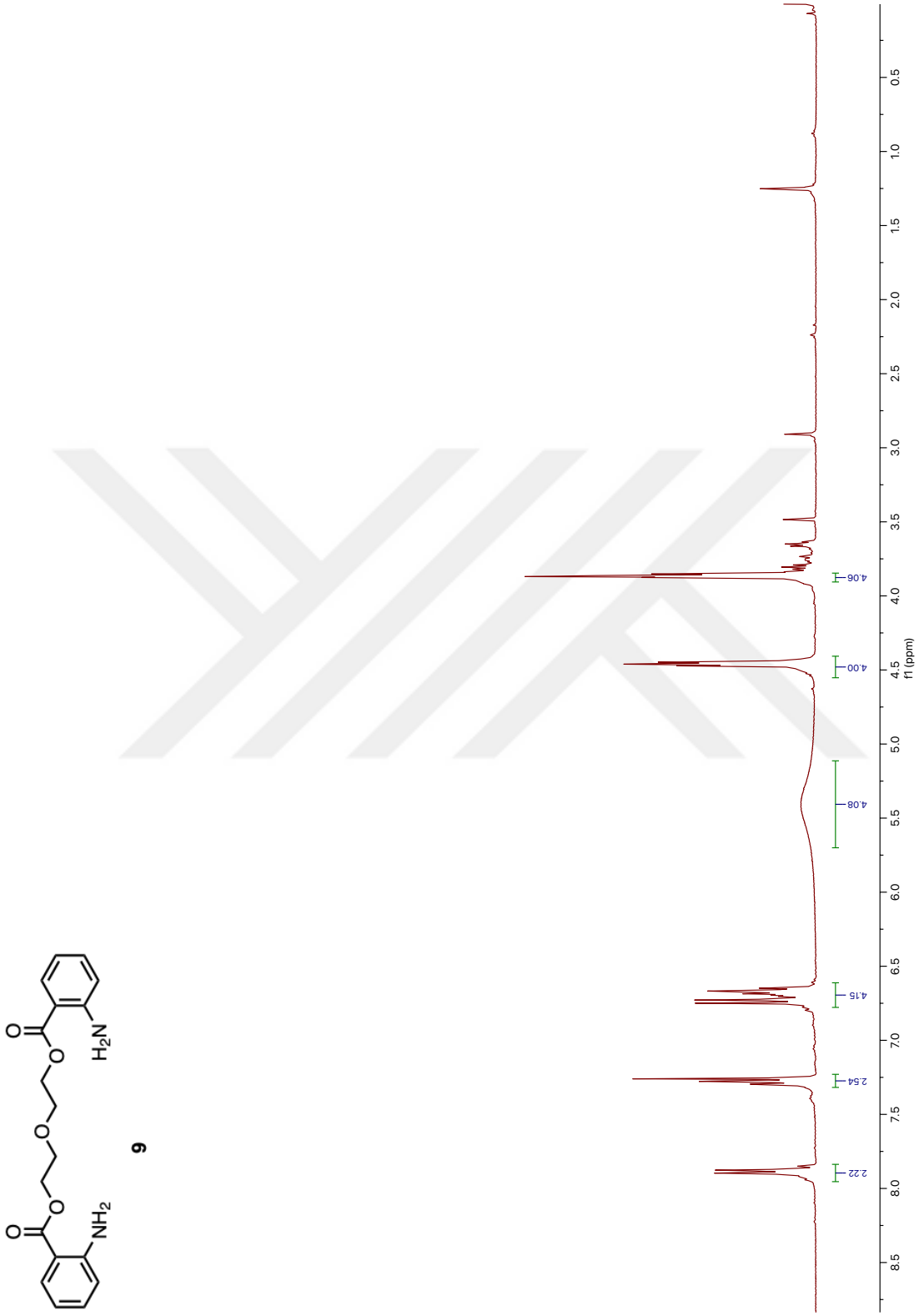

Figure 51. ^{1}H NMR Spectrum of Compound **9**

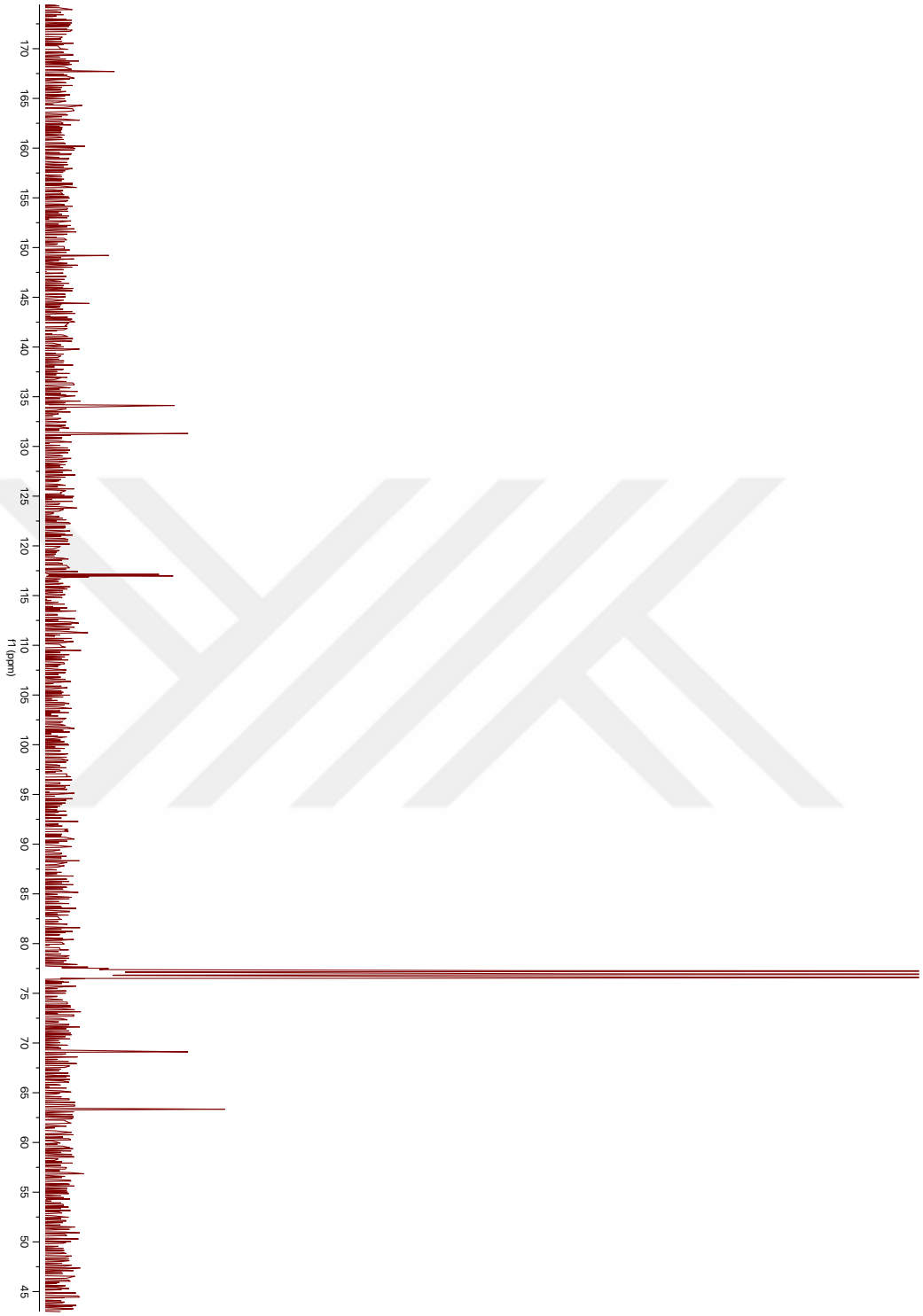

Figure 52. ^{13}C NMR Spectrum of Compound **9**

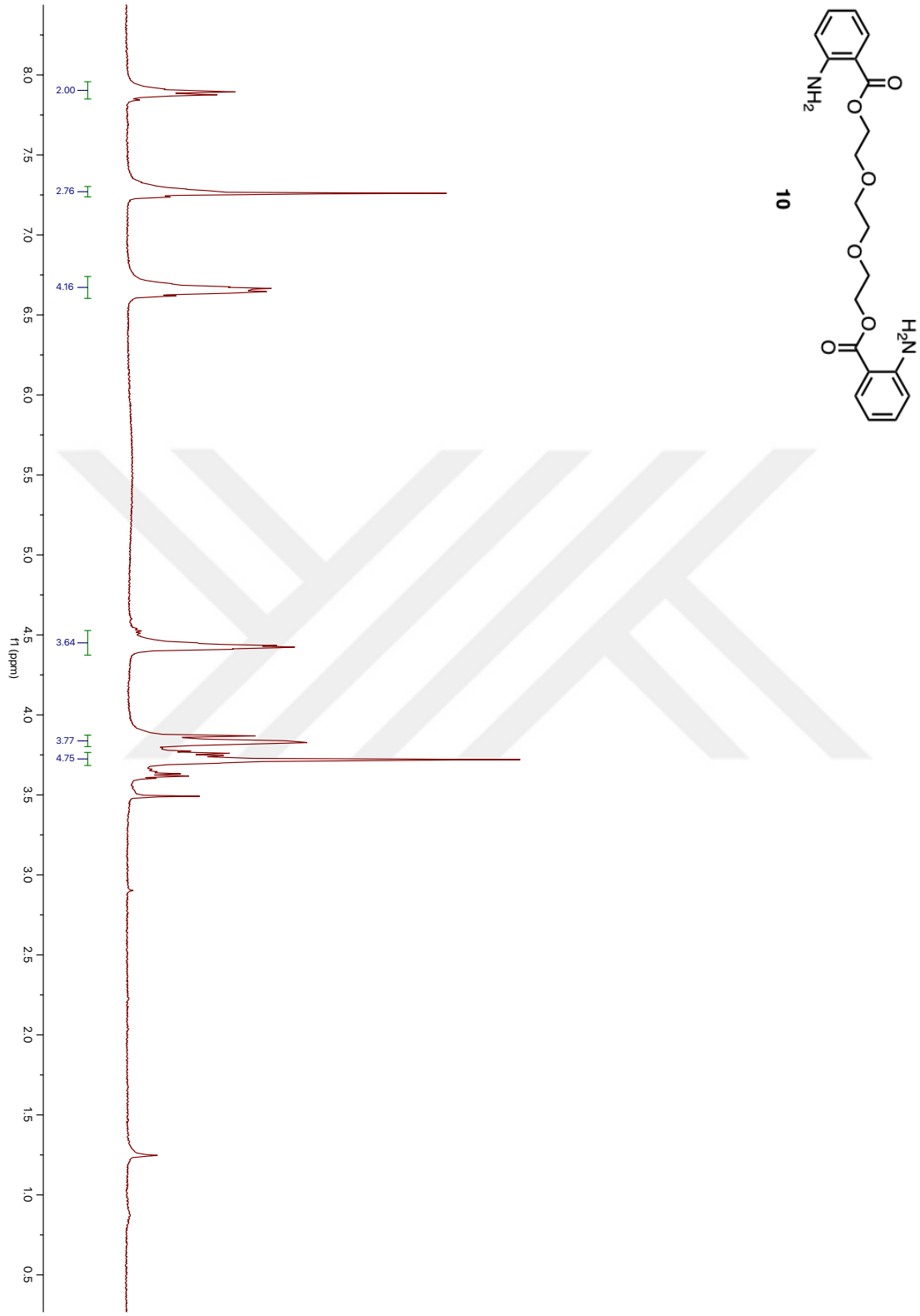

Figure 53. ^{1}H NMR Spectrum of Compound **10**

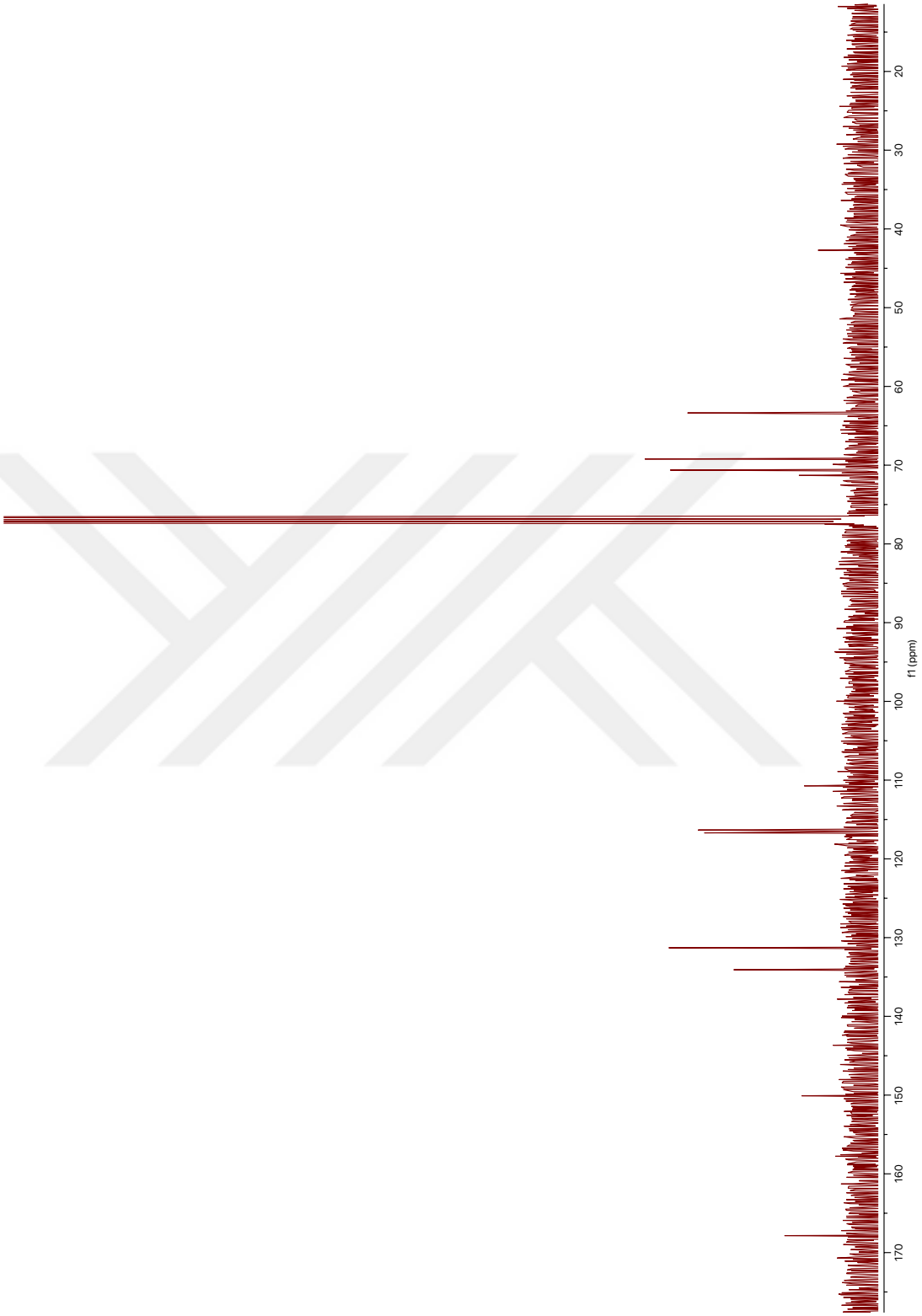

Figure 54. ^{13}C NMR Spectrum of Compound **10**

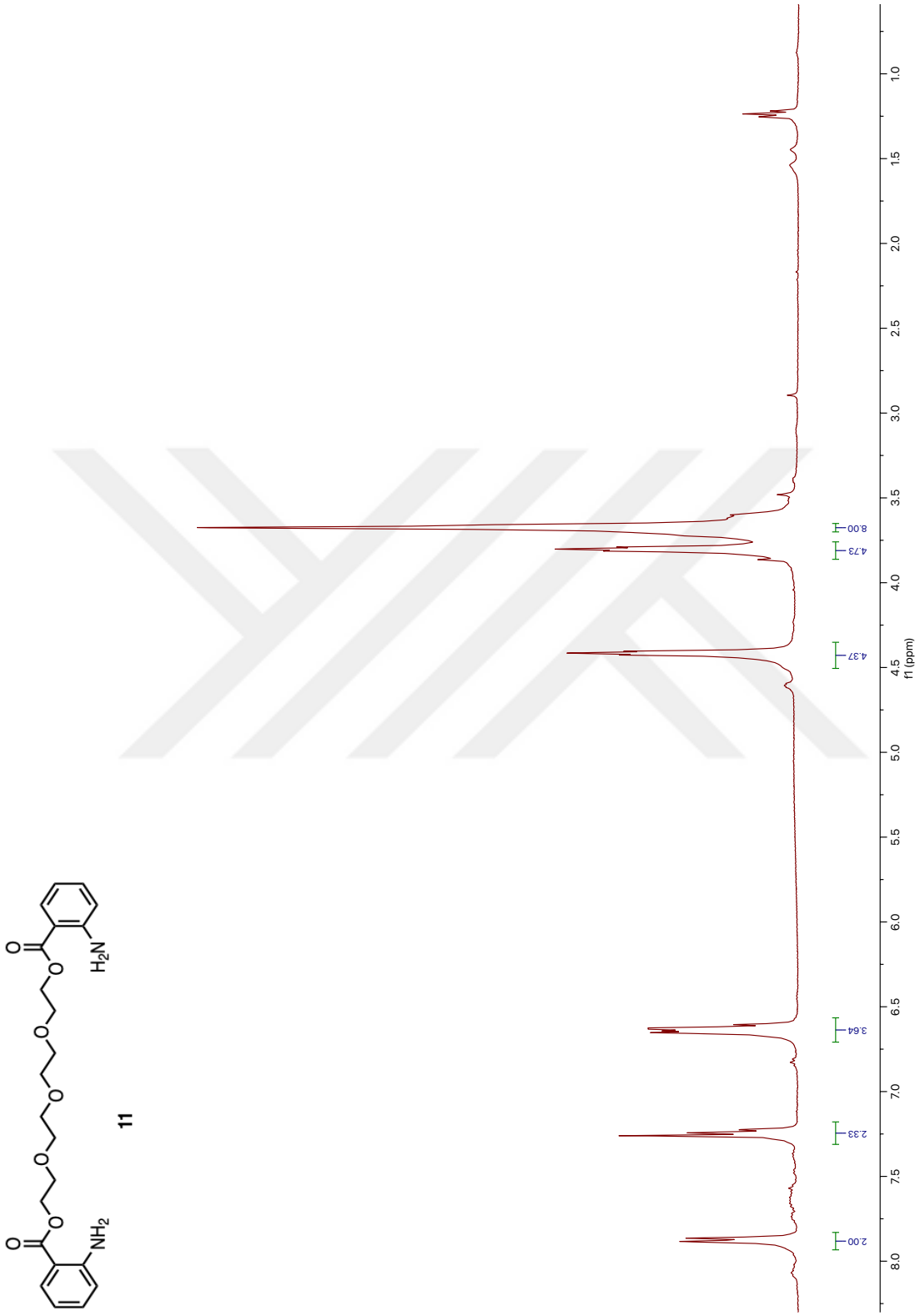

Figure 55. ^{1}H NMR Spectrum of Compound **11**

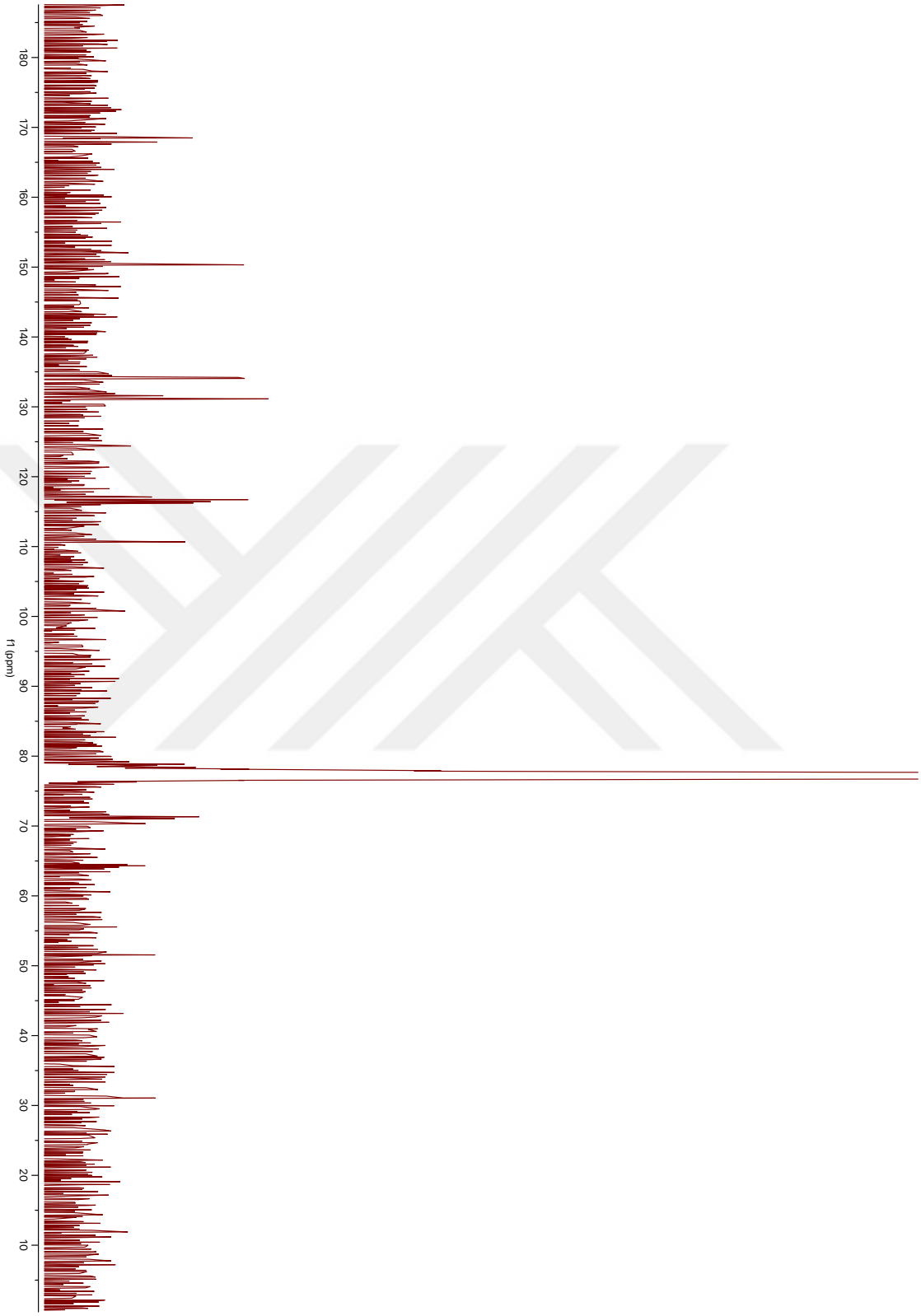

Figure 56. ^{13}C NMR Spectrum of Compound **11**

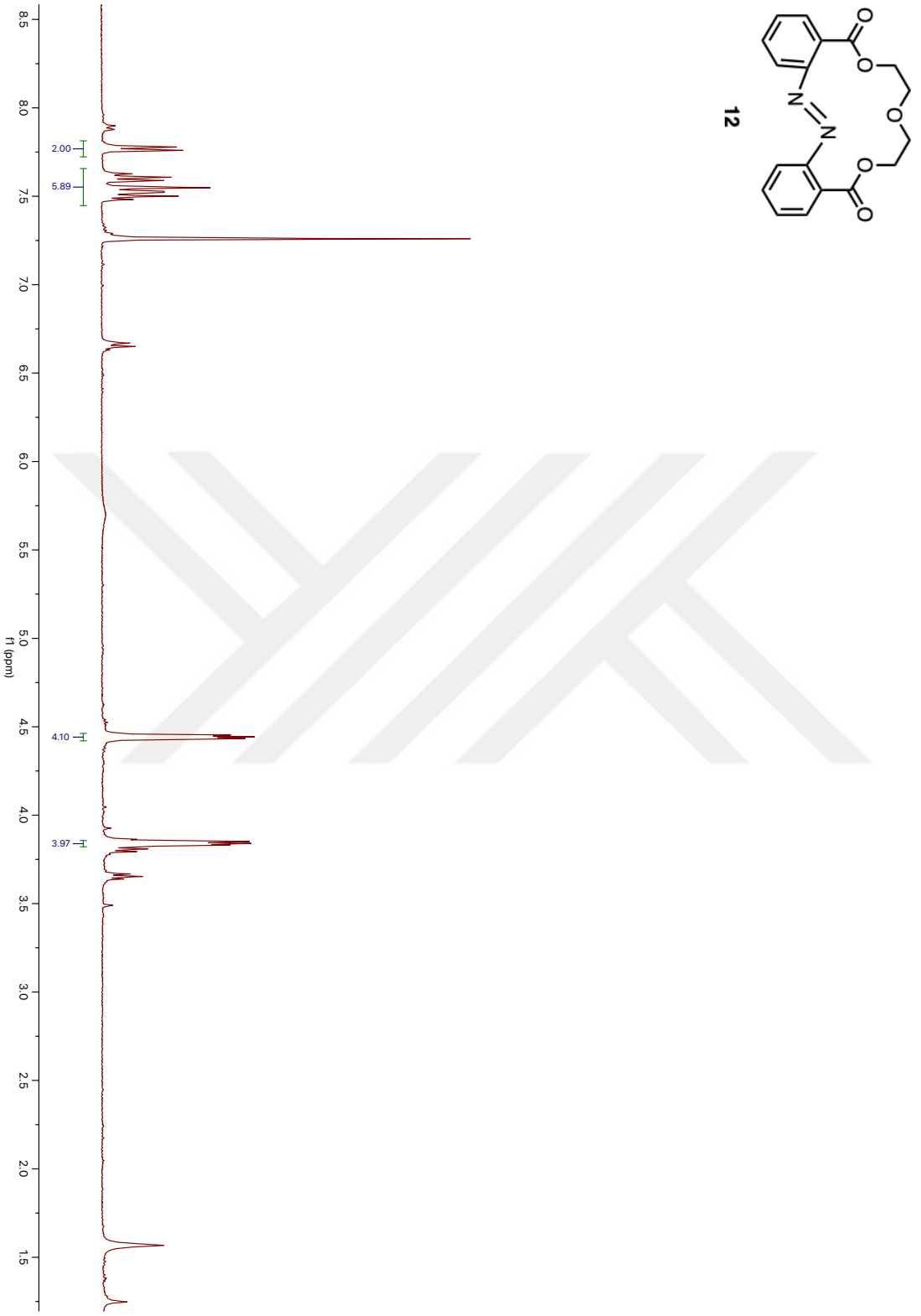

Figure 57. ^{1}H NMR Spectrum of **Cycle I**, Compound **12**

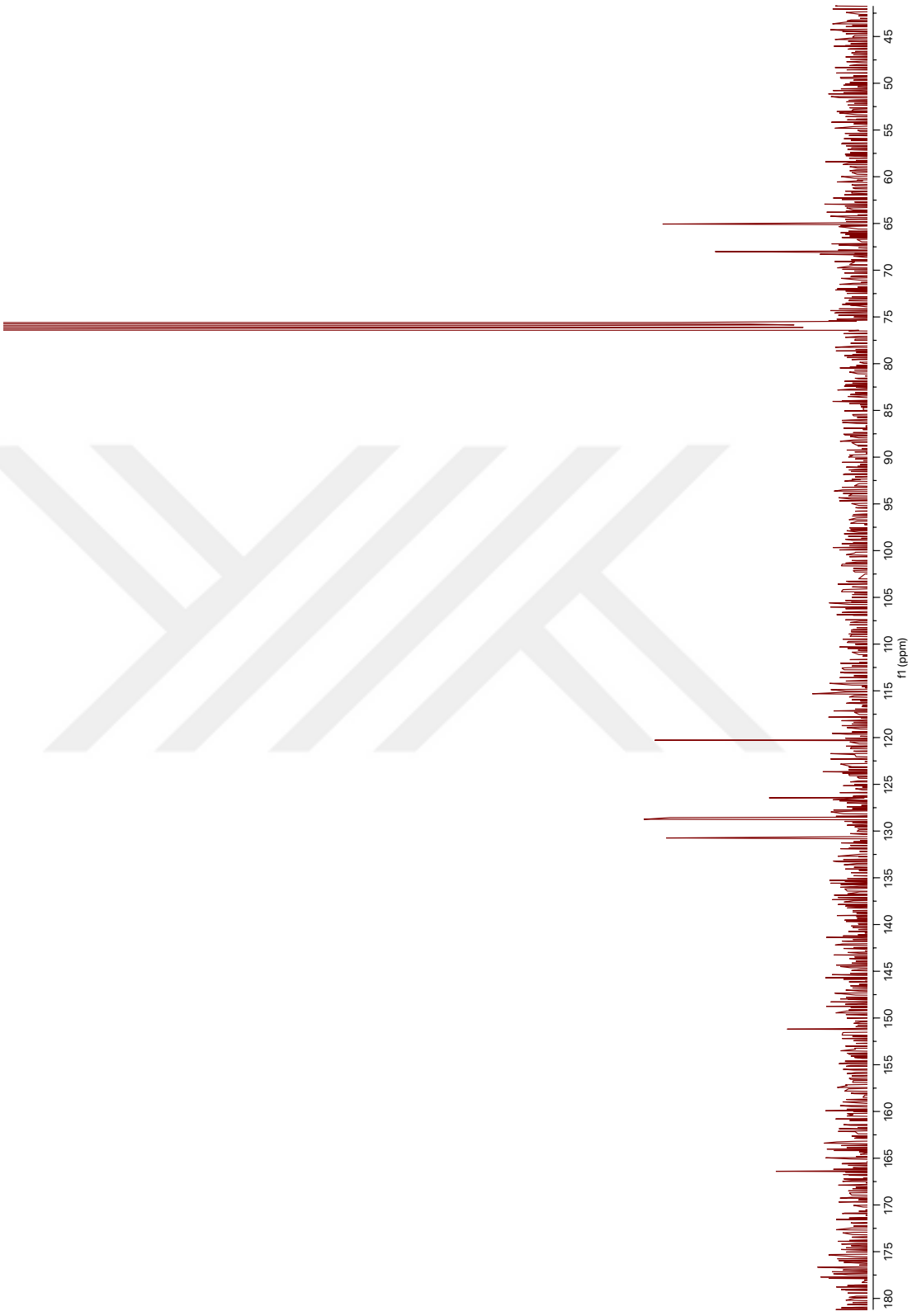

Figure 58. ^{13}C NMR Spectrum of **Cycle I**

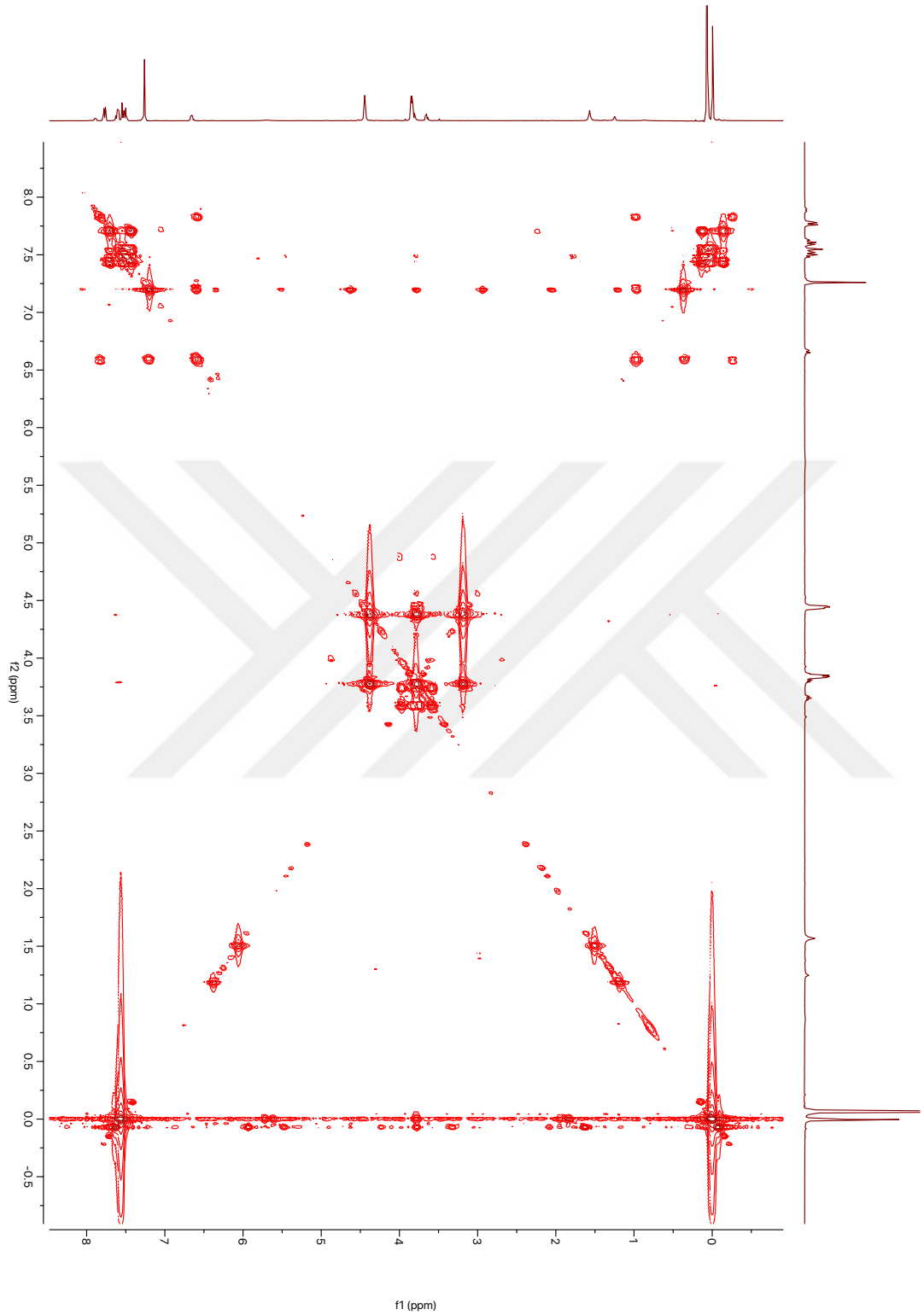

Figure 59. COSY NMR Spectrum of **Cycle I**

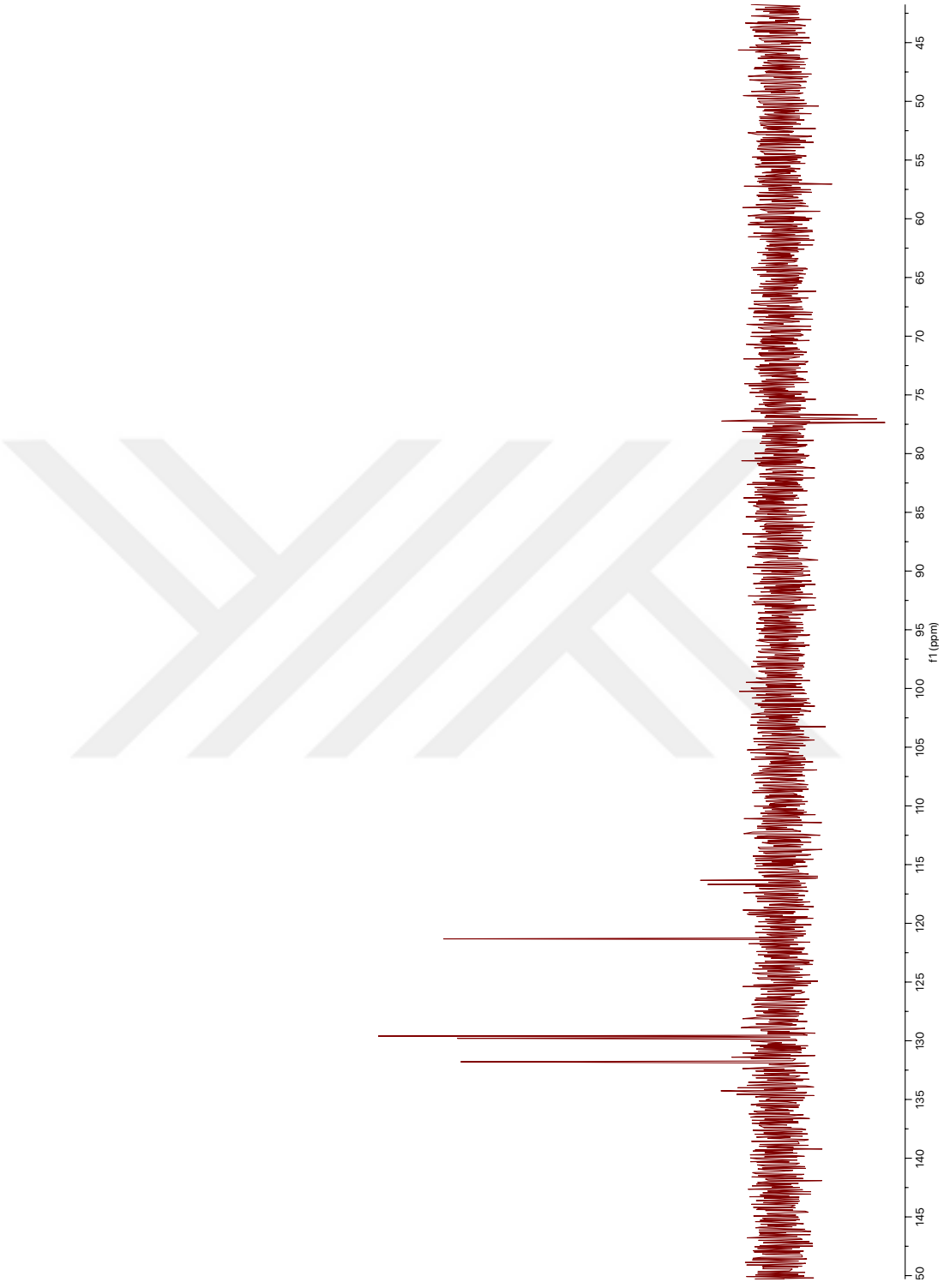

Figure 60. DEPT90 NMR Spectrum of **Cycle I**

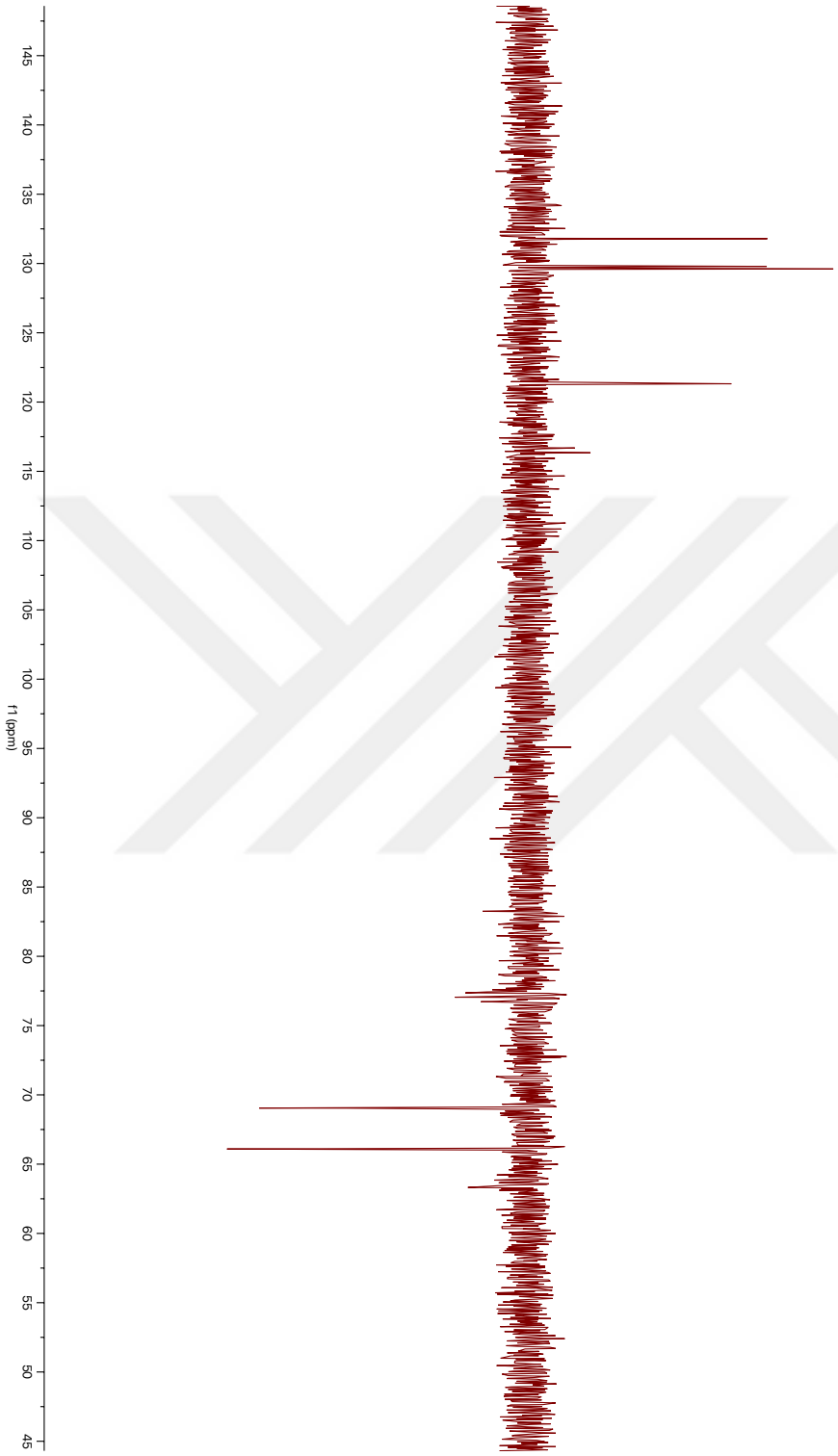

Figure 61. DEPT135 NMR Spectrum of **Cycle I**

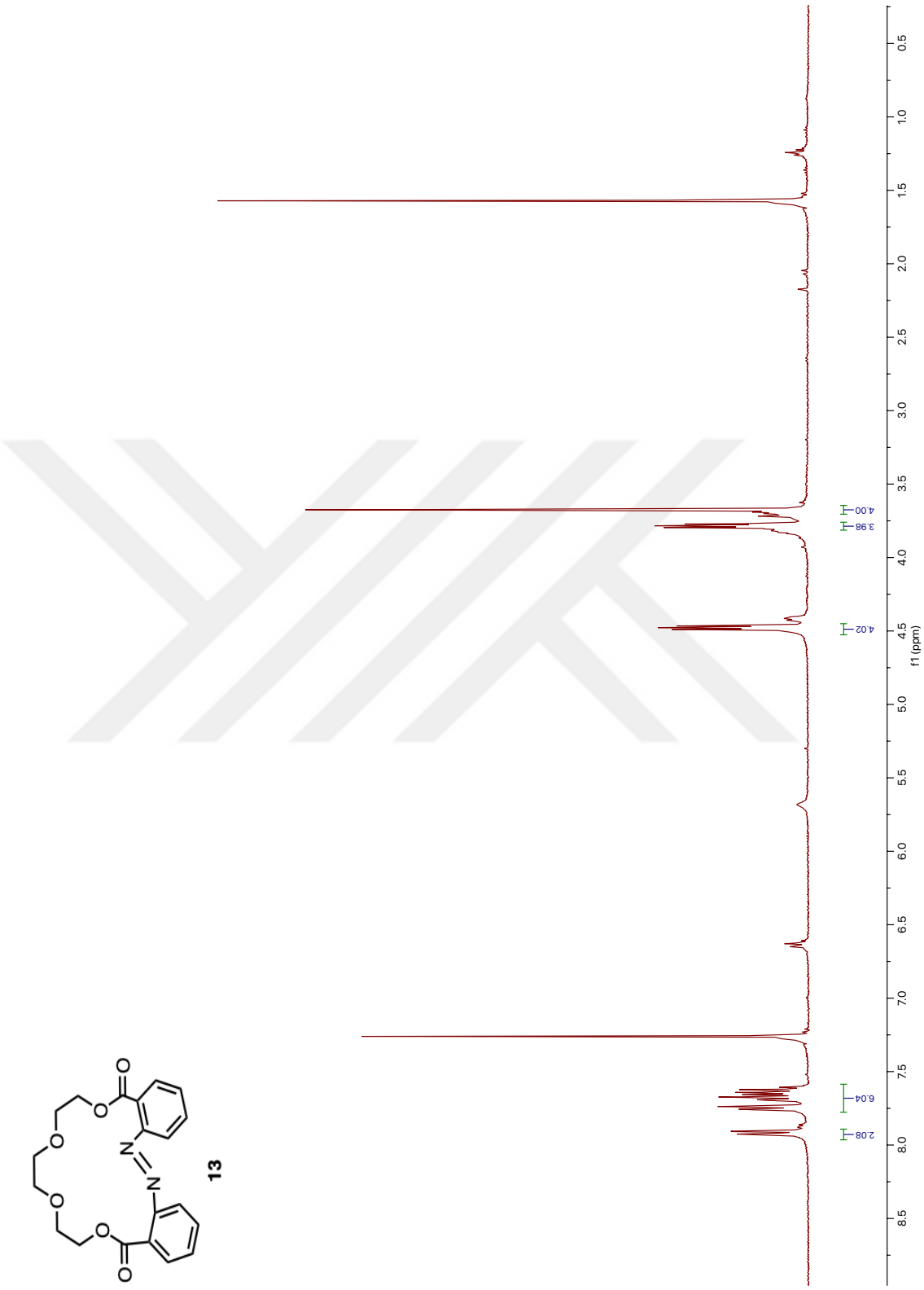

Figure 62. ^{1}H NMR Spectrum of **Cycle II,** Compound **13**

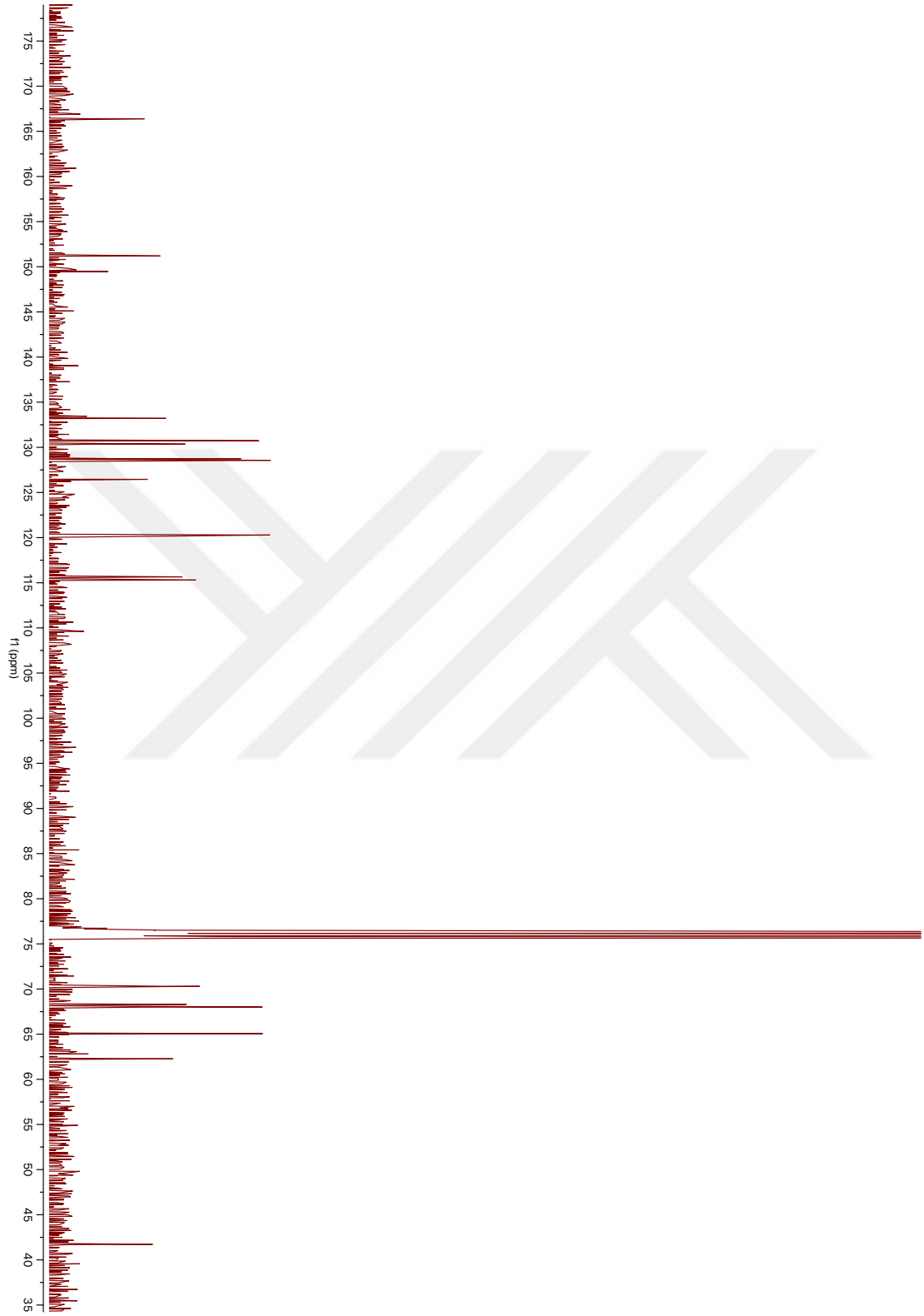

Figure 63. ^{13}C NMR Spectrum of **Cycle II**

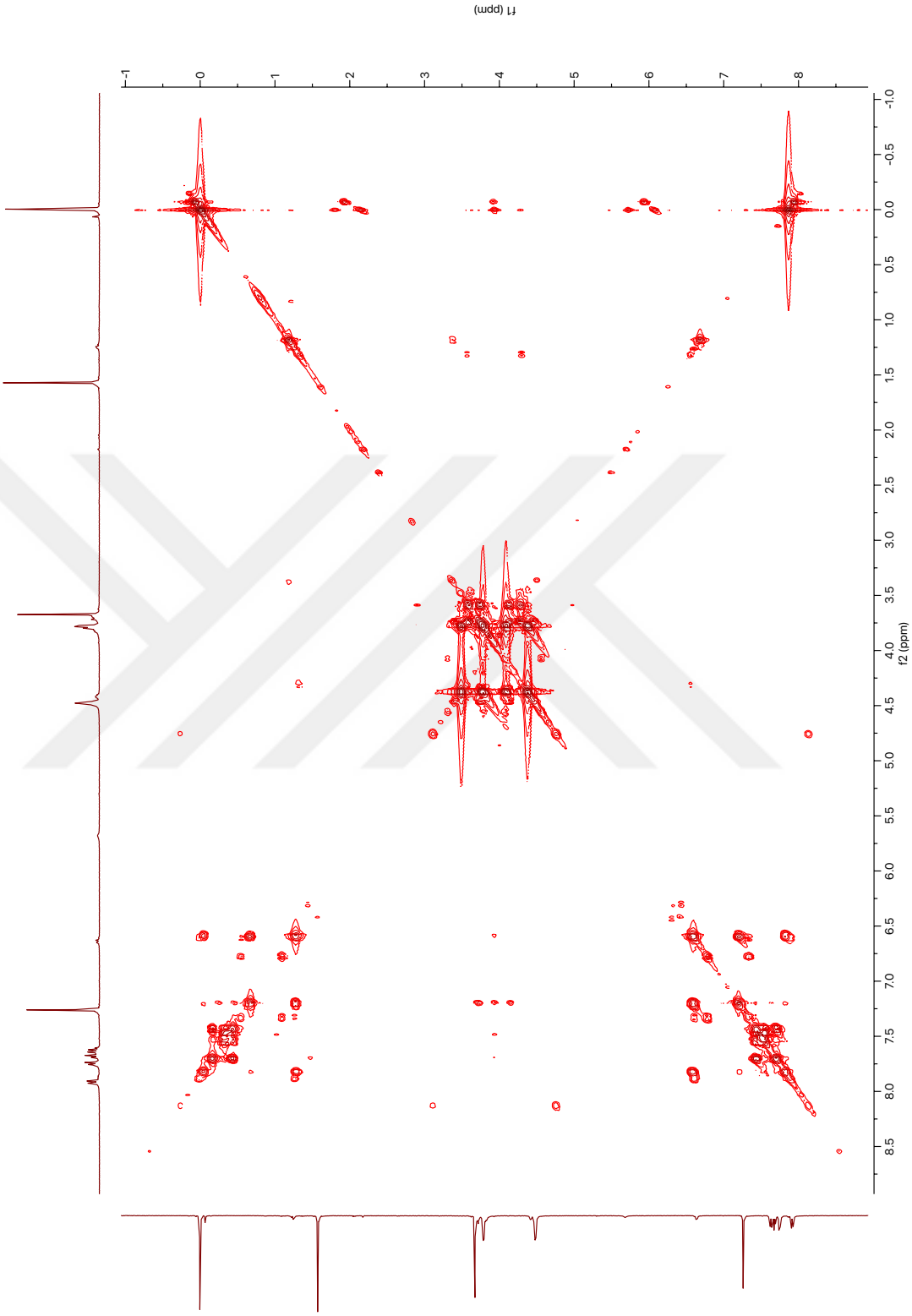

Figure 64. COSY NMR Spectrum of **Cycle II**

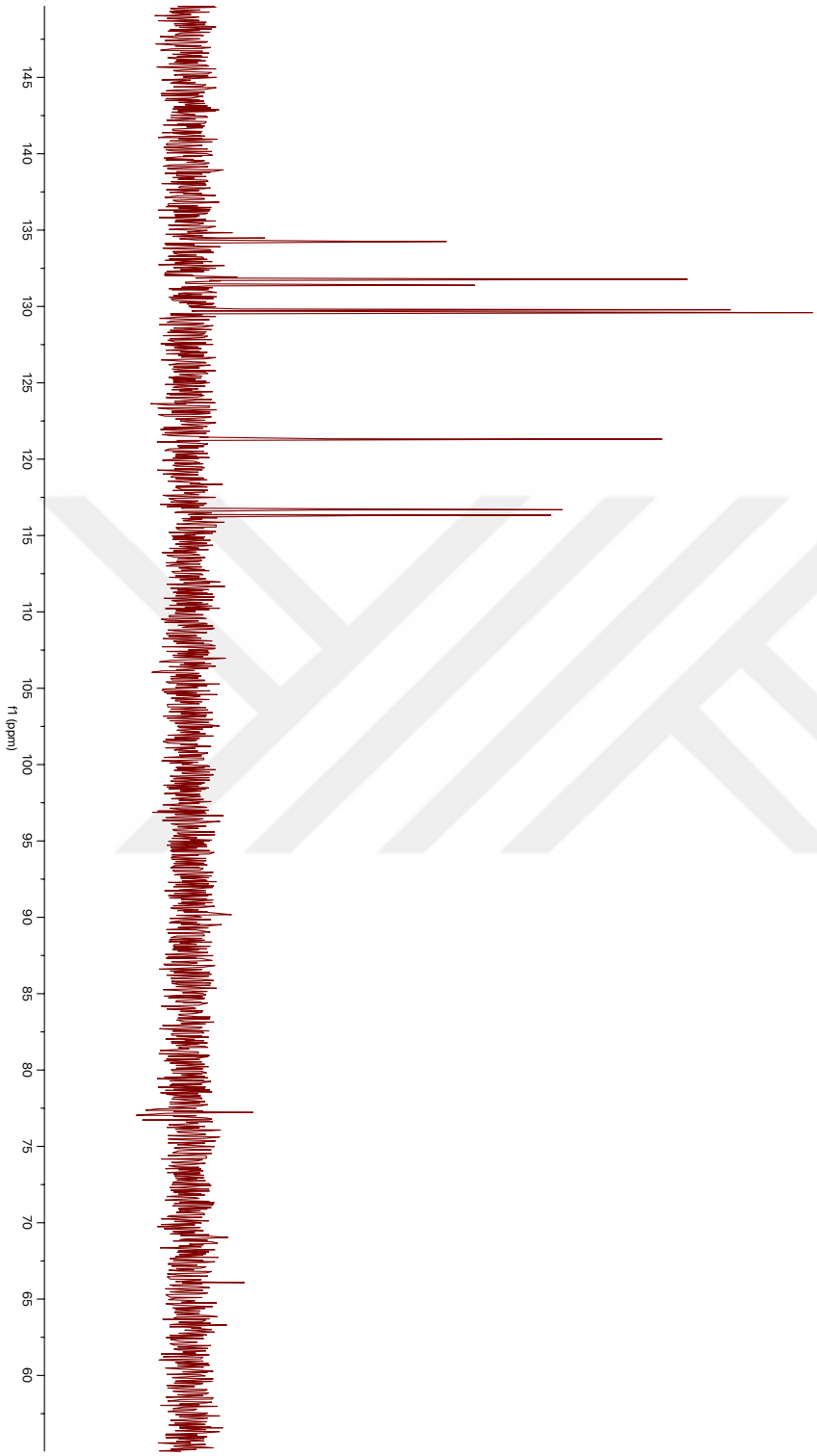

Figure 65. DEPT90 NMR Spectrum of **Cycle II**

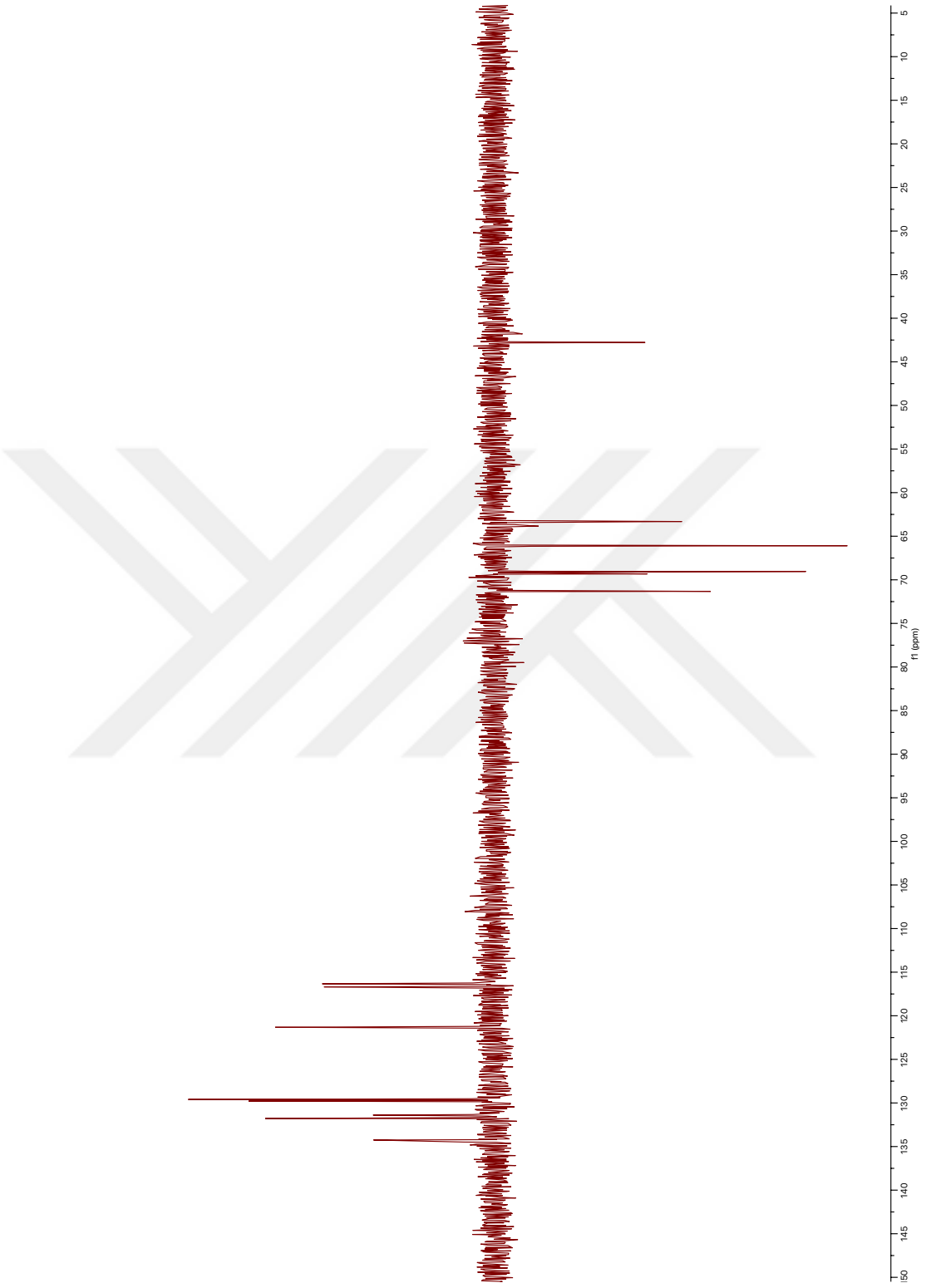

Figure 66. DEPT135 NMR Spectrum of **Cycle II**

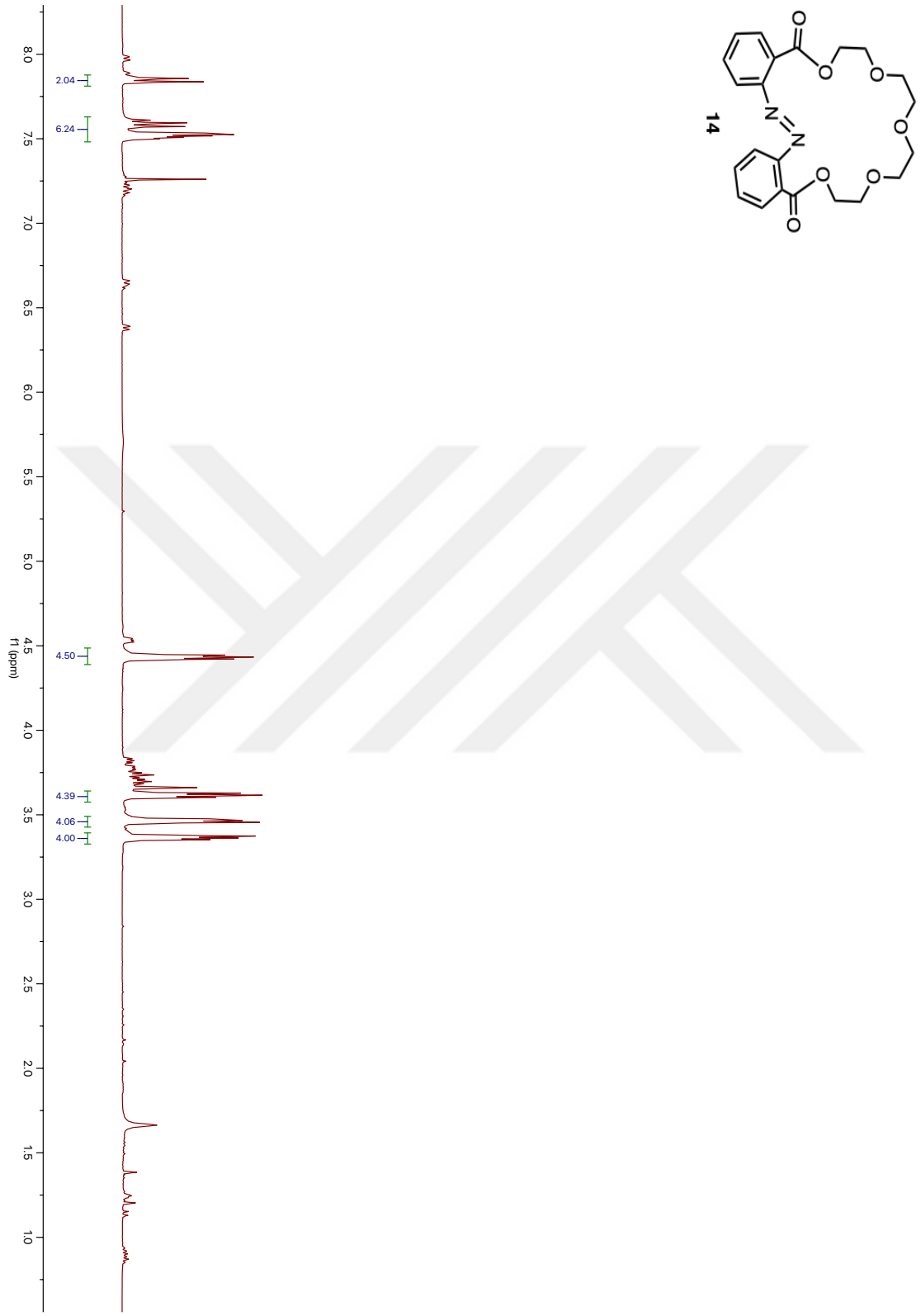

Figure 67. ^{1}H NMR Spectrum of **Cycle III,** Compound **14**

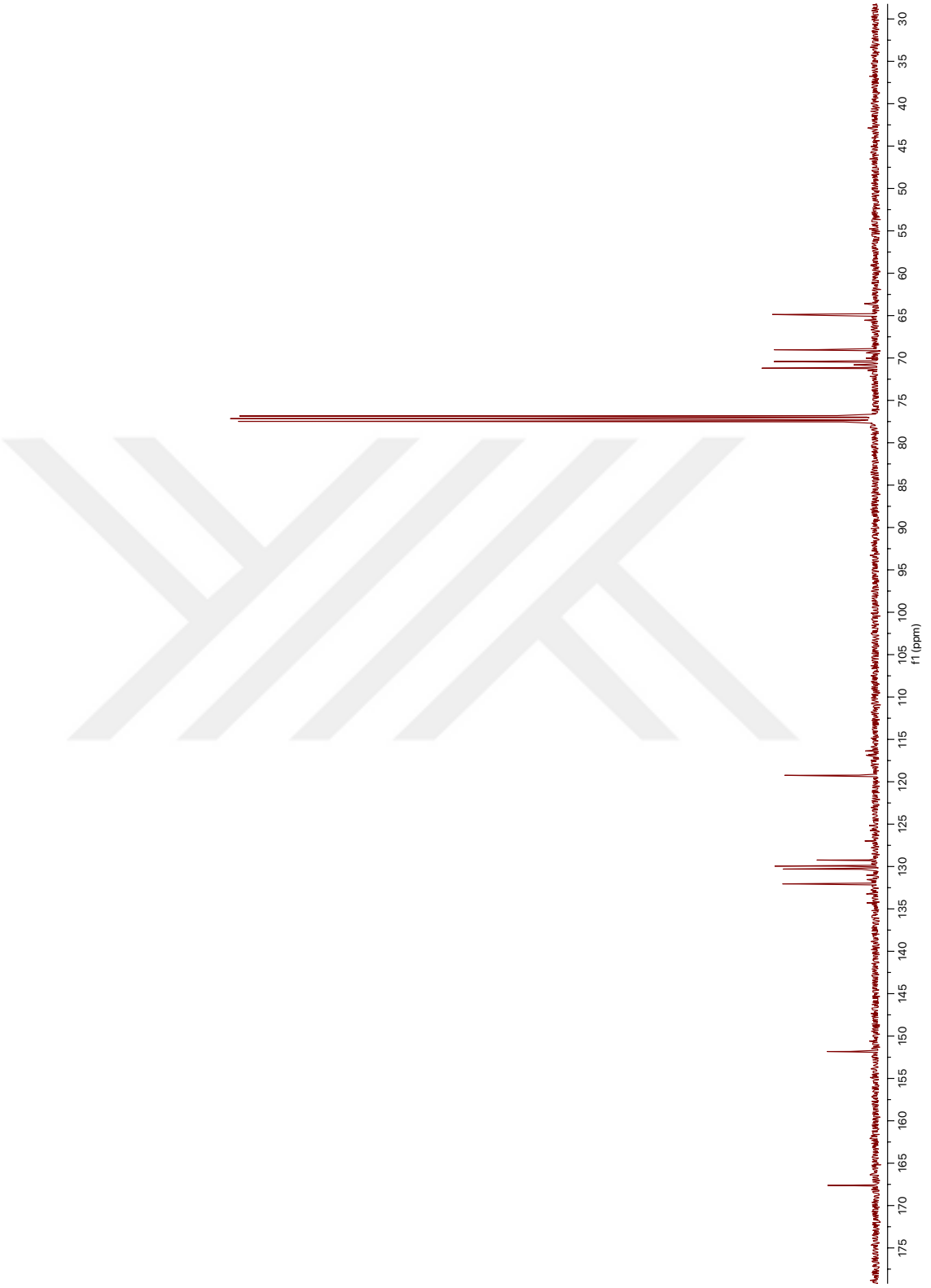

Figure 68. ^{13}C NMR Spectrum of **Cycle III**

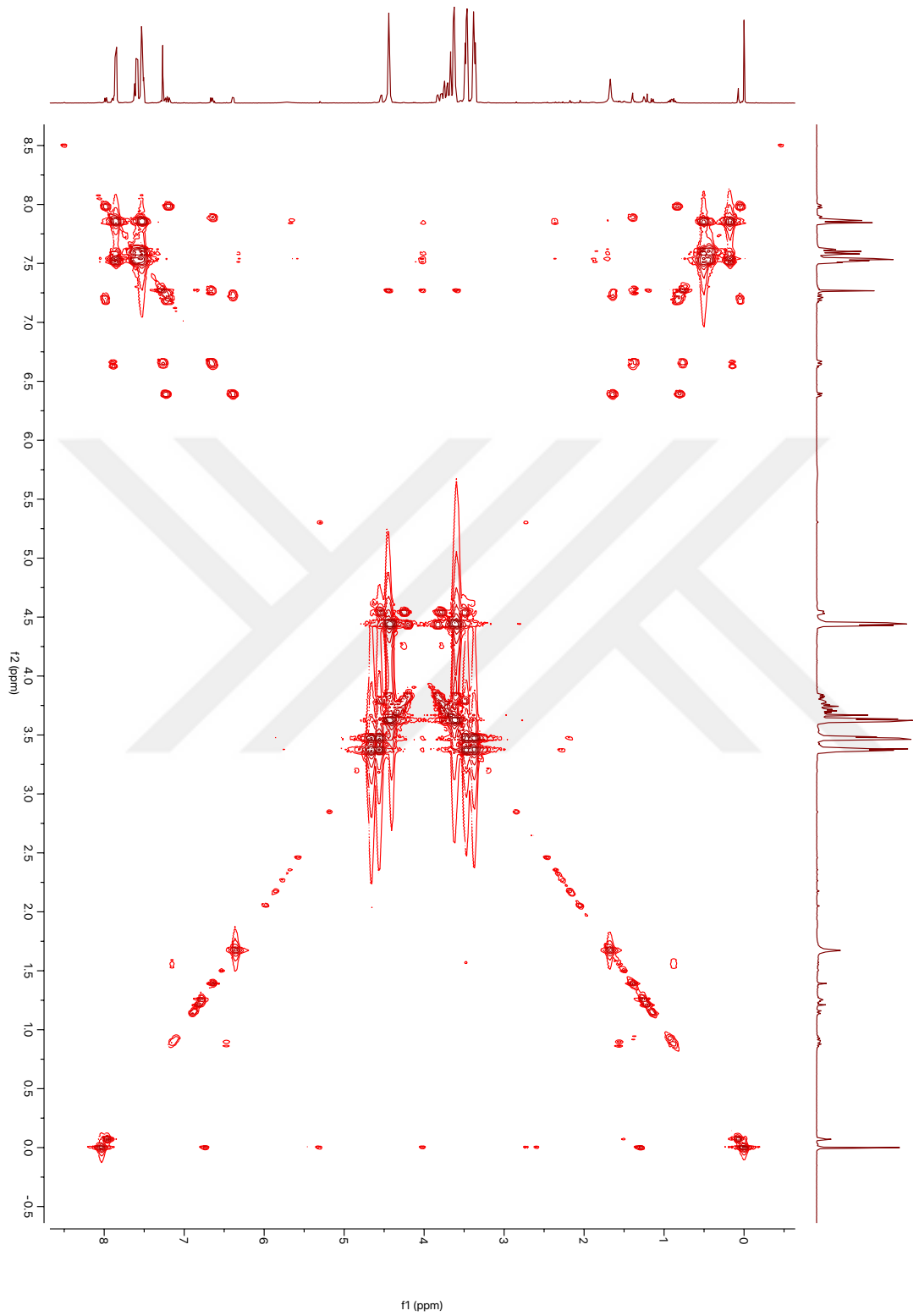

Figure 69. COSY NMR Spectrum of **Cycle III**

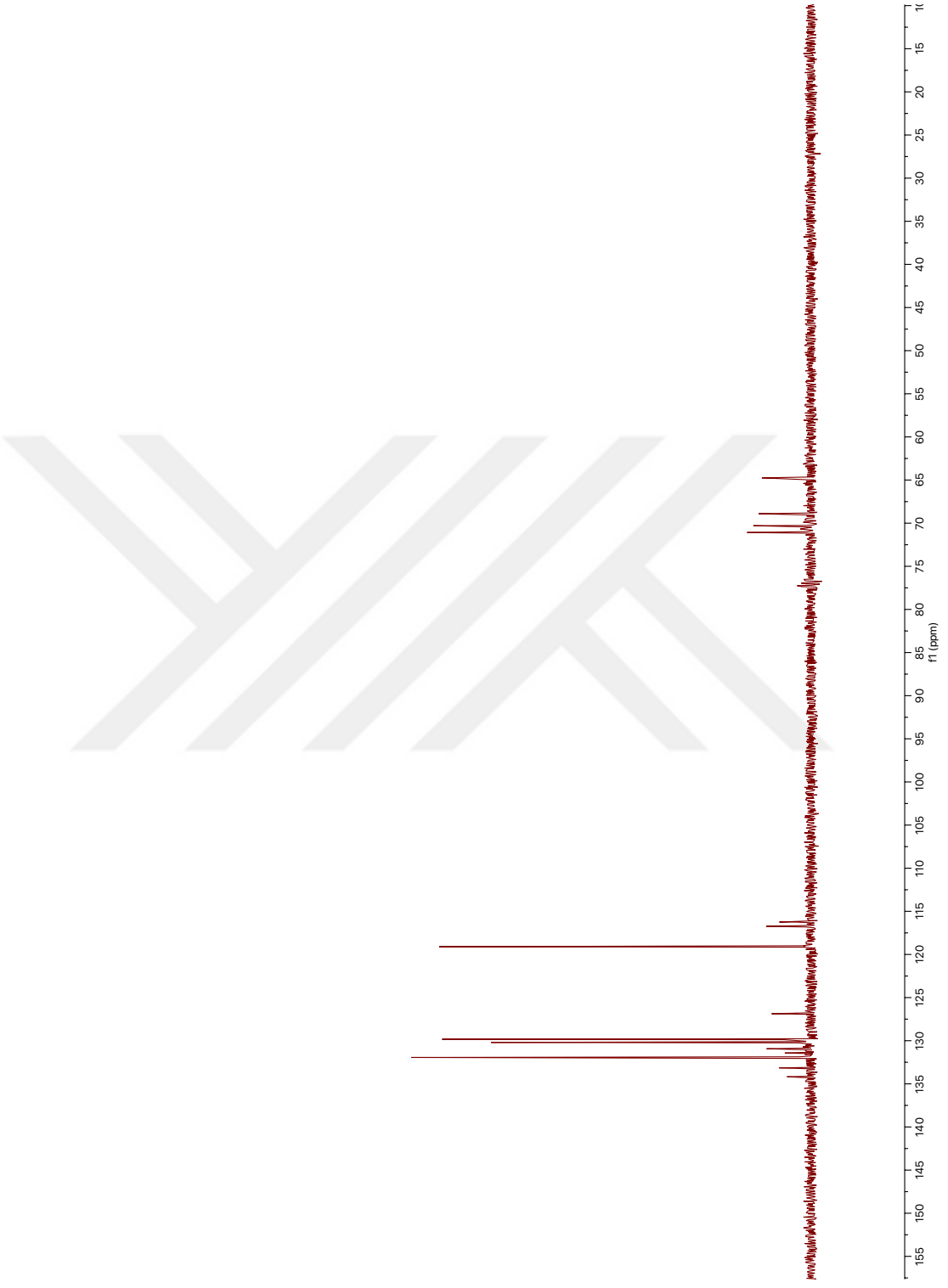

Figure 70. DEPT90 NMR Spectrum of **Cycle III**

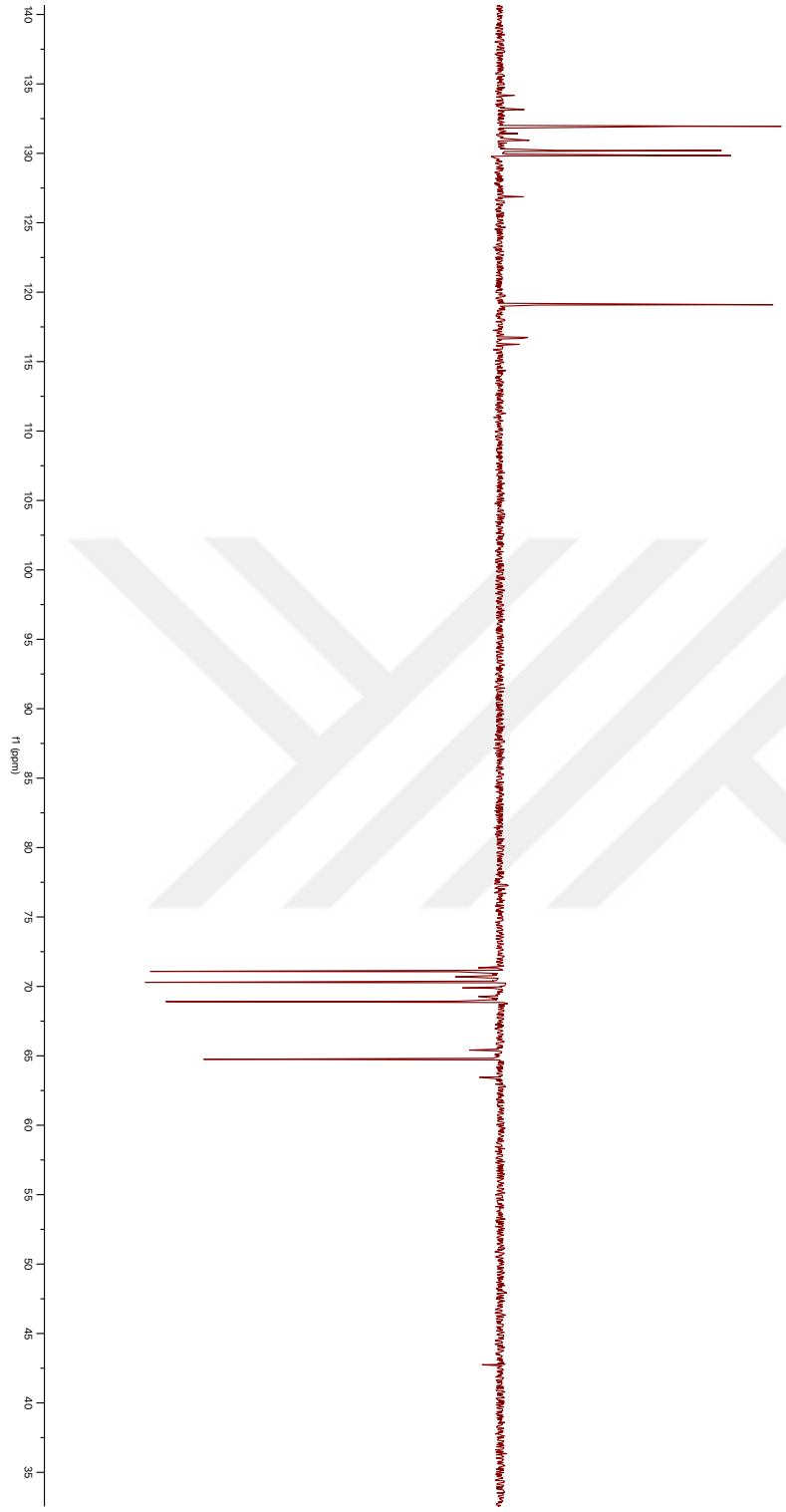

Figure 71. DEPT135 NMR Spectrum of **Cycle III**

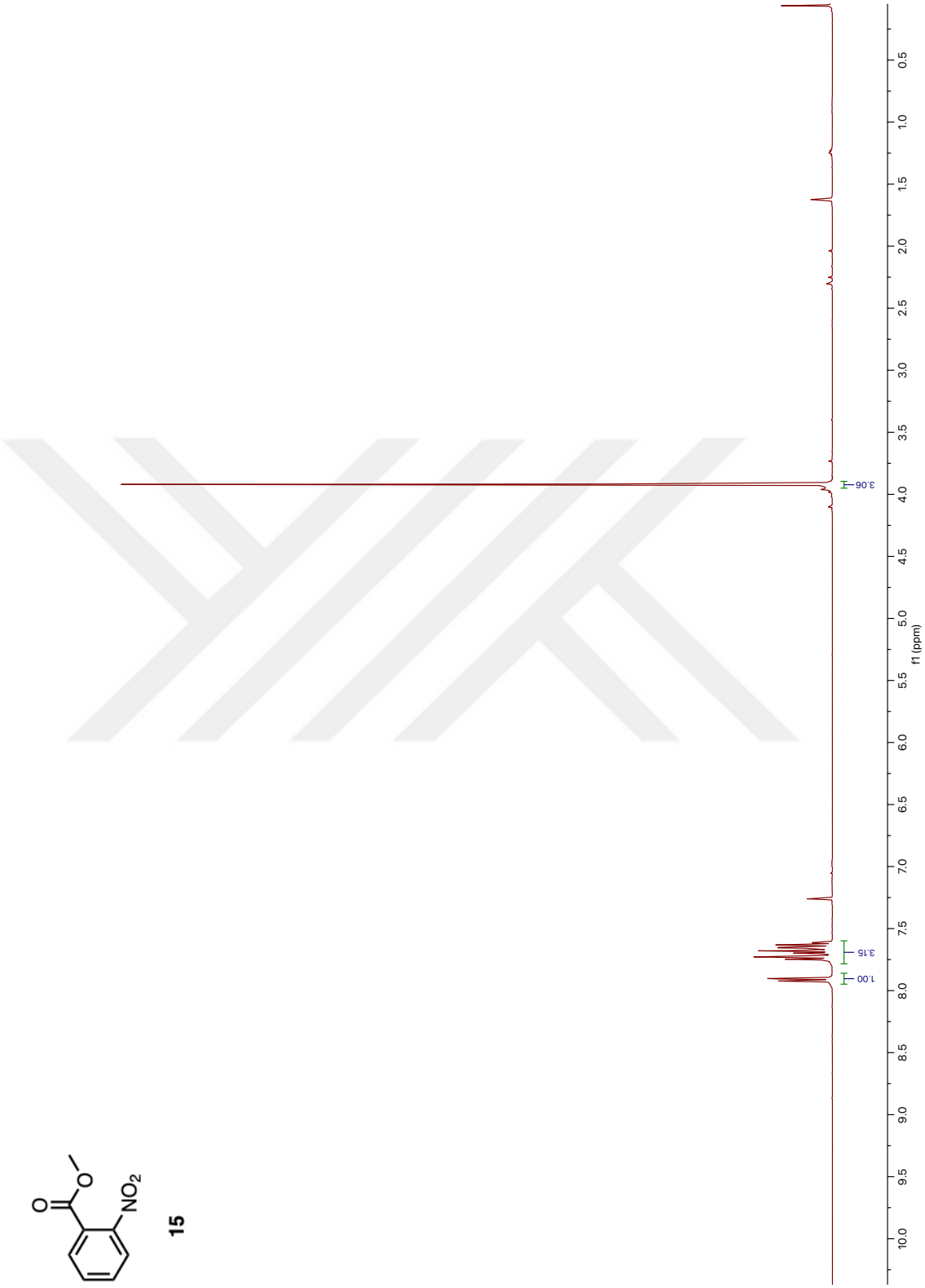

Figure 72. ^{1}H NMR Spectrum of Compound **15**

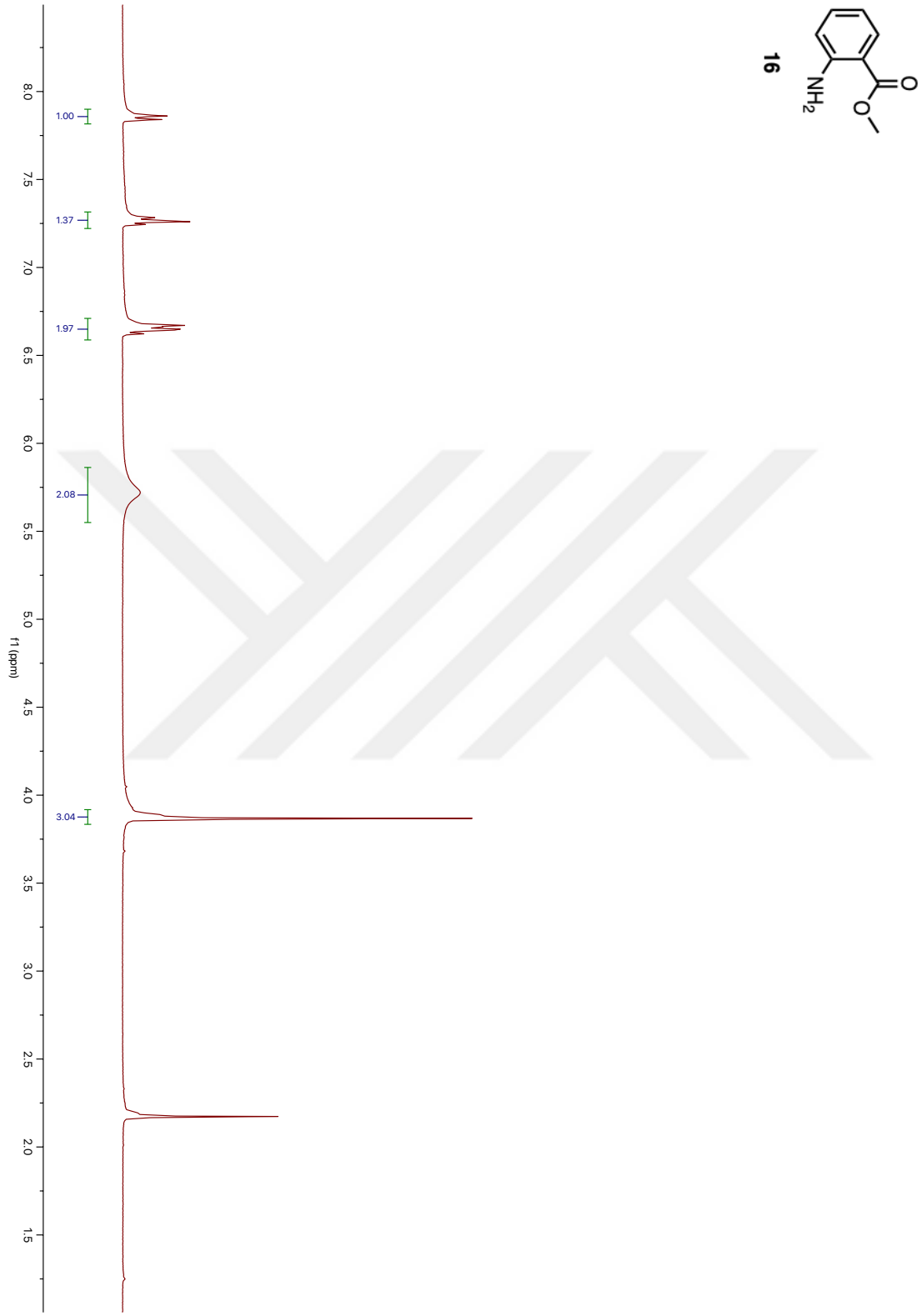

Figure 73. ^{1}H NMR Spectrum of Compound **16**

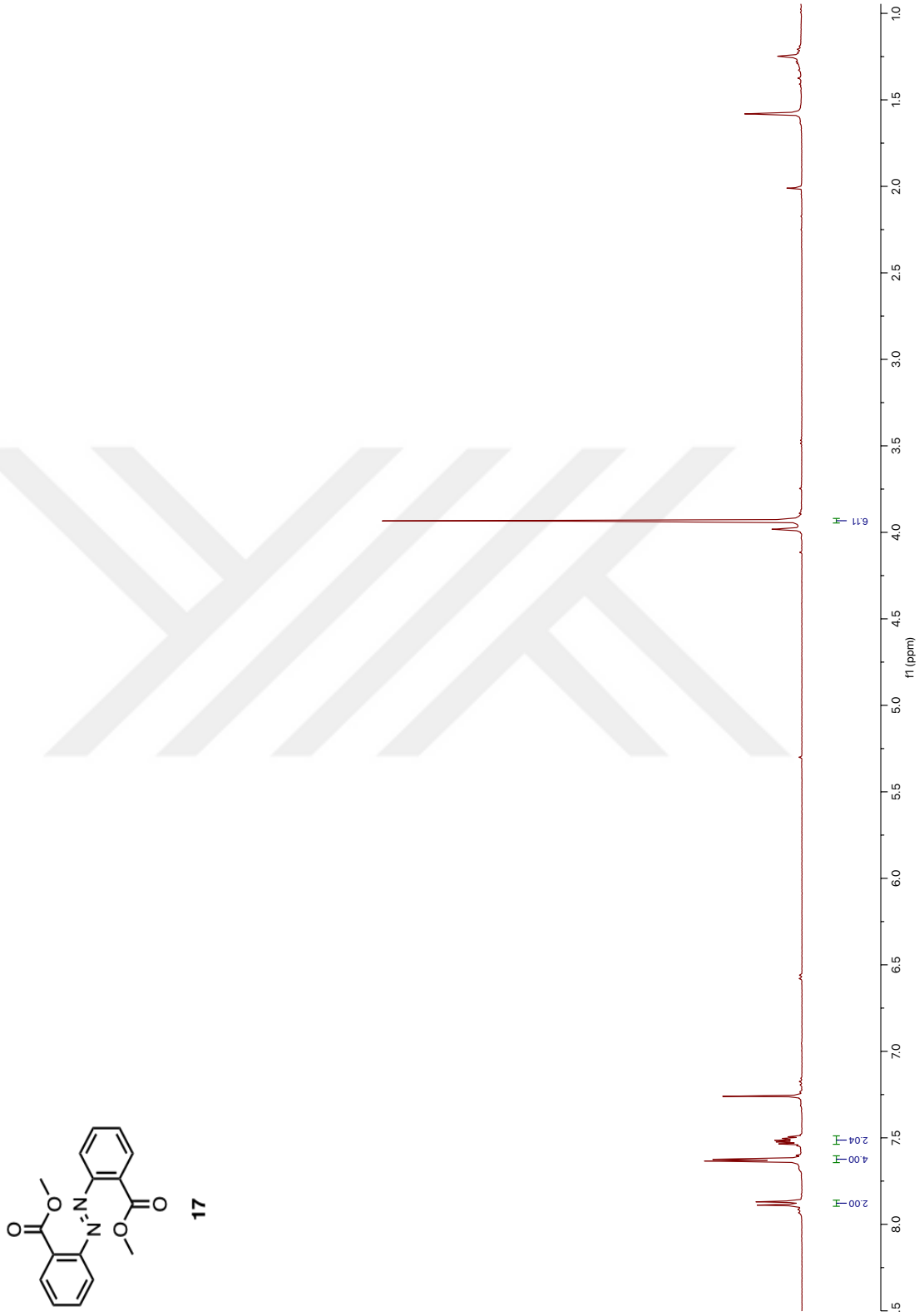

Figure 74. ^{1}H NMR Spectrum of Compound **17**

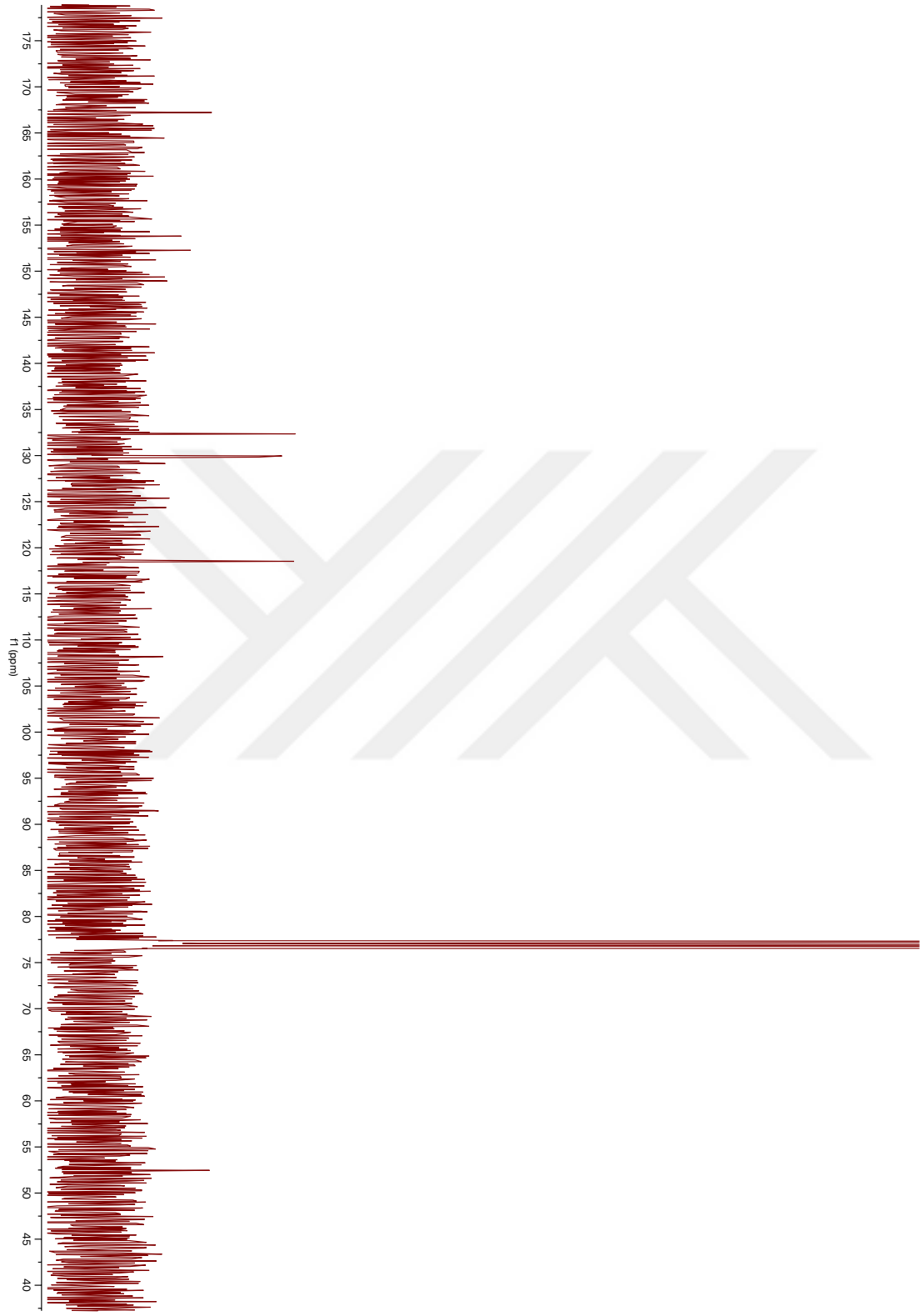

Figure 75. ^{13}C NMR Spectrum of compound **17**

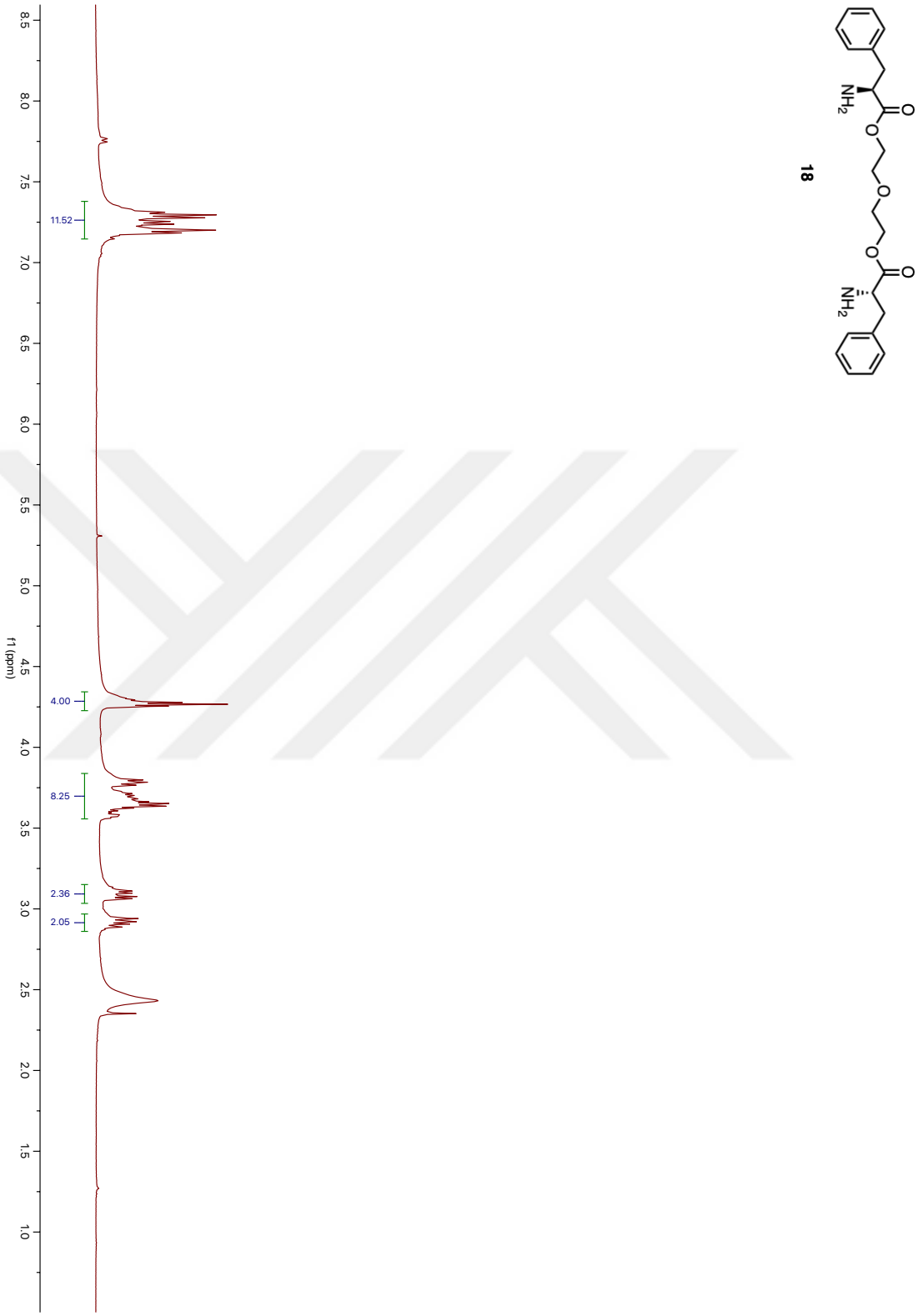

Figure 76. ^{1}H NMR Spectrum of Compound **18**

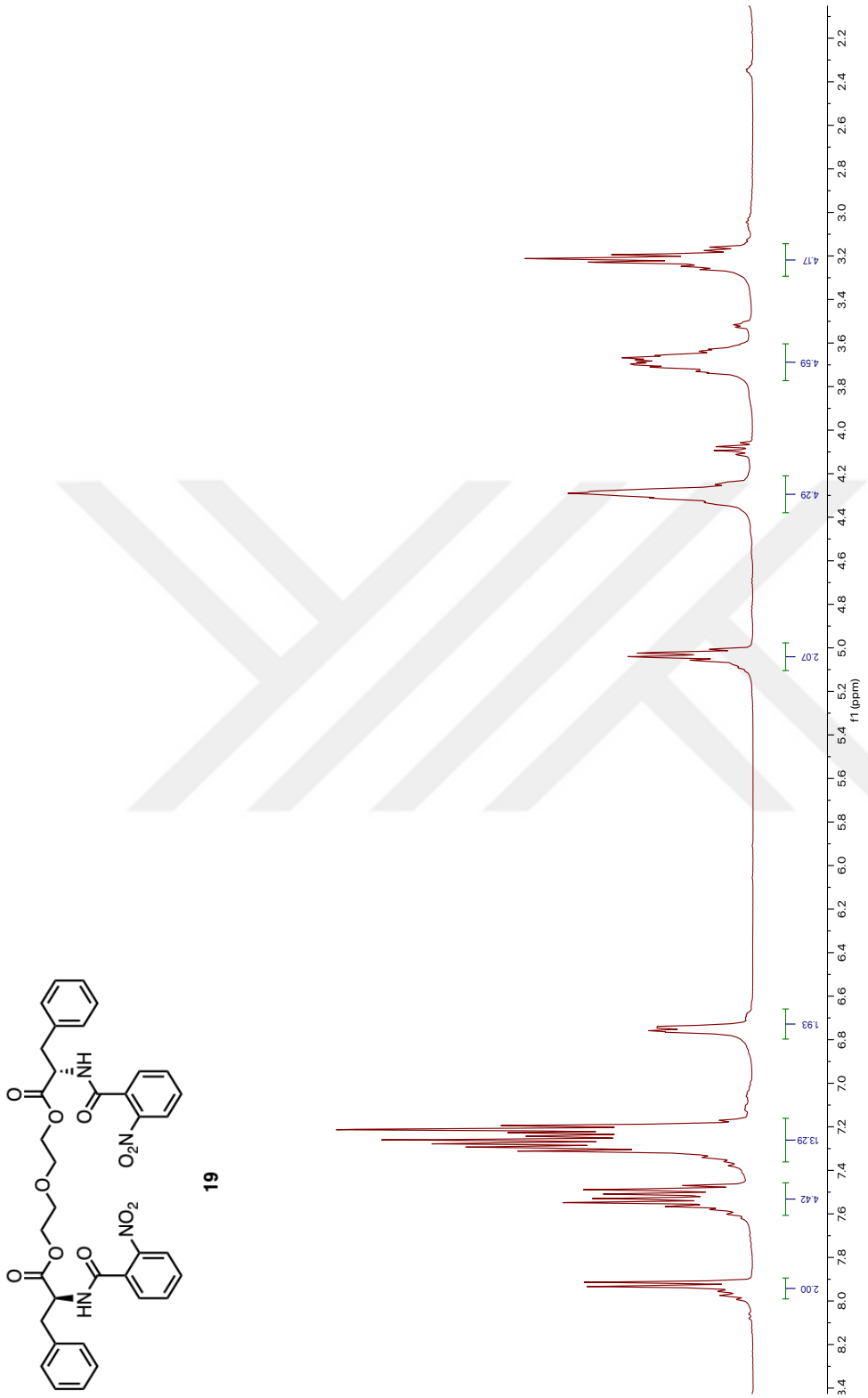

Figure 77. ^{1}H NMR Spectrum of Compound **19**

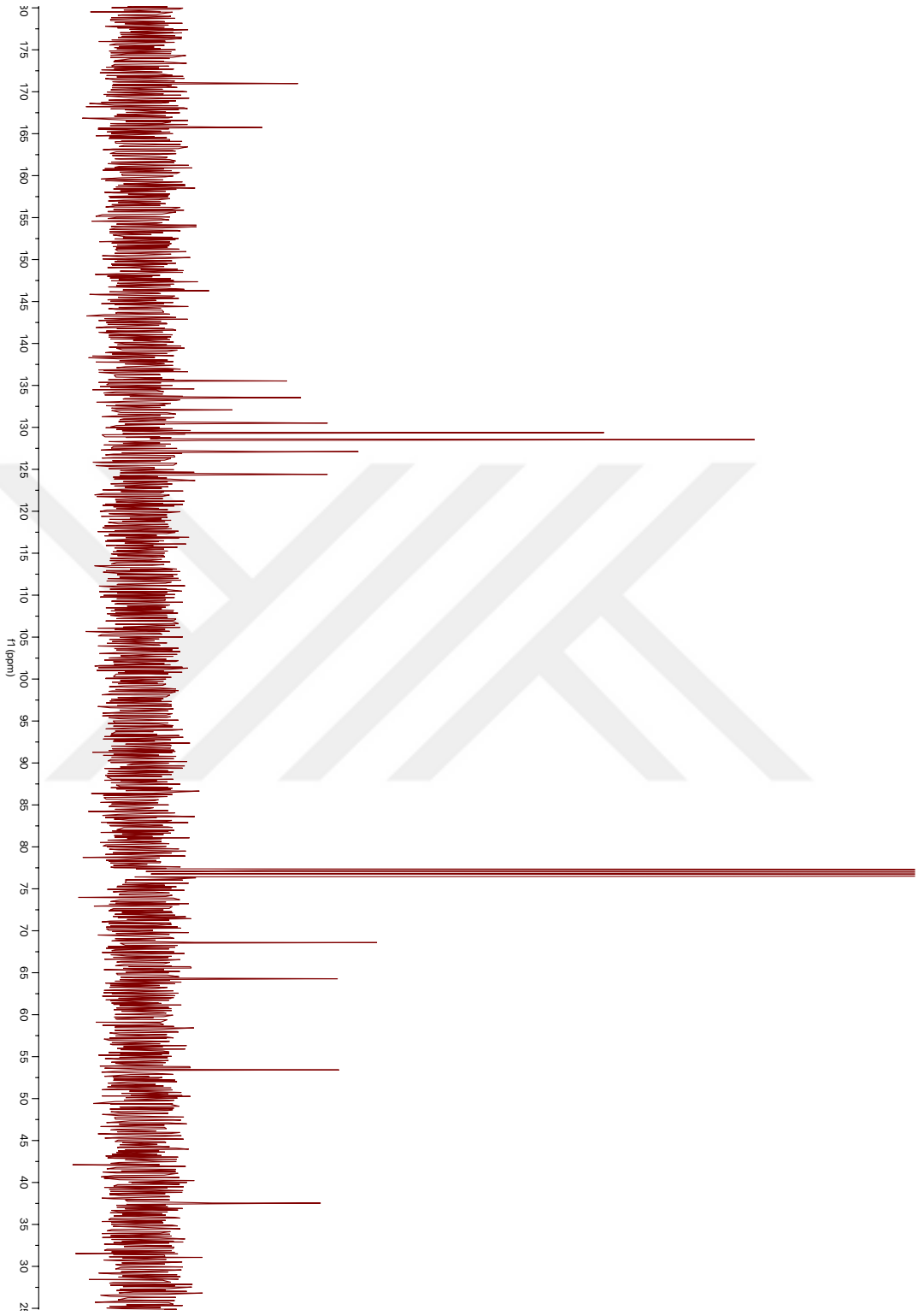

Figure 78. ^{13}C NMR Spectrum of compound **19**

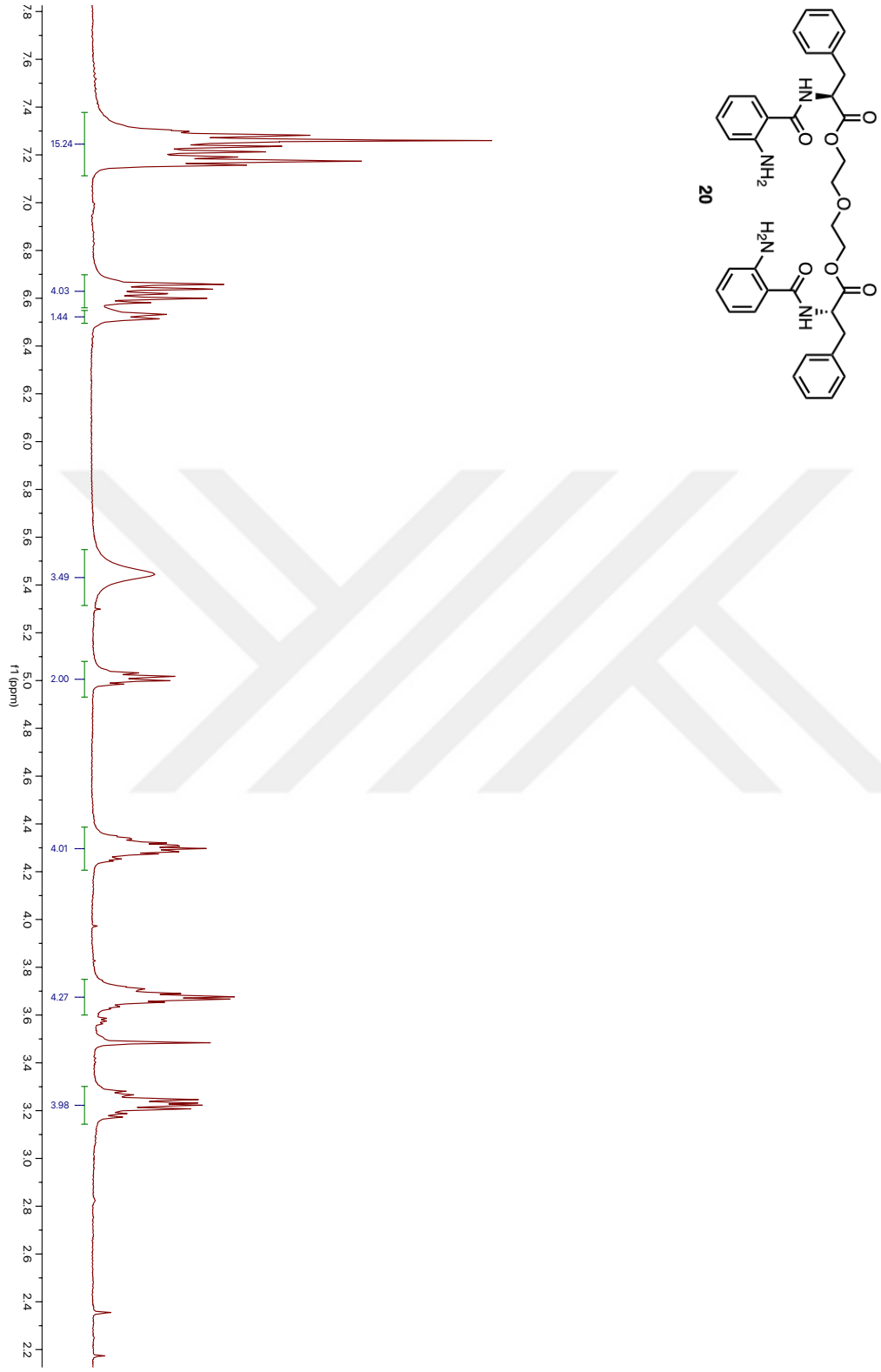

Figure 79. ^{1}H NMR Spectrum of Compound **20**

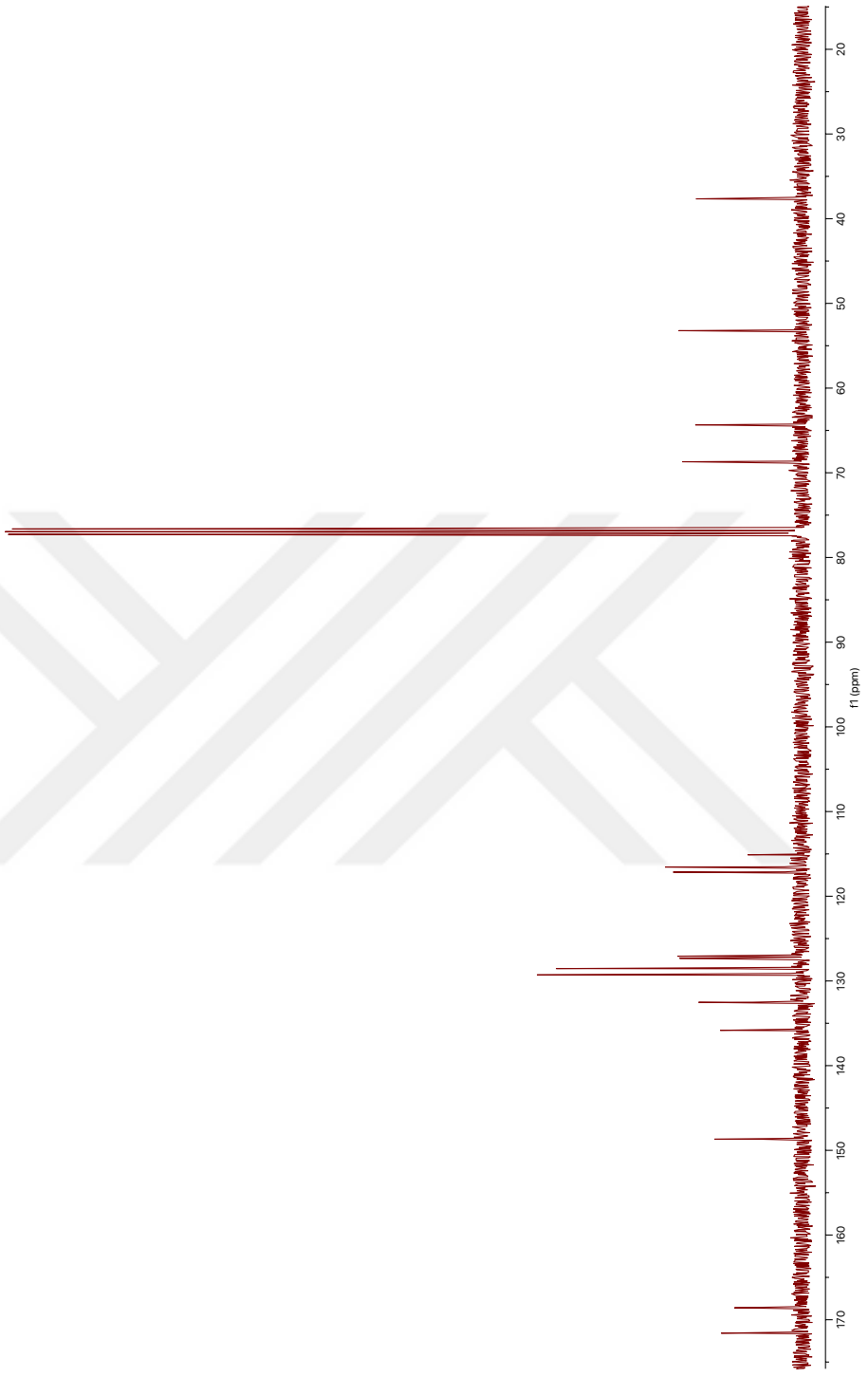

Figure 80. ^{13}C NMR Spectrum of compound **20**

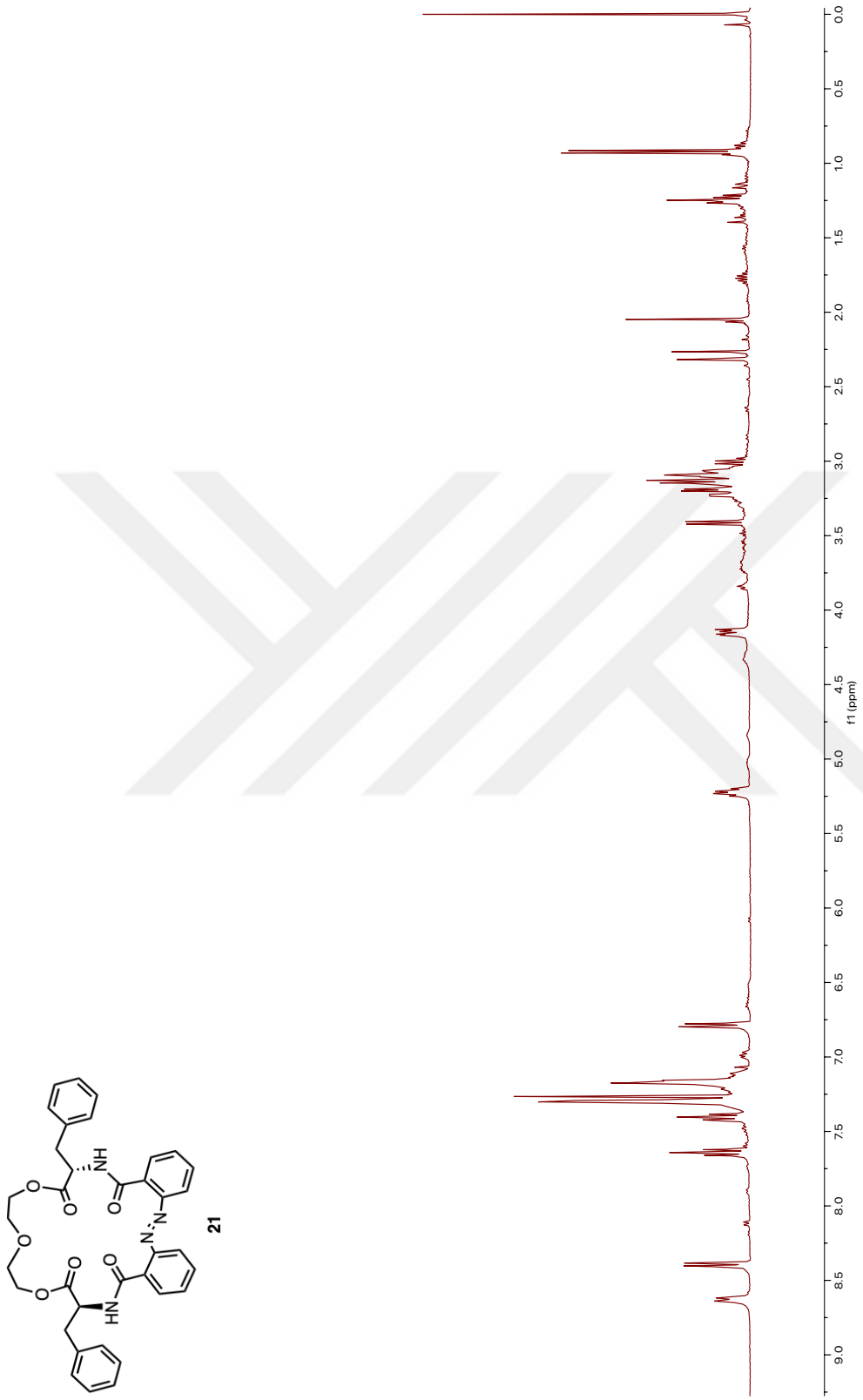

Figure 81. ^{1}H NMR Spectrum of **Cycle IV**

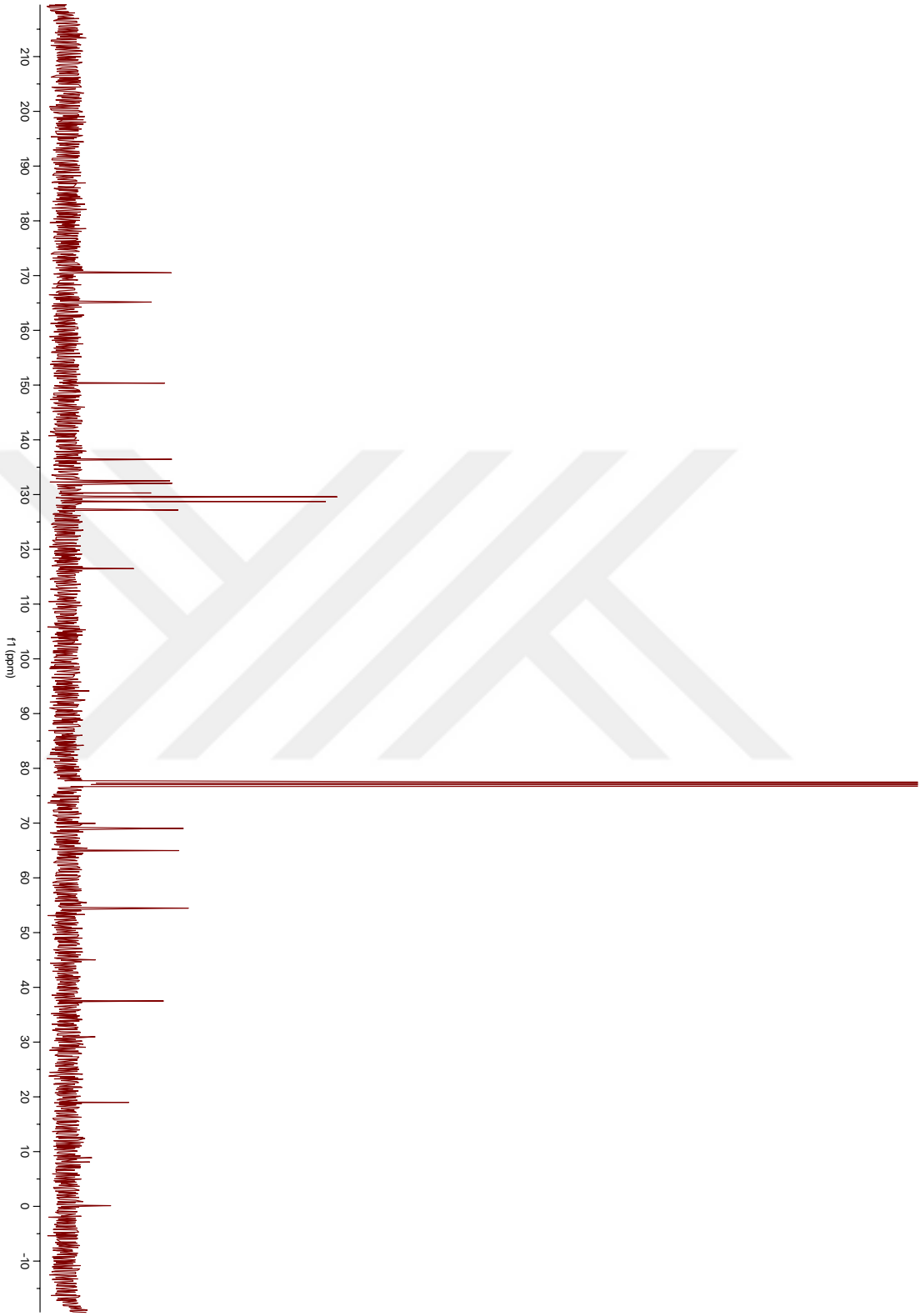

Figure 82. ^{13}C NMR Spectrum of **Cycle IV**

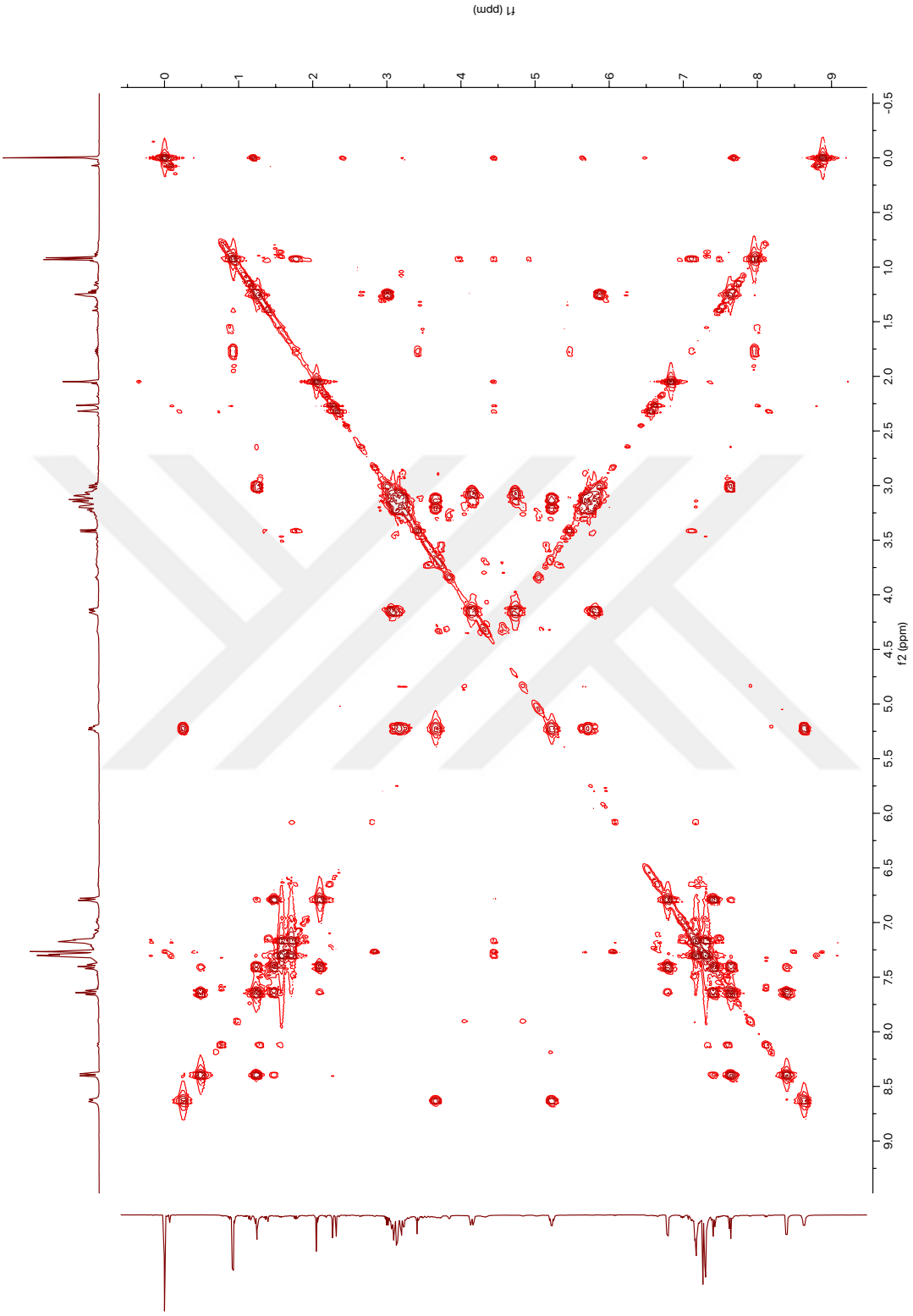

Figure 83. COSY NMR Spectrum of **Cycle IV**

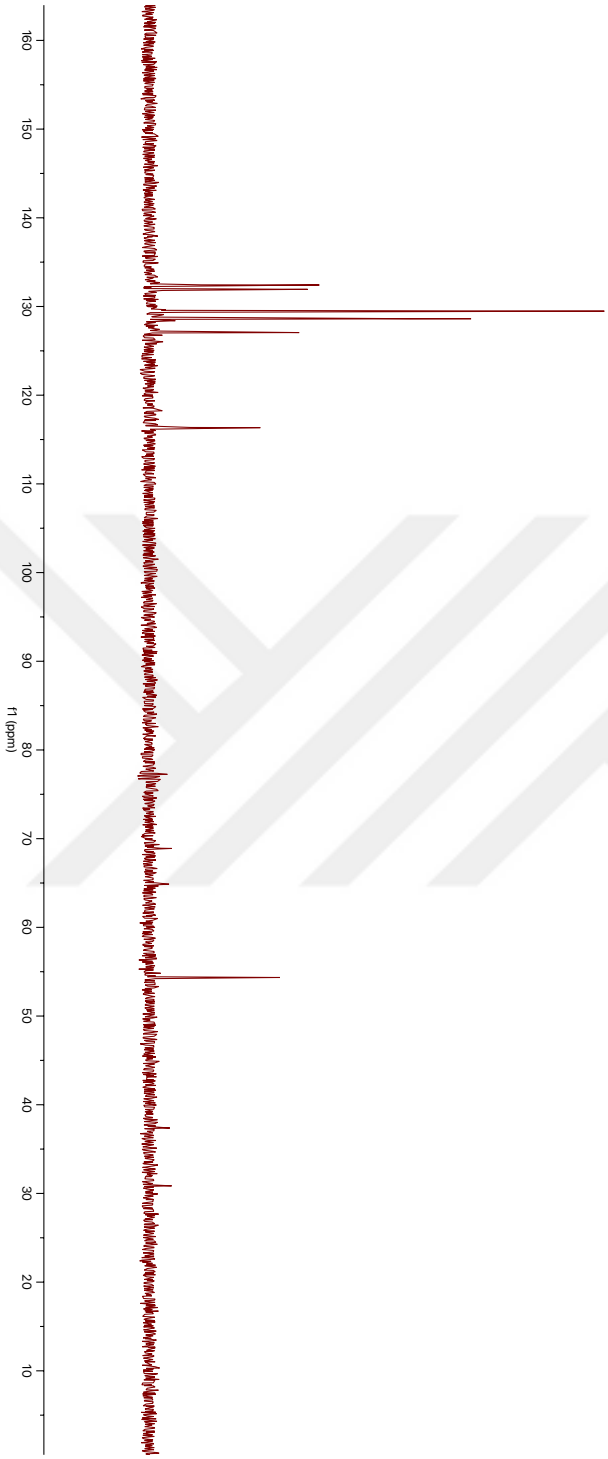

Figure 84. DEPT90 NMR Spectrum of **Cycle IV**

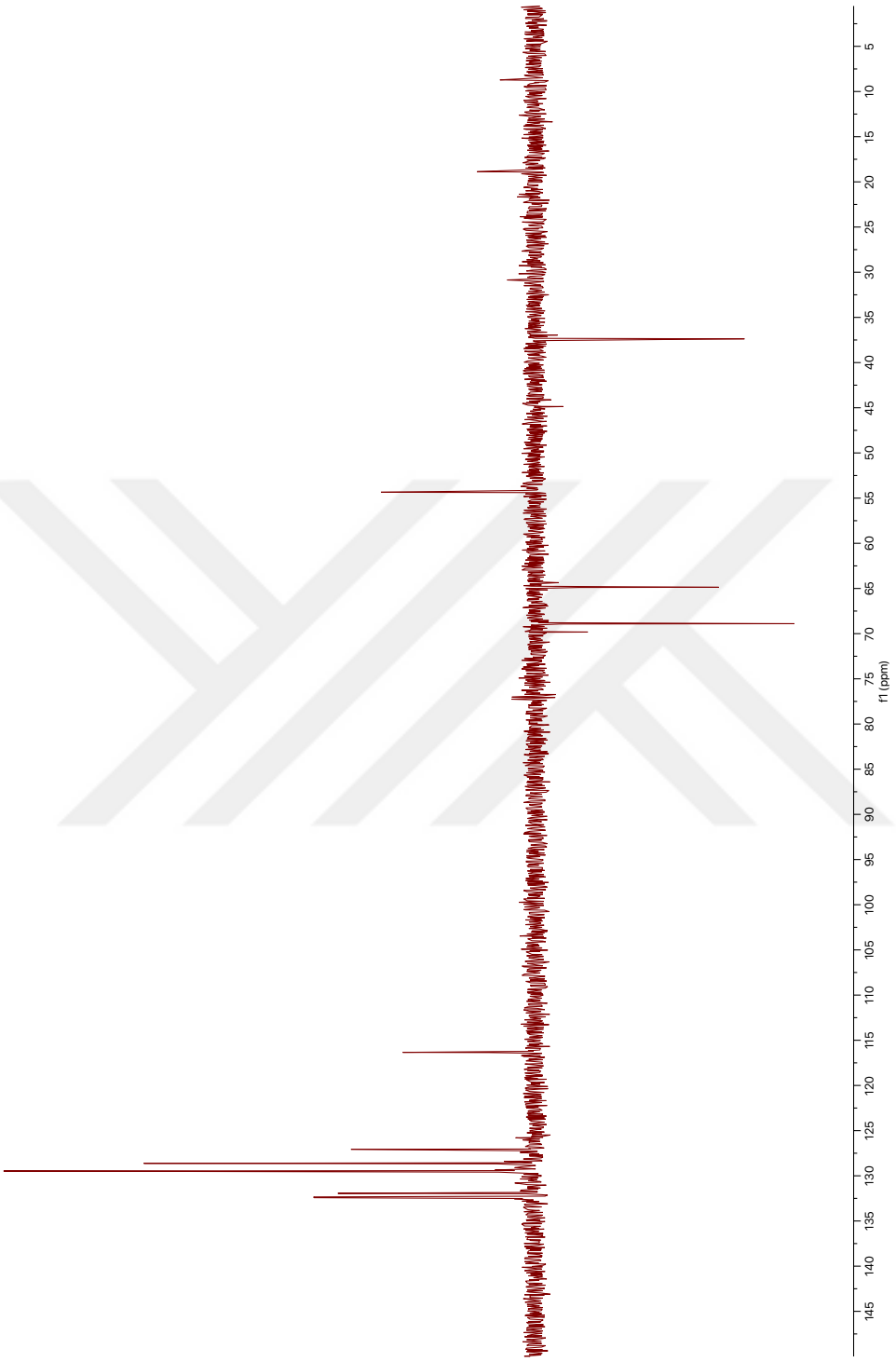

Figure 85. DEPT135 NMR Spectrum of **Cycle IV**

B. IR Spectra

IR spectra were recorded at Thermo Scientific Nicolet iS10 ATR-IR spectrometer.

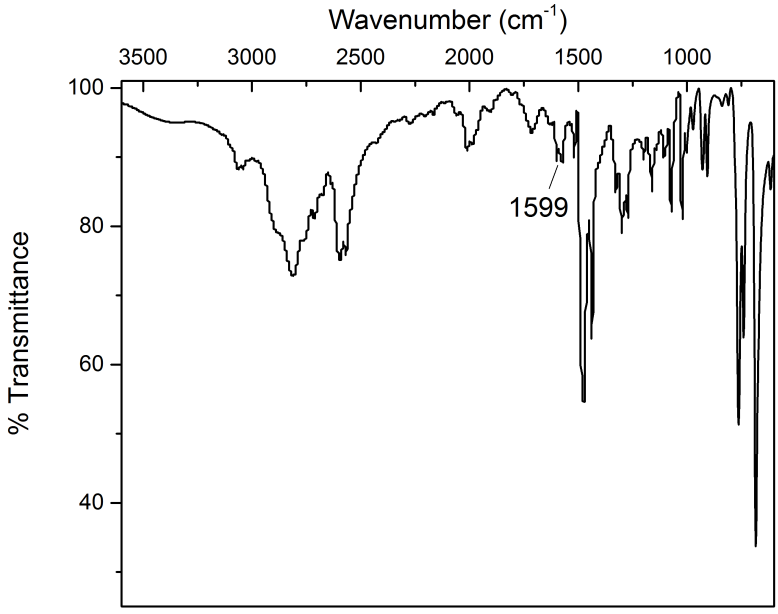

Figure 86. IR Spectrum of Azobenzene

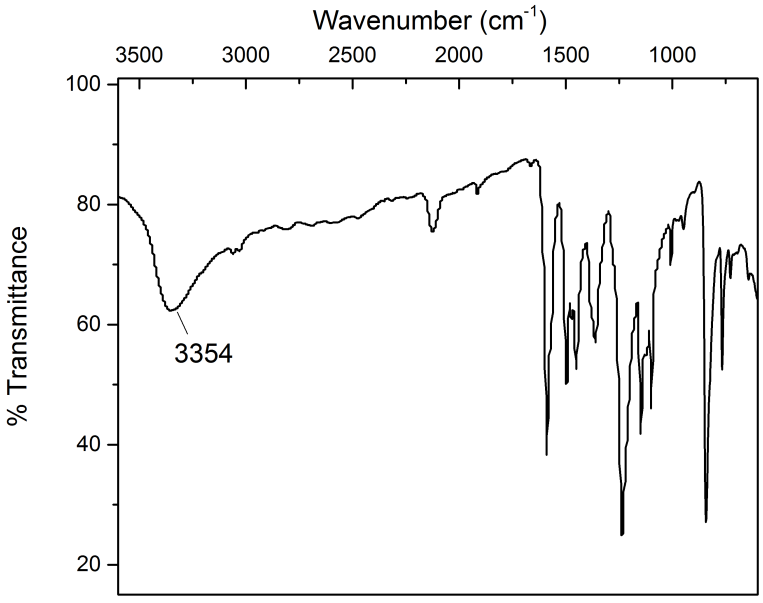

Figure 87. IR Spectrum of 4,4'-dihydroxyazobenzene

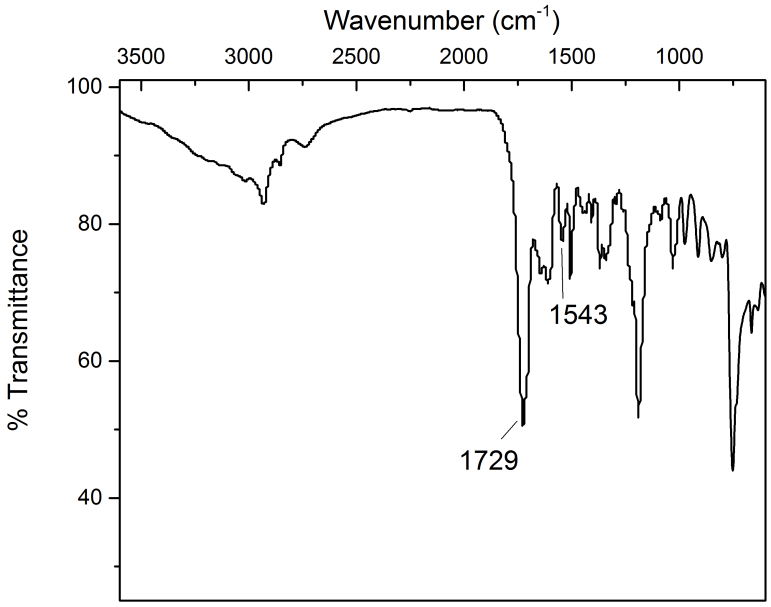

Figure 88. IR Spectrum of Compound **4**

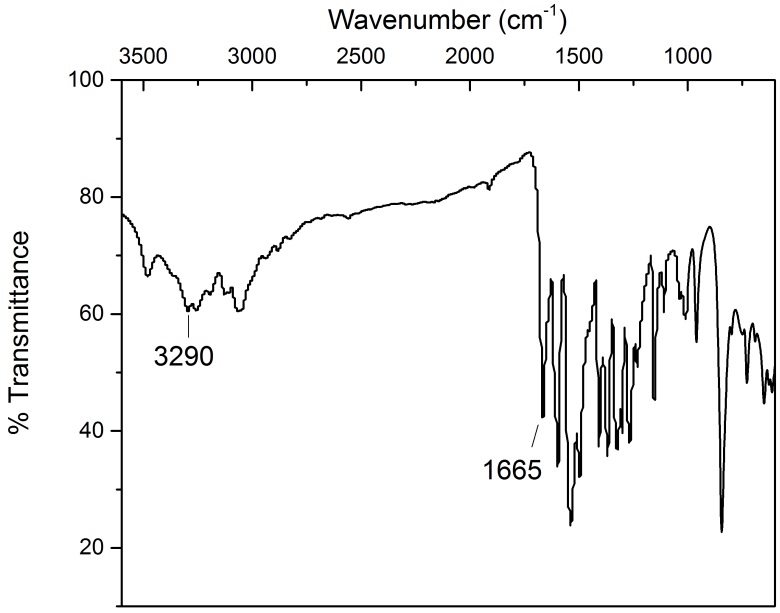

Figure 89. IR Spectrum of Compound **5**

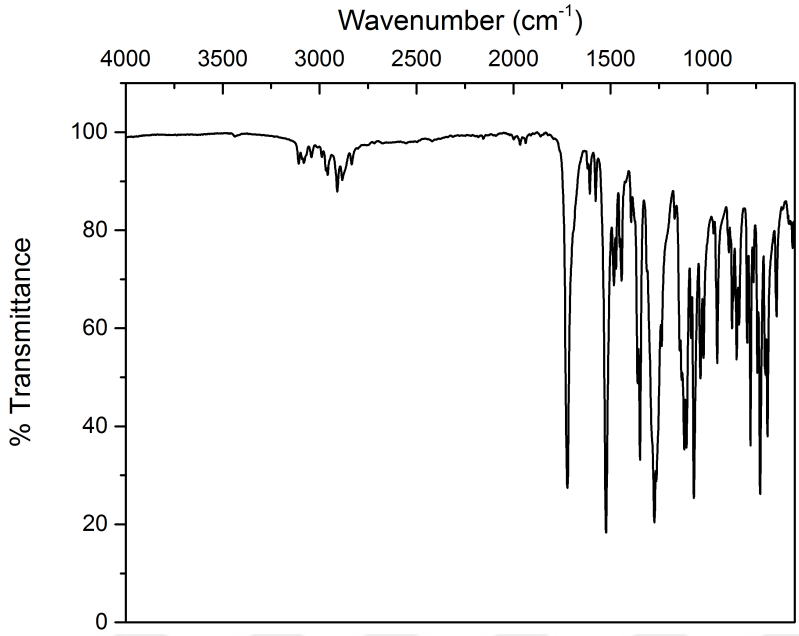

Figure 90. IR Spectrum of Compound **6**

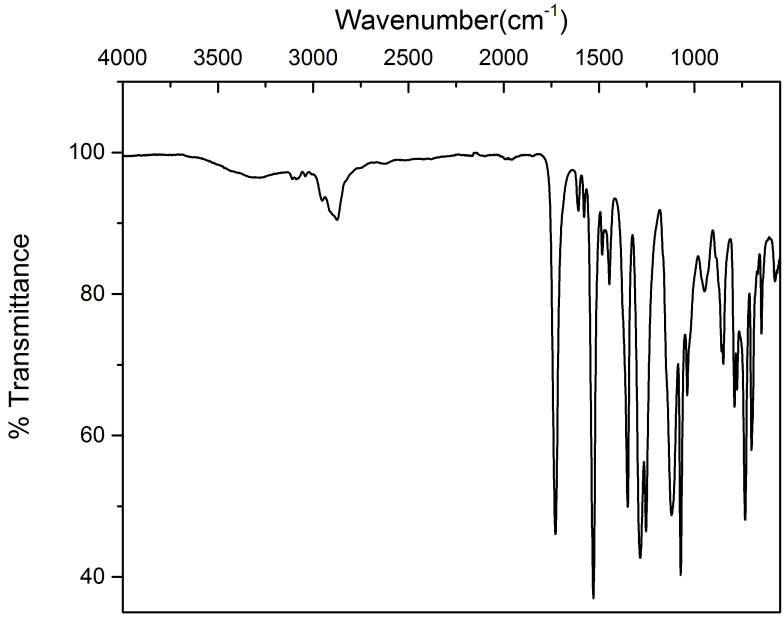

Figure 91. IR Spectrum of Compound **7**

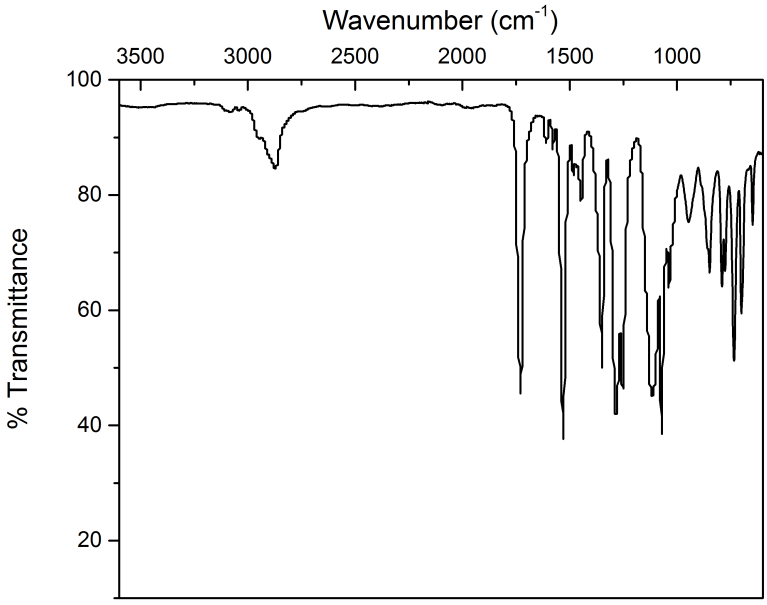

Figure 92. IR Spectrum of Compound **8**

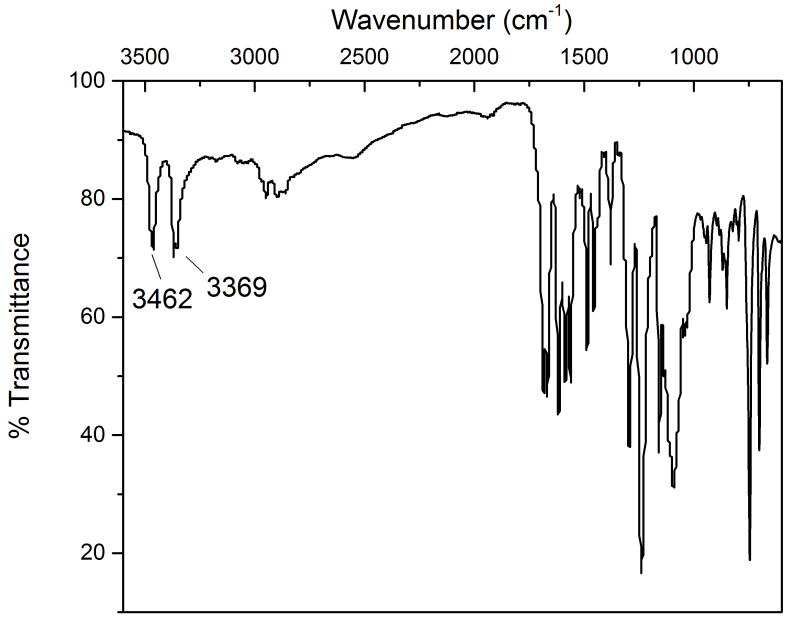

Figure 93. IR Spectrum of Compound **9**

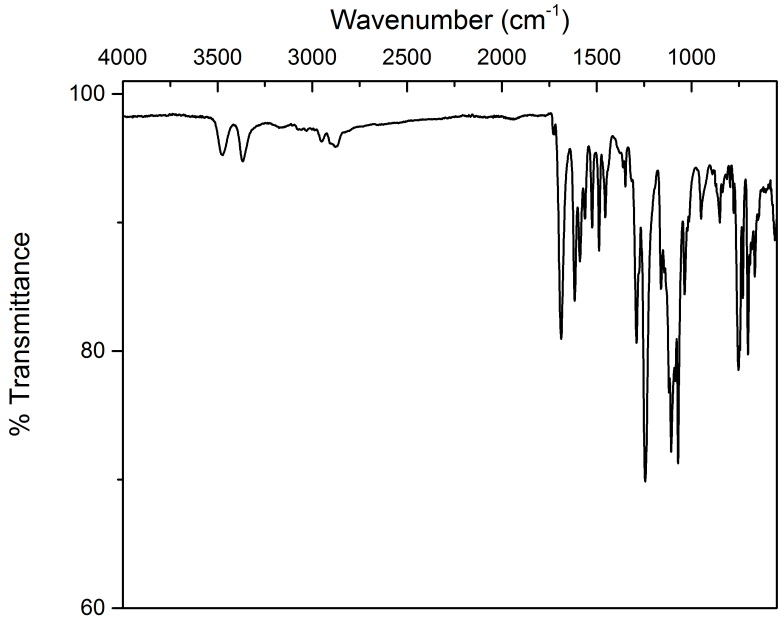

Figure 94. IR Spectrum of Compound **10**

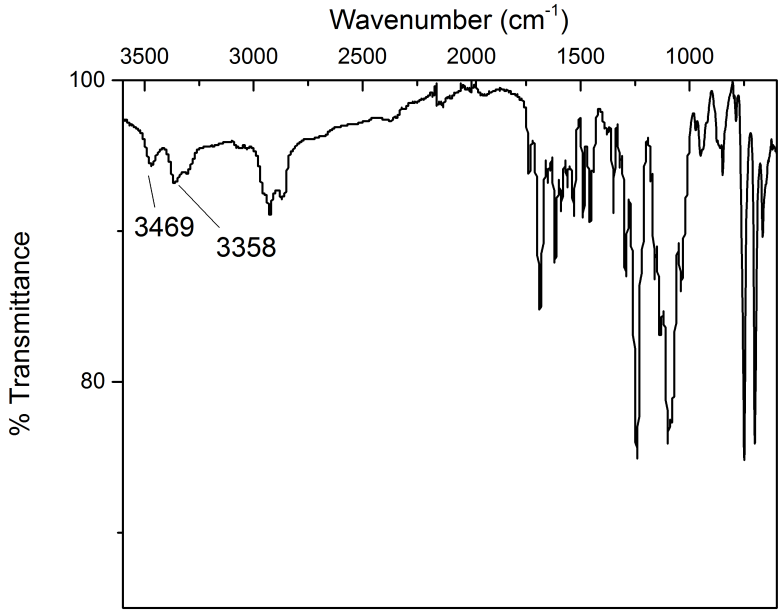

Figure 95. IR Spectrum of Compound **11**

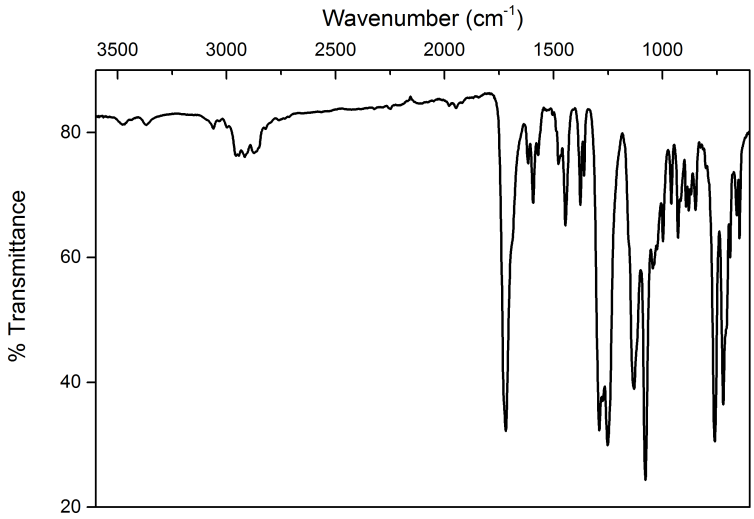

Figure 96. IR Spectrum of Cycle **I**

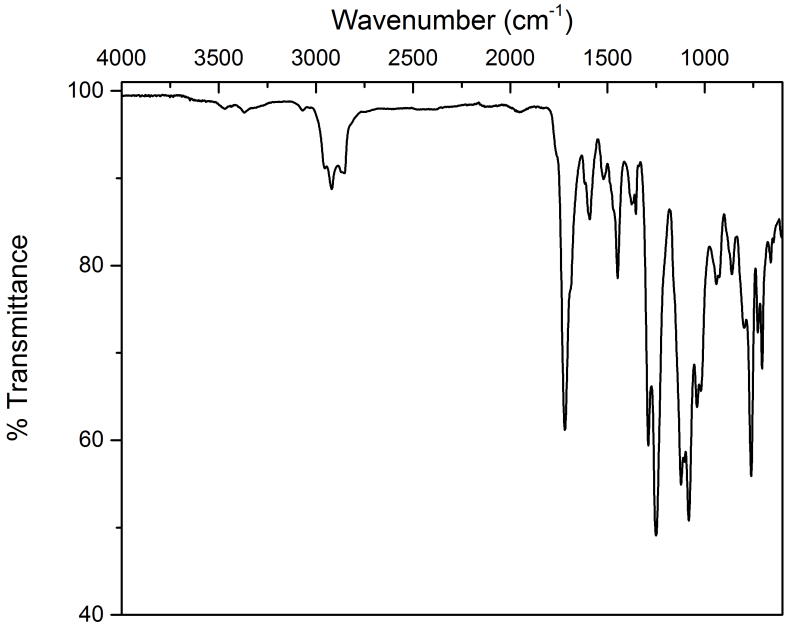

Figure 97. IR Spectrum of Cycle **II**

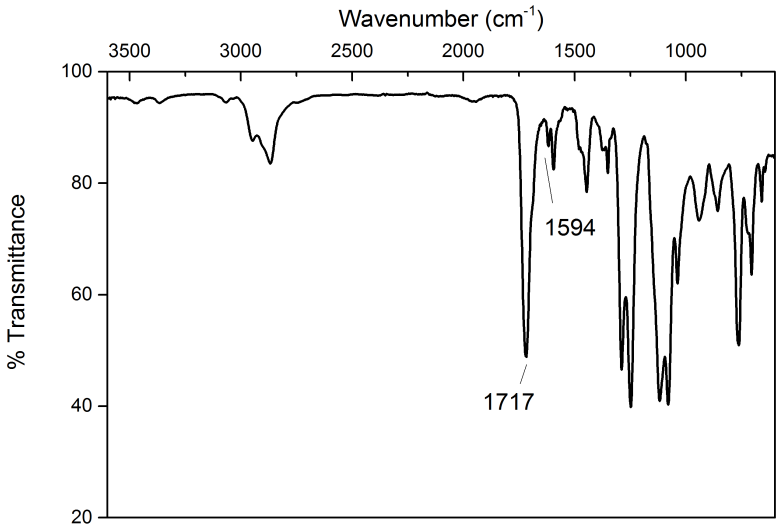

Figure 98. IR Spectrum of Cycle **III**

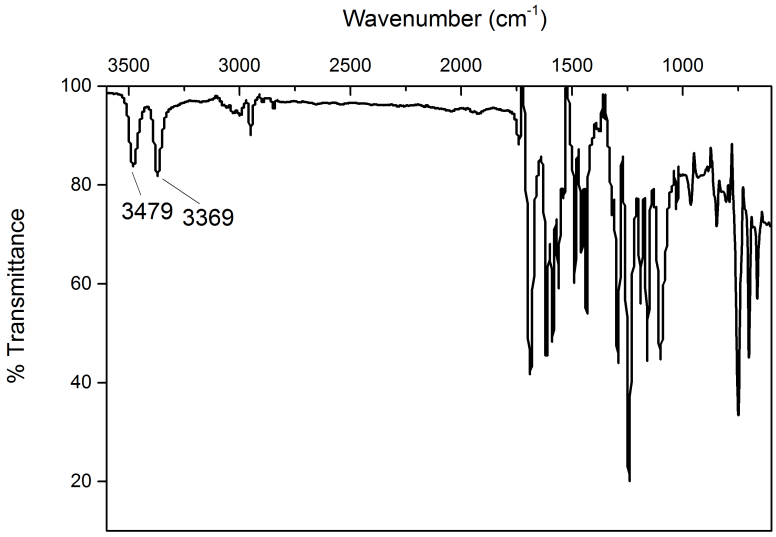

Figure 99. IR Spectrum of Compound **16**

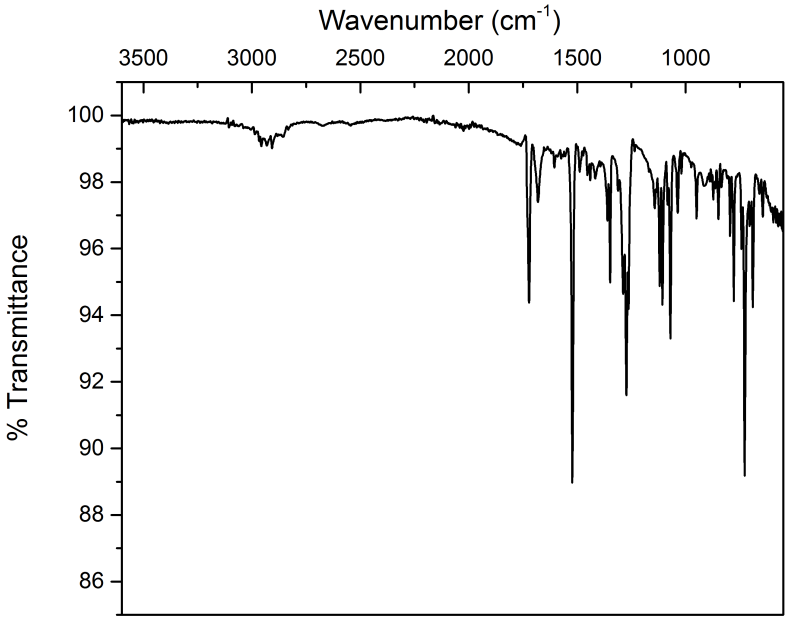

Figure 100. IR Spectrum of Compound **17**

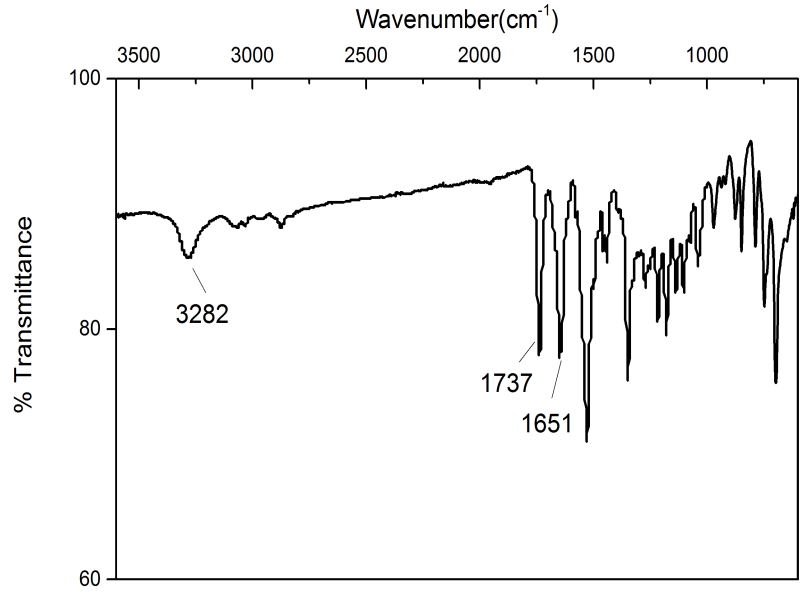

Figure 101. IR Spectrum of Compound **19**

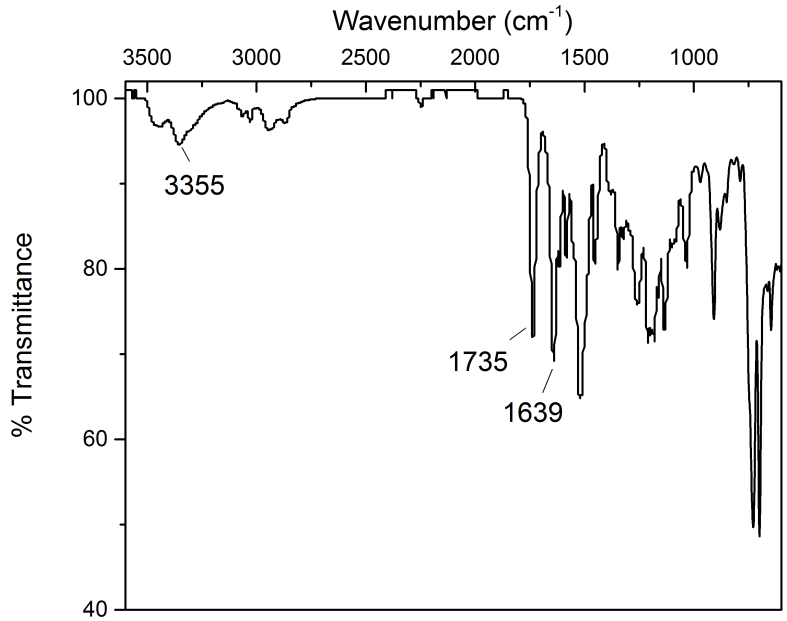

Figure 102. IR Spectrum of Compound **20**

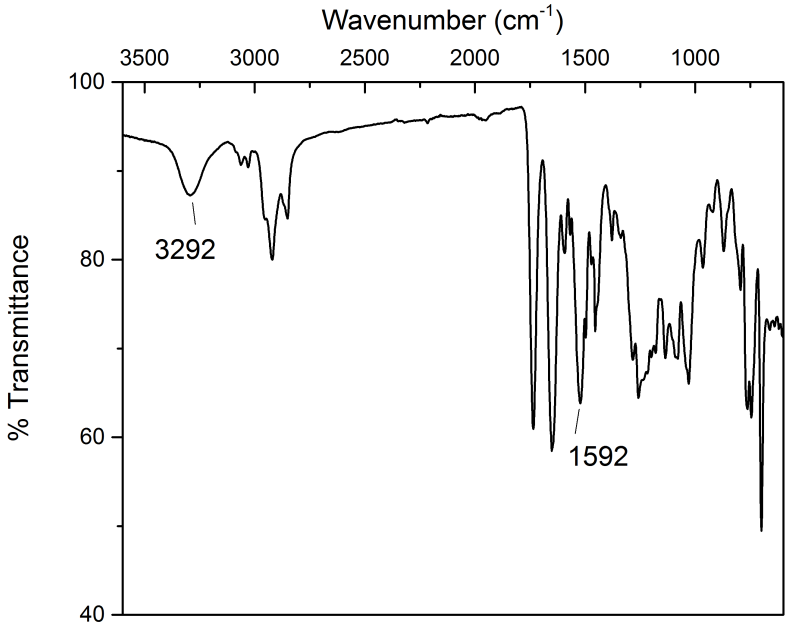

Figure 103. IR Spectrum of **Cycle IV**

C. FLUORESCENCE Spectra

Fluorescence spectra were recorded at Perkin Elmer LS55 spectrofluorometer.

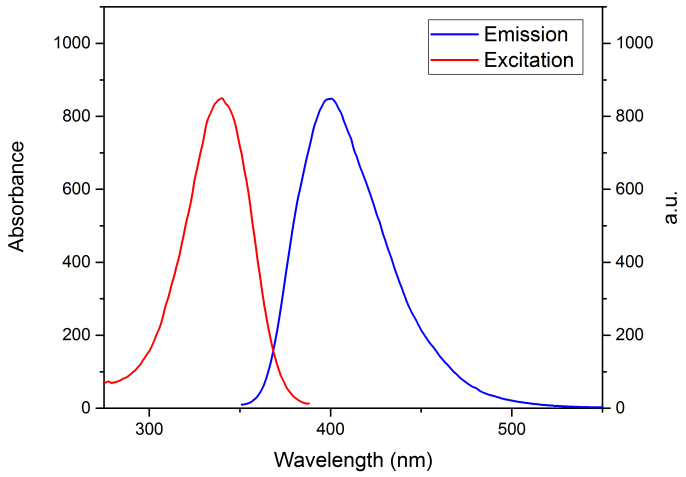

Figure 104. Fluorescence absorption and emission spectra of **Cycle I** in acetonitrile

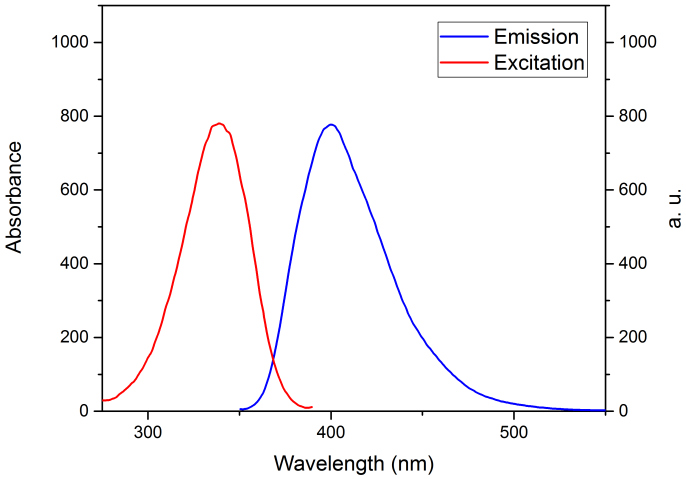

Figure 105. Fluorescence absorption and emission spectra of **Cycle II** in acetonitrile

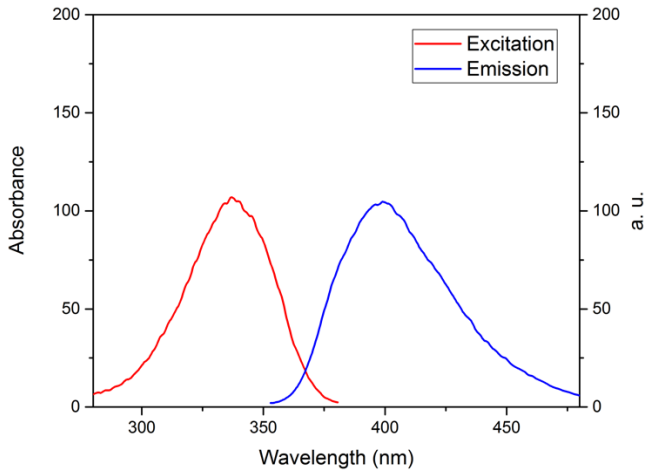

Figure 106. Fluorescence absorption and emission spectra of **Cycle III** in acetonitrile

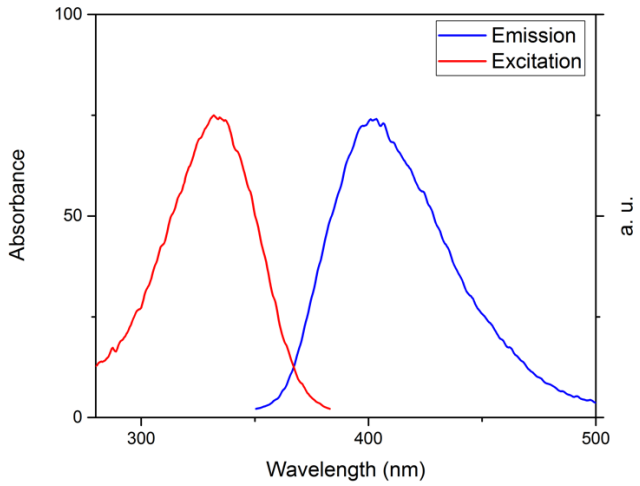

Figure 107. Fluorescence absorption and emission spectra of **Cycle IV** in acetonitrile

D. HRMS Spectra

High Resolution Mass Spectra (HRMS) Spectra were processed in positive mode on (ES+) using Time of Flight mass analyzer.

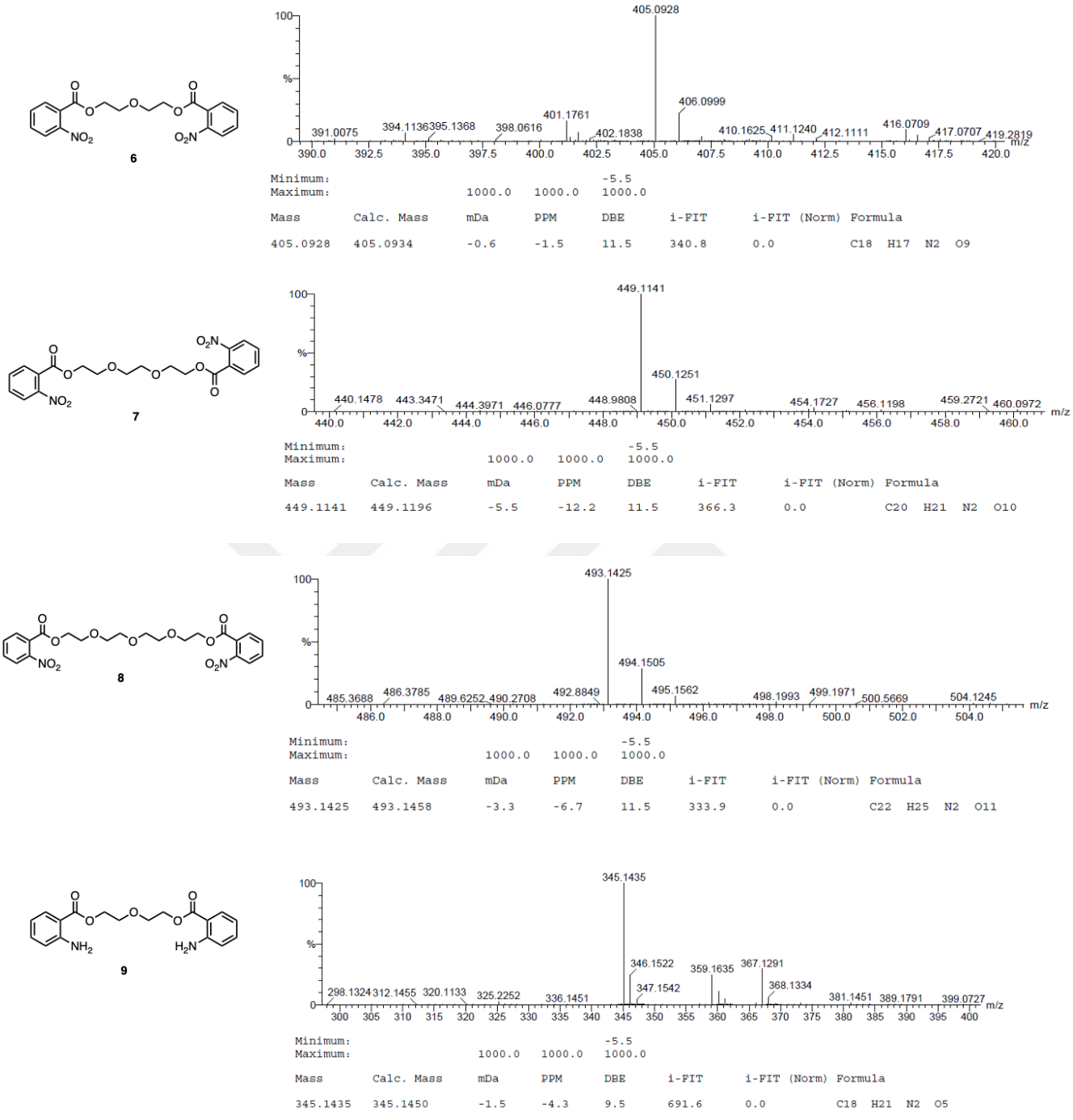

Figure 108. HRMS Spectra of Compound **6,7,8**, and **9**

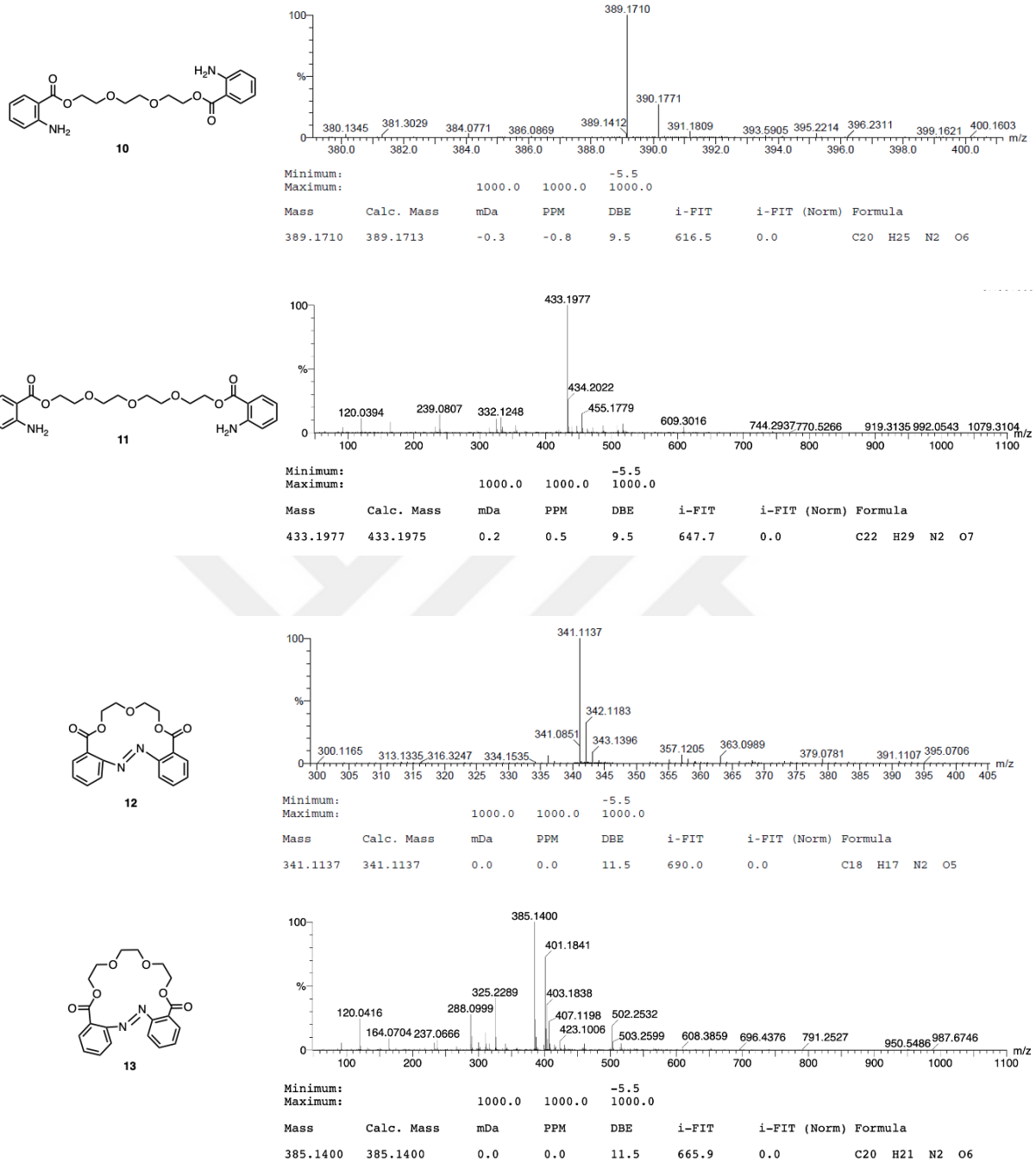

Figure 109. HRMS Spectra of Compound **10,11,** Cycle **I,** and Cycle **II**

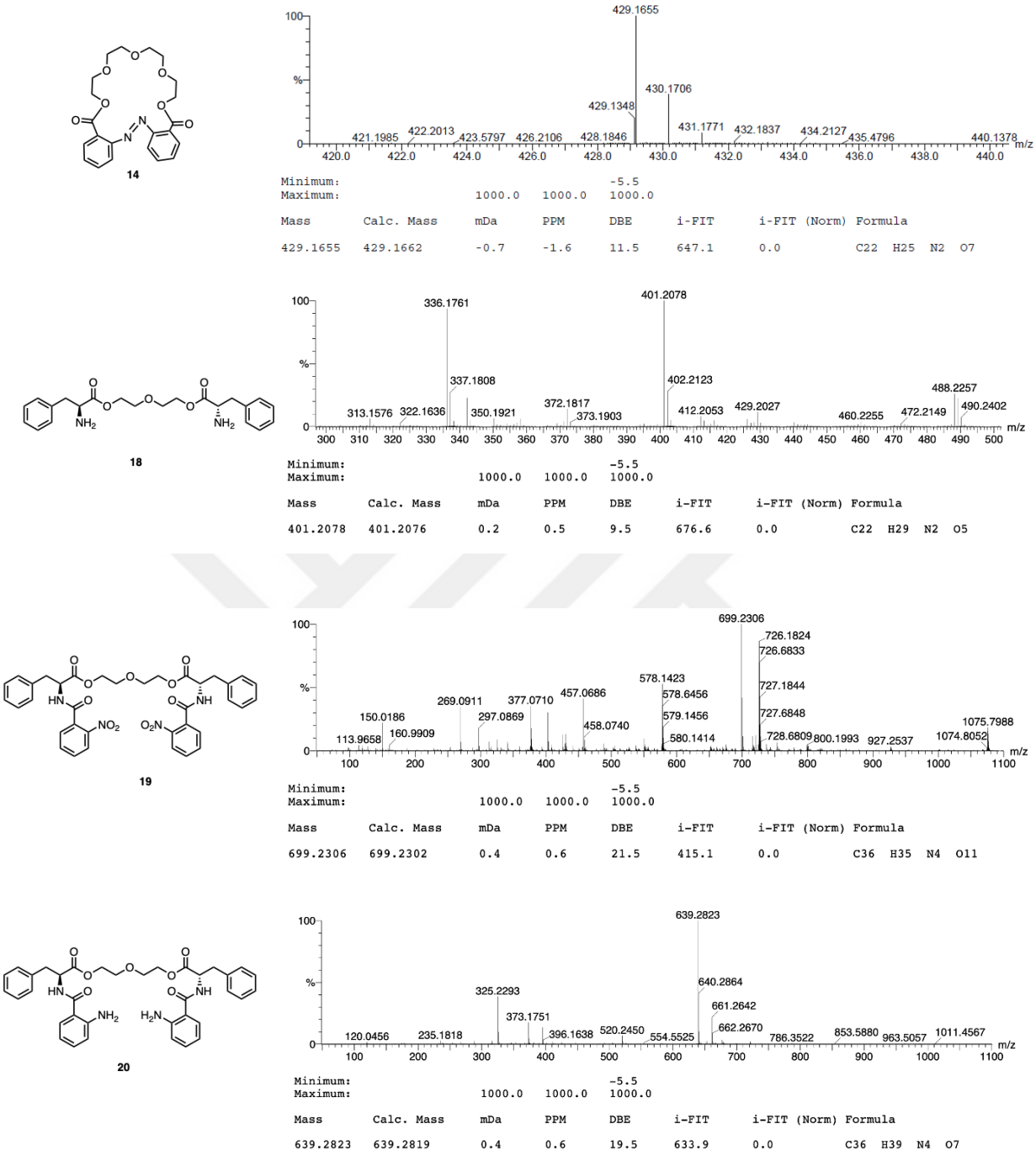

Figure 110. HRMS Spectra of Cycle **III**, Compound **18,19**, and **20**

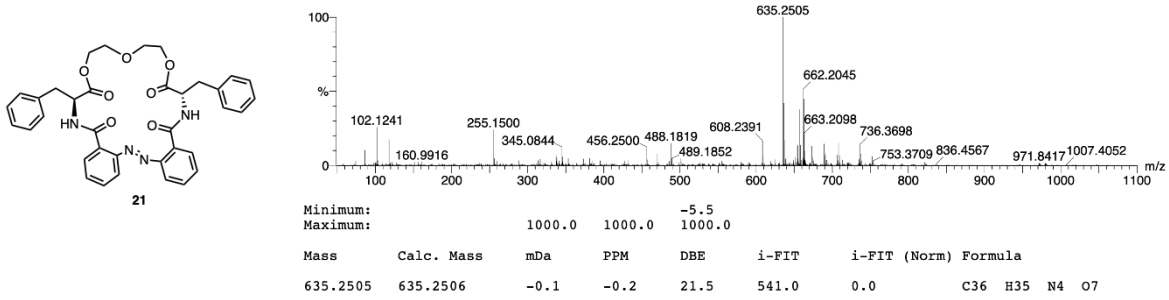

Figure 111. HRMS Spectra of Cycle **IV**

E. XYZ Coordinates of Optimized Structures

For Compound 17

Trans

Coordinates (Angstroms)

X	Y	Z
1.237680	-2.250899	-0.034529
2.189125	-3.262997	0.037455
3.550715	-2.947253	0.051418
3.951768	-1.615254	-0.003882
3.010055	-0.579749	-0.063494
1.636275	-0.905702	-0.080757
1.868650	-4.300935	0.067211
4.296465	-3.735795	0.095900
5.003396	-1.349051	-0.001292
3.568102	0.807354	-0.078815
0.675526	0.121198	-0.290547
-0.447146	-0.134512	0.211064
-1.424153	0.870420	-0.013669

-2.784758	0.493872	-0.059430
-3.763203	1.492250	-0.156427
-3.407066	2.837896	-0.214470
-2.058971	3.203329	-0.169831
-1.073933	2.226323	-0.066628
-4.806332	1.200209	-0.195871
-4.178607	3.598560	-0.291037
-1.776829	4.252134	-0.207868
-0.021644	2.480893	-0.006244
0.176322	-2.469359	-0.087931
2.753593	1.726076	0.483805
4.675403	1.078333	-0.501493
3.281119	3.062414	0.512781
2.523841	3.663101	1.017689
4.224787	3.090272	1.063775
3.452733	3.430850	-0.502148
-3.178877	-0.946556	-0.080216
-4.444703	-1.118966	0.374055
-2.489502	-1.867090	-0.469319
-4.926113	-2.471123	0.337898
-5.946180	-2.427454	0.720797
-4.913828	-2.857953	-0.684790
-4.306360	-3.115037	0.967390

Cis

Coordinates (Angstroms)

X	Y	Z
-0.320735	1.876985	0.456231
-1.072884	0.904685	-0.216580

-2.423438	0.695722	0.131942
-2.989826	1.458472	1.162349
-2.236361	2.414609	1.838218
-0.901626	2.620896	1.480834
-0.519745	0.339363	-1.413911
0.519958	-0.338947	-1.413751
1.072784	-0.904438	-0.216337
0.320637	-1.876868	0.456229
0.901463	-2.620862	1.480852
2.236120	-2.414558	1.838419
2.989654	-1.458362	1.162671
2.423364	-0.695537	0.132313
0.308157	-3.370192	1.998129
2.687217	-2.996632	2.636569
4.025241	-1.283015	1.432184
3.196404	0.377768	-0.543272
-3.196374	-0.377678	-0.543639
-4.025422	1.283047	1.431759
-2.687497	2.996623	2.636392
-0.308374	3.370147	1.998289
0.702061	2.055332	0.138943
4.532170	0.201133	-0.430393
2.701239	1.325548	-1.125765
5.338193	1.227030	-1.031803
6.371126	0.930183	-0.847976
5.139833	1.288841	-2.104767
5.128972	2.198547	-0.575705
-4.532161	-0.201857	-0.429873
-2.701020	-1.324853	-1.126944

-5.337957	-1.227861	-1.031415
-6.370941	-0.932609	-0.845327
-5.141430	-1.287736	-2.104836
-5.126651	-2.199810	-0.577229
-0.702109	-2.055439	0.138918

For Cycle I

Trans

Coordinates (Angstroms)

X	Y	Z
-0.559697	-1.124673	-0.121240
-1.937316	-1.260857	0.217306
-2.427514	-2.357290	0.946974
-3.785729	-2.487394	1.203367
-4.683582	-1.534025	0.711826
-4.207622	-0.445696	-0.012232
-2.834278	-0.274083	-0.238848
-1.716635	-3.098331	1.293029
-4.148815	-3.335296	1.777824
-5.749162	-1.637295	0.896285
-4.892189	0.296827	-0.408241
-2.470145	0.978958	-0.981606
0.097689	-2.181683	0.051112
1.482191	-2.099311	-0.233416
1.999798	-3.212007	-0.910183
3.336490	-3.258070	-1.292980
4.184357	-2.197777	-0.968897
3.688156	-1.107043	-0.257487
2.342277	-1.037389	0.128947

1.317719	-4.022355	-1.147673
3.715331	-4.119902	-1.835062
5.232504	-2.225826	-1.252406
4.349919	-0.294799	0.020832
1.906186	0.082924	1.021890
-1.441300	1.654131	-0.436606
-3.125599	1.399129	-1.915416
2.622997	1.203851	0.752276
1.086959	0.000249	1.909757
2.267307	2.409059	1.448361
2.130355	3.508333	0.403214
1.342688	2.241250	2.005007
3.069377	2.648639	2.157144
1.972891	4.476715	0.904960
3.056505	3.575885	-0.177333
1.099665	3.225072	-0.524608
-0.187083	3.675300	-0.140568
-1.225743	2.971472	-0.986936
-0.392205	3.475385	0.921292
-0.271053	4.763441	-0.301335
-2.173536	3.518840	-0.974425
-0.889681	2.891233	-2.024622

Cis

Coordinates (Angstroms)

X	Y	Z
1.169077	-0.410247	1.908992
0.983100	0.809963	1.742704
1.710130	-1.258911	0.873553

1.379675	1.525306	0.555269
0.877579	-1.971577	-0.013146
1.469794	-2.800038	-0.978963
2.849161	-2.977273	-1.030461
3.657483	-2.336983	-0.090150
3.090353	-1.489149	0.858486
-0.604769	-2.019940	0.185752
0.823299	-3.326398	-1.672200
3.286644	-3.631608	-1.778510
4.732926	-2.492110	-0.093778
3.714792	-0.999392	1.599048
2.754013	1.677007	0.309057
3.215952	2.504137	-0.710260
2.312019	3.211169	-1.503794
0.952418	3.102832	-1.239845
0.464834	2.285496	-0.208469
3.462458	1.162201	0.945026
4.285523	2.595067	-0.879139
2.664064	3.853721	-2.305176
0.224569	3.663997	-1.815484
-1.014083	2.335035	-0.006211
-1.473502	1.407087	0.850206
-1.730670	3.148553	-0.563813
-2.886924	1.470821	1.148738
-1.253872	-2.258083	-0.987484
-1.142179	-1.951119	1.265783
-2.663871	-2.556046	-0.922854
-2.846739	-3.246644	-1.751058
-2.891985	-3.040956	0.029503

-3.513987	-1.306987	-1.085379
-4.549578	-1.609657	-1.321866
-3.137661	-0.712196	-1.932578
-3.183553	2.515335	1.271207
-3.719437	0.803266	0.065997
-2.990058	0.928300	2.089404
-3.448281	-0.581590	0.118704
-4.786630	1.006817	0.257098
-3.467302	1.227726	-0.914450

For Cycle II

Trans

Coordinates (Angstroms)

X	Y	Z
-0.426872	3.178871	-1.301461
0.369021	4.168082	-1.865402
1.698668	4.299261	-1.461628
2.214231	3.430376	-0.506257
1.436740	2.411069	0.066378
0.082877	2.300006	-0.330284
-1.453485	3.038778	-1.618001
-0.045793	4.828249	-2.622257
2.333964	5.066357	-1.894999
3.242914	3.516187	-0.176327
-0.771758	1.263353	0.142876
-1.960541	1.647964	0.282135
-2.908993	0.627177	0.540585
-3.894743	0.945501	1.483559
-4.879850	0.022758	1.820928

-2.948987	-0.619928	-0.121988
-3.951100	-1.534899	0.226382
-4.907912	-1.223386	1.190717
-3.852312	1.922789	1.954258
-5.627412	0.277553	2.566784
-3.980023	-2.494321	-0.279124
-5.680350	-1.945840	1.438049
2.170433	1.582221	1.079729
3.325545	1.814115	1.380133
1.444752	0.581924	1.629952
2.163618	-0.301745	2.514188
2.411599	-1.642410	1.832965
3.103781	0.171449	2.797850
1.531036	-0.442830	3.395672
3.040945	-1.394927	0.591648
1.459895	-2.174245	1.697043
3.049804	-2.254973	2.492882
0.673173	-2.621766	-0.927730
-0.487712	-2.680964	-1.914600
-1.646538	-2.263759	-1.161249
-0.678153	-3.705555	-2.241595
-0.343555	-2.030704	-2.778675
-2.006670	-0.956184	-1.237879
-1.641236	-0.198299	-2.108439
3.690205	-2.491108	-0.032247
2.785149	-3.623215	-0.527093
4.445840	-2.928503	0.645148
4.212740	-2.053417	-0.888286
1.822016	-3.232950	-1.490965

2.289115	-4.125685	0.320161
3.428180	-4.365343	-1.016391
0.361070	-3.166136	-0.022610
0.867715	-1.580164	-0.646482

Cis

Coordinates (Angstroms)

X	Y	Z
-3.372150	-1.451987	-0.296394
-2.216965	-1.418416	0.497406
-1.191226	-2.363513	0.275519
-1.363434	-3.314745	-0.737310
-2.519952	-3.351918	-1.515796
-3.523471	-2.411224	-1.296246
0.030215	-2.465478	1.157602
1.247287	-2.560910	0.547142
1.475959	-2.043930	-0.773649
2.968389	-2.055870	-1.058173
3.644543	-1.051317	-0.321356
4.600112	-0.327736	-1.068938
5.175399	0.793672	-0.205930
4.223106	1.566411	0.499255
3.094300	2.015219	-0.224462
2.161075	2.613922	0.824652
0.833030	2.833658	0.296195
-0.008293	1.774595	0.363260
0.331110	0.671530	0.746054
-2.182482	-0.602683	1.675712
-2.343882	0.627107	1.681190

-2.495972	1.469970	0.519693
-3.791753	1.882307	0.178964
-3.992125	2.867429	-0.783349
-2.900314	3.499317	-1.385066
-1.611829	3.145000	-1.001551
-1.390734	2.131206	-0.056862
-0.039432	-2.583776	2.353933
-5.005491	3.152755	-1.052490
-3.054608	4.275698	-2.128189
-4.638263	1.432853	0.689832
-0.752567	3.649557	-1.430055
-0.590774	-4.062298	-0.891549
-2.637085	-4.116336	-2.278341
-4.433099	-2.427387	-1.890019
-4.172656	-0.750554	-0.098493
1.082423	-1.026884	-0.844948
0.982436	-2.671412	-1.523845
3.089999	-1.890387	-2.140250
3.385885	-3.045457	-0.821984
2.500073	3.595432	1.160392
2.106704	1.925382	1.669283
5.437629	-0.966998	-1.397822
4.136646	0.083931	-1.981808
5.816428	0.368771	0.572110
5.803002	1.427733	-0.857393
3.368296	2.760811	-0.989702
2.579024	1.182134	-0.713049

For Cycle III

Trans

Coordinates (Angstroms)

X	Y	Z
3.394525	-1.816797	-1.609079
3.567754	-3.092866	-2.133749
2.782832	-4.151918	-1.669802
1.831826	-3.924737	-0.678735
1.651753	-2.649648	-0.127974
2.444624	-1.580667	-0.603932
3.962802	-0.971701	-1.980970
4.303280	-3.258896	-2.916164
2.904897	-5.148082	-2.085236
1.208675	-4.731647	-0.308689
2.177624	-0.261514	-0.159018
3.171734	0.507283	-0.175718
2.852601	1.852786	0.138688
3.850220	2.568736	0.809668
3.624064	3.878296	1.226458
1.624187	2.476961	-0.174042
1.411192	3.790031	0.256777
2.398385	4.488218	0.955174
4.788460	2.063207	1.016295
4.400611	4.419675	1.759322
0.466807	4.270793	0.022146
2.213787	5.510942	1.271609
0.630452	-2.547834	0.959816
-0.272736	-3.353021	1.095141
0.865070	-1.527688	1.809826
-0.060478	-1.335509	2.893566

-1.017523	-0.177557	2.616647
-0.590143	-2.271106	3.084918
0.554860	-1.082808	3.762965
-1.930163	-0.373940	1.558365
-0.441979	0.710194	2.339456
-1.553634	0.033676	3.560079
-1.710928	1.421912	-1.376557
-0.636416	1.966923	-0.572896
0.607915	1.834539	-1.075321
0.863866	1.339352	-2.151479
-2.889024	-1.408652	1.747213
-4.148624	-1.049266	0.981655
-3.153718	-1.506041	2.813347
-2.484920	-2.366645	1.399843
-3.842976	-0.974729	-0.398023
-4.536986	-0.091890	1.361068
-4.917262	-1.820370	1.164949
-2.996565	2.070275	-0.882513
-1.741613	0.339831	-1.237300
-1.535353	1.652332	-2.429774
-4.064513	1.718737	-1.756854
-2.884223	3.163406	-0.897806
-3.194698	1.759487	0.148803
-5.137078	0.981582	-1.199540
-4.911581	-0.531384	-1.219764
-6.015398	1.199767	-1.820868
-5.362975	1.334397	-0.181948
-4.645288	-0.831561	-2.238306
-5.851727	-1.041403	-0.945153

Cis

Coordinates (Angstroms)

X	Y	Z
5.004292	-0.661703	-0.531346
3.629802	-0.568658	-0.794939
3.011444	0.698327	-0.822488
3.792890	1.833845	-0.554160
5.147818	1.730921	-0.252521
5.753716	0.472434	-0.236323
1.609484	0.897753	-1.321513
0.839700	1.833688	-0.686640
0.845469	1.991063	0.748039
-0.063443	3.249347	1.108027
1.338910	3.120756	1.014757
1.867908	3.235082	-0.302219
3.372745	3.070396	-0.244905
3.678309	1.733665	0.101477
5.001657	1.355248	-0.201481
5.171501	-0.118956	0.112603
4.294835	-0.857412	-0.712974
4.361933	-2.256718	-0.539236
3.043146	-2.855140	-0.987807
2.056606	-2.560173	0.018979
0.818552	-2.192667	-0.399223
0.469230	-2.167090	-1.557497
-3.015360	-1.813930	-1.171588
-2.042559	-2.333487	-0.597501
-1.462980	-1.836689	0.615178
-2.270882	-1.583465	1.734745

-1.697964	-1.308364	2.973982
-0.309329	-1.280680	3.115200
0.499900	-1.561957	2.016134
-0.056991	-1.857923	0.765181
-1.197492	0.370063	-2.323368
-2.340069	-1.117174	3.829573
0.141236	-1.054838	4.077159
-3.349032	-1.627967	1.633089
1.578806	-1.557247	2.113656
-3.325764	2.812480	-0.616674
-5.730718	2.625986	-0.056547
-6.813457	0.375830	-0.017458
-5.467157	-1.643650	-0.563890
-0.367416	1.118461	1.204197
-1.869935	2.074682	1.126017
-0.271844	3.476569	2.160718
-0.429215	4.093533	0.499707
3.122808	-3.944782	-1.075541
2.723657	-2.440149	-1.945680
4.539946	-2.517974	0.515901
5.220210	1.528887	-1.268375
5.734198	1.933436	0.389605
4.944813	-0.302576	1.175356
6.224282	-0.401239	-0.063052
3.780565	3.315693	-1.240183
3.809680	3.774512	0.482676
1.629576	4.229175	-0.718707
5.183782	-2.691369	-1.134268
1.445883	2.474685	-0.967106

For Cycle IV

Trans

Coordinates (Angstroms)

X	Y	Z
2.483192	2.997459	2.850611
3.181909	2.544161	3.964030
2.682068	0.808751	1.803603
3.400661	0.377164	2.927877
3.653506	1.230819	4.000123
4.213860	0.870732	4.858407
3.358109	3.213784	4.801487
3.791772	-0.635178	2.944946
1.480867	2.606099	0.646183
1.658912	3.828617	0.417385
0.867812	4.393497	-0.613100
1.479571	5.474914	-1.261643
0.851737	6.131137	-2.316197
-0.421914	5.726223	-2.713389
-1.051677	4.671120	-2.050578
-0.429854	3.987333	-0.997891
-0.934722	6.237563	-3.523261
-2.059946	4.385460	-2.336903
2.468474	5.767785	-0.923147
1.349009	6.957295	-2.816372
-1.239089	2.946540	-0.259181
2.450585	-0.138267	0.655044
2.453243	0.204247	-0.519043
2.275503	-1.447852	1.053918

-1.428105	2.972016	0.953543
-1.839786	2.041011	-1.084306
1.928119	-2.493492	0.112726
1.955974	-1.616963	2.000767
-2.693148	0.980812	-0.584044
-1.570930	1.973700	-2.058396
-4.852895	0.612781	0.796666
4.312757	-2.709629	-0.842062
0.809841	-3.323085	0.741414
-2.844594	-0.022325	-1.721907
-2.541441	0.215309	-2.875250
0.447045	-3.201365	1.893596
0.320416	-4.233192	-0.121815
-3.370991	-1.182247	-1.304557
-6.007220	-0.051216	0.366247
-4.420012	0.419430	2.116834
-5.119079	-0.423854	2.979634
-6.268841	-1.083095	2.538045
-6.713066	-0.891995	1.228959
-6.359659	0.096171	-0.652547
-6.817706	-1.735793	3.211963
-7.612041	-1.393716	0.879240
-3.532273	0.943279	2.465038
-4.770131	-0.560952	3.999864
5.449715	-2.433707	-0.073773
4.299878	-2.308643	-2.184728
5.392933	-1.649495	-2.743905
6.522028	-1.380173	-1.967042
6.547712	-1.774192	-0.629382

7.422189	-1.570504	-0.016703
5.476871	-2.743101	0.968671
5.363229	-1.344286	-3.786529
7.375011	-0.866539	-2.402553
3.423644	-2.511275	-2.796681
-0.785367	-5.040739	0.336460
-3.519044	-2.210292	-2.305335
-1.867933	-5.041229	-0.724589
-1.158303	-4.627593	1.274391
-0.415122	-6.057580	0.506831
-2.252966	-3.703420	-0.959668
-2.707898	-5.646960	-0.345692
-1.509274	-5.509063	-1.655962
-3.498894	-3.556019	-1.612999
-2.700576	-2.129773	-3.023227
-4.468072	-2.061250	-2.832945
-4.325229	-3.640162	-0.890390
-3.641454	-4.329255	-2.385632
-4.078449	1.535552	-0.116810
-4.670044	1.802400	-1.000597
-3.848785	2.462393	0.416640
-2.214139	0.489335	0.269979
3.126624	-3.427357	-0.237608
3.436340	-3.942126	0.680372
2.753928	-4.193326	-0.926956
1.562537	-2.023999	-0.806797
2.240656	2.148458	1.760136
2.097906	4.009502	2.802513

Cis

Coordinates (Angstroms)

X	Y	Z
-3.512190	-1.482976	2.221582
-3.237648	-1.925021	3.512622
-1.502938	-0.101839	2.271401
-1.209497	-0.612956	3.539082
-2.075620	-1.506676	4.165265
-1.848315	-1.872025	5.162432
-3.924632	-2.609514	4.001995
-0.297633	-0.283528	4.025788
-2.905985	-0.002046	0.309392
-3.265544	-0.637245	-0.703597
-3.413989	-2.067877	-0.747439
-4.678271	-2.490533	-1.185849
-4.974279	-3.844107	-1.303274
-3.990099	-4.793632	-1.019045
-2.720255	-4.374019	-0.635279
-2.395782	-3.014412	-0.509656
-4.205531	-5.854129	-1.110950
-1.940995	-5.096097	-0.415962
-5.423159	-1.732262	-1.408178
-5.965270	-4.154565	-1.622396
-0.956187	-2.744913	-0.134155
-0.522284	0.892366	1.693702
0.688903	0.753549	1.876491
-1.044260	1.974342	1.055552
-0.371830	-3.504116	0.638935
-0.315609	-1.714293	-0.752672

-0.171150	2.915956	0.368417
-1.997764	1.895503	0.713141
1.125031	-1.543362	-0.601636
-0.772822	-1.126582	-1.440478
3.351513	-2.854874	-0.901296
-2.142044	3.860760	-0.987412
0.959353	3.359752	1.302395
1.504831	-0.201434	-1.211897
0.768098	0.450965	-1.932529
0.811383	3.818640	2.410506
2.150525	3.258834	0.671977
2.761810	0.126658	-0.913671
4.389825	-2.610324	-1.807415
3.678887	-3.274517	0.395888
5.010185	-3.430882	0.779492
6.038523	-3.178873	-0.131632
5.724400	-2.771729	-1.429122
4.150392	-2.295629	-2.821218
7.076135	-3.304353	0.166221
6.517075	-2.584425	-2.149370
2.879988	-3.484680	1.103541
5.245407	-3.754787	1.789965
-3.433526	4.278411	-0.641542
-1.962006	3.176748	-2.199693
-3.044086	2.926221	-3.042152
-4.325734	3.356302	-2.690392
-4.518196	4.032373	-1.486184
-5.511497	4.368356	-1.199919
-3.588946	4.807207	0.296248

-2.885966	2.391210	-3.974733
-5.167668	3.161038	-3.349229
-0.972780	2.825328	-2.482832
3.316099	3.548276	1.463762
3.311173	1.297872	-1.557499
4.543410	3.312724	0.602410
3.321180	2.891036	2.337680
3.279641	4.588317	1.807482
4.754745	1.932355	0.346429
5.417283	3.696869	1.148410
4.457339	3.885417	-0.332180
4.712300	1.517208	-1.005972
2.661714	2.152651	-1.368053
3.355061	1.116109	-2.638093
5.265347	0.573615	-1.048630
5.225296	2.243596	-1.657350
1.901566	-2.707276	-1.303809
1.811970	-2.582754	-2.389895
1.364507	-3.620275	-1.033153
1.374829	-1.528287	0.462410
-0.971104	4.161320	-0.070666
-1.319827	4.676999	0.830236
-0.267400	4.837769	-0.574401
0.279868	2.435685	-0.505685
-2.639979	-0.584453	1.591319
-4.403494	-1.820818	1.705405